

T401

**Synthesis, spectral and structural studies of  
transition metal complexes of N(4)-substituted  
semicarbazones**

Thesis submitted to the

**Cochin University of Science and Technology**

In partial fulfillment of the  
requirements for the degree of

**DOCTOR OF PHILOSOPHY**

Under the Faculty of Science

By

**Binu Varghese**



**Department of Applied Chemistry  
Cochin University of Science and Technology**

**Kochi-682 022**

**February 2009**

**Synthesis, spectral and structural studies of transition metal complexes  
of N(4)-substituted semicarbazones**

**Ph. D. Thesis under the faculty of Science**

T401

**Author:**

Binu Varghese

Research fellow, Department of Applied Chemistry

Cochin University of Science and Technology,

Kochi, India

E mail: binumv2002@yahoo.com

**Research advisor:**

Dr. M. R. Prathapachandra Kurup

Professor

Department of Applied Chemistry

Cochin University of Science and Technology,

Kochi, India

E mail: mrp@cusat.ac.in



Department of Applied Chemistry

Cochin University of Science and Technology,

Kochi, India

February 2009

**Front cover:** Crystal structure of copper(II) complex of 2-benzoylpyridine-*N*(4)-phenylsemicarbazone



Phone Off. 0484-2862423  
0484-2575804  
Phone Res. 0484-2576904  
Fax: 0484-2577595  
Email: mrp@cusat.ac.in  
mrp\_k@yahoo.com

**DEPARTMENT OF APPLIED CHEMISTRY**  
**COCHIN UNIVERSITY OF SCIENCE AND TECHNOLOGY**  
KOCHI - 682 022, INDIA

---

**Prof. M.R. Prathapachandra Kurup**  
**Professor**

12<sup>th</sup> February 2009

---

**CERTIFICATE**

This is to certify that the thesis entitled **“Synthesis, spectral and structural studies of transition metal complexes of N(4)-substituted semicarbazones”** submitted by Ms. Binu Varghese, in partial fulfillment of the requirements for the degree of Doctor of Philosophy, to the Cochin University of Science and Technology, Kochi-22, is an authentic record of the original research work carried out by her under my guidance and supervision. The results embodied in this thesis, in full or in part, have not been submitted for the award of any other degree.

**M. R. Prathapachandra Kurup**  
(Supervisor)

## DECLARATION

I hereby declare that the work presented in this thesis entitled **“Synthesis, spectral and structural studies of transition metal complexes of N(4)-substituted semicarbazones”** is entirely original and was carried out independently under the supervision of Dr. M. R. Prathapachandra Kurup, Department of Applied Chemistry, Cochin University of Science and Technology and has not been included in any other thesis submitted previously for the award of any other degree.

12-02-09

Kochi-22



Binu Varghese

## ACKNOWLEDGEMENT

*The research described in this thesis was done at the Department of Applied Chemistry, CUSAT. I am grateful to all those who inspired me during this research work and I wish to express my deep feeling of gratitude towards them, without whose valuable suggestions and encouragement, the accomplishment of this thesis would have been impossible.*

*First and foremost, I wish to place on record my heartfelt gratefulness to my revered guide Prof. (Dr.) M.R. Prathapachandra Kurup, Department of Applied Chemistry for his intensive guidance and whole hearted support and inspiration throughout my research work,*

*I am greatly obliged to Dr. Girish Kumar (Head of the Department) and Prof. (Dr.) K.K. Mohammed Yusuff (Doctoral Committee member) for their kind consideration. I acknowledge all faculty members of the Department of Applied Chemistry for their support and advice. I also acknowledge all the non-teaching staff of the Department in taking care of all issues regarding the administration of my academic program.*

*I am indebted to Prof. (Dr.) P. Mathur, National Single Crystal X-ray Diffraction Facility, IIT-Bombay and Dr. E. Suresh, Analytical Sciences Division, CSMCRI, Bhavanagar, Gujarat, for single crystal X-ray diffraction studies. Acknowledgements are also due to the services provided by the Sophisticated Analytical Instrumentation Facility, IIT Bombay, IIT, Roorkee and IISc, Bangalore and Sophisticated Test and Instrumentation Centre, Kochi-22.*

*I am grateful to Dr. V. Suni and Dr. P.F. Raphael for their help during the initial stages of my research possession. I am much obliged to S.R. Sheeja, Suja Krishnan, Dr. E.B. Seena, Dr. U.L. Kala, Sreesha Sasi, Leji Latheef, Bessy, Dr. Mini and Dr. Manoj for their boundless support and timely help whenever I need it most. I am thankful to my lab mates Laly miss, Reena chechy, Nancy, Renjusha, Neema, Roji, Dhanya, Shimi, Jessy miss, Annie miss, Jayakumar sir, Ananya and Sarika for their encouragement in my ways.*

*I owe a special debt of gratitude and thanks to Dr. Winny Varghese, Principal, Mar Athanasius College, Kothamangalam for providing the facilities available for doing my research work. I am also grateful to Dr. M.M. Joseph, HOD of Chemistry and the faculty of Chemistry department for their whole hearted support and inspiration throughout my research work,*

*I also express my feeling of gratitude to my beloved parents, brothers, sister and in-laws for imparting moral support, love, confidence and affection with their earnest prayers and sustained support. I place on record the assistance from my husband Sinosh for his symbiotic support, love and patience for keeping me in a*

*pleasant mood. He has been an endearing source of encouragement in all my activities. I also express my deep sense of love to my daughter Sweeta who missed lot of my care and attention during the course of this investigation.*

*Above all I praise the God Almighty for having given me His strength and blessings to carry this work to conclusion.*

*Binu Varghese*

## PREFACE

The work from which this thesis originated was carried out by the author in the Department of Applied Chemistry, CUSAT, Kochi, during the period 2004-2009. The thesis is an introduction to our attempts to evaluate the coordination behaviour of a few compounds of our interest. Semicarbazones and their metal complexes have been an active area of research during the past years because of the beneficial biological activities of these substances. Tridentate NNO semicarbazone systems formed from heterocyclic and aromatic carbonyl compounds and their transition metal complexes are well-authenticated compounds in this field and their synthesis and characterization are well desirable. Hence, we decided to develop a research program aimed at the synthesis and characterization of novel semicarbazones derived from 2-benzoylpyridine and 2-acetylpyridine and their transition metal complexes. In addition to various physico-chemical methods of analysis, single crystal X-Ray diffraction studies were also used for the characterization of the complexes.

The thesis has been divided into seven chapters carrying a detailed account of the novel ligands and their complexes with some first row transition metal ions. Chapter 1 is a review of applications and recent developments in the field of semicarbazones and their metal complexes. A brief introduction to the various analytical methods is also included in this chapter. Chapter 2 deals with the syntheses and characterization of the ligands, 2-benzoylpyridine-*N*(4)-phenylsemicarbazone and 2-acetylpyridine-*N*(4)-phenylsemicarbazone. Chapter 3 describes the syntheses and physico-chemical characterizations of copper(II) complexes of 2-benzoylpyridine-*N*(4)-phenylsemicarbazone along with the crystal

structure of complex **(1a)**. Chapter 4 deals with the syntheses and physico-chemical characterizations of copper(II) complexes of 2-acetylpyridine-*N*(4)-phenylsemicarbazone along with the crystal structure of complex **(10a)**. Syntheses and spectral characterizations of manganese(II) complexes of the ligands are discussed in Chapter 5. Chapter 6 comprises syntheses and spectral characterizations of cobalt(III) complexes. Chapter 7 describes the syntheses and physico-chemical characterizations of zinc(II) complexes. Summary of the thesis is also given at the end.



# CONTENTS

	<b>Page No.</b>
<b>CHAPTER 1</b>	
Semicarbazones - A brief introduction	
1.1	General introduction 1
1.2	Biological activity of semicarbazones 2
1.3	Stereochemistry, bonding and nature of coordination of semicarbazones 3
1.4	Scope and significance of the present work 5
1.5	Introduction to the relevant analytical techniques 7
1.5.1	Elemental analysis 8
1.5.2	Magnetic susceptibility measurements 8
1.5.3	Infrared spectroscopy 9
1.5.4	Electronic spectroscopy 10
1.5.5	NMR spectroscopy 12
1.5.6	EPR spectroscopy 12
1.5.7	Conductivity measurements 14
1.5.8	X-ray crystallography 14
	References 15
<b>CHAPTER 2</b>	
Syntheses and characterization of semicarbazone ligands	
2.1	Introduction 18
2.2	Experimental 20
2.2.1	Materials 20
2.2.2	Syntheses of ligands 20
2.2.2.1	Synthesis of HL <sup>1</sup> 20
2.2.2.2	Synthesis of HL <sup>2</sup> 21
2.3	Characterization techniques 22
2.4	Results and discussion 22
2.4.1	Analytical data 22
2.4.2	IR spectra 23
2.4.3.	Electronic spectra 25
2.4.4	NMR spectrum of HL <sup>1</sup> 26
2.4.5	NMR spectrum of HL <sup>2</sup> 29
	References 32

### CHAPTER 3

#### Syntheses, structural and spectral characterization of copper(II) complexes of 2-benzoylpyridine-*N*(4)-phenylsemicarbazone

3.1	Introduction	34
3.2	Experimental	35
3.2.1	Materials	35
3.2.2	Syntheses of complexes	35
3.2.3	Analytical methods	38
3.2.4	X-Ray crystallography	39
3.3.	Results and discussion	41
3.3.1	Analytical measurements	41
3.3.2	Crystal structure of $[\text{Cu}_2\text{L}^1_2(\text{OAc})_2]$ ( <b>1a</b> )	42
3.3.3	IR spectra	49
3.3.4	Electronic spectra	56
3.3.5	EPR spectra	61
	References	80

### CHAPTER 4

#### Syntheses, structural and spectral characterization of copper(II) complexes of 2-acetylpyridine-*N*(4)-phenylsemicarbazone

4.1	Introduction	83
4.2	Experimental	84
4.2.1	Materials	84
4.2.2	Syntheses of complexes	84
4.2.3	Analytical methods	87
4.2.4	X-Ray crystallography	88
4.3	Results and discussion	89
4.3.1	Analytical measurements	89
4.3.2	Crystal structure of $[\text{Cu}_2\text{L}^2_2(\mu\text{-N}_3)_2]$ ( <b>10a</b> )	91
4.3.3	IR spectra	98
4.3.4	Electronic spectra	105
4.3.5	EPR Spectra	110
	References	127

## CHAPTER 5

### Syntheses and spectral characterization of manganese(II) complexes of *N*(4)-phenylsemicarbazones

5.1	Introduction	130
5.2	Experimental	131
5.2.1.	Materials	131
5.2.2.	Syntheses of complexes	132
5.2.3.	Analytical methods	134
5.3.	Results and discussion	134
5.3.1.	Analytical measurements	134
5.3.2	IR spectra	136
5.3.3.	Electronic spectra	142
5.3.4.	EPR spectra	145
	References	153

## CHAPTER 6

### Syntheses and spectral characterization of cobalt(III) complexes of *N*(4)-phenylsemicarbazones

6.1	Introduction	155
6.2.	Experimental	156
6.2.1.	Materials	156
6.2.2.	Syntheses of complexes	156
6.2.3.	Analytical methods	158
6.3.	Results and discussion	158
6.3.1.	Analytical measurements	158
6.3.2.	IR spectra	160
6.3.3.	Electronic spectra	165
	References	168

## CHAPTER 7

### Syntheses and spectral characterization of zinc(II) complexes of *N*(4)-phenylsemicarbazones

7.1.	Introduction	170
7.2.	Experimental	173
7.2.1.	Materials	173
7.2.2.	Syntheses of complexes	173
7.2.3.	Analytical methods	175
7.3.	Results and discussion	175

7.3.1.	Analytical measurements	175
7.3.2.	Infrared spectra	177
7.3.3.	Electronic spectra	182
	References	186
	<b>Summary and conclusion</b>	<b>188</b>

## SEMICARBAZONES-A BRIEF INTRODUCTION

### 1.1. General introduction

Coordination compounds are substances with characteristic chemical structures in which a central metal atom is surrounded by non-metal atoms (or groups of atoms), called ligands, joined to it by chemical bonds. The importance of coordination complexes in our day to day life is increasing due to their complex structures and interesting magnetic, electronic and optical properties. The diversity in structures exhibited by the coordination complexes of multidentate ligands have led to their usage as sensors, models for enzyme mimetic centers, medicines etc. The ligands chosen are of prime importance in determining the properties of coordination compounds. The presence of nitrogen and oxygen atoms in the ligands enhances their coordinating possibilities. Moreover, the presence of these atoms in the coordination sphere leads to their biological activity.

The applications of coordination compounds in chemistry and technology are many and diverse. Naturally occurring coordination compounds are vital to living organisms. Coordination compounds can be used for the analysis of various substances. These include the selective precipitation of metal ions as complexes, the formation of colored complexes and the preparation of complexes.

## **1.2. Biological activity of semicarbazones**

Semicarbazones are associated with diverse pharmacological activities, such as antibacterial and antifungal, antihypertensive, hypolipidemic, antineoplastic, hypnotic and anticonvulsant. Several studies have reported the anticonvulsant activity of semicarbazones derived from aromatic and unsaturated carbonyl compounds. Semicarbazones (SCs), as well as their sulfur analogs, thiosemicarbazones (TSCs), are compounds possessing a wide spectrum of biological applications. The semicarbazones have been screened for their anti-fungal, antibacterial, biocidal, and anti-convulsant [1-4] activities. Aryl semicarbazones have documented increasing advances in antiseptic drug design and were found to act by blocking the voltage-gated sodium ion channels. Various aryl substituted semicarbazones act as potential anticonvulsant agents.

The search for new anticonvulsant drugs continues to be an active area of investigation in medicinal chemistry. Aryl semicarbazones are potent anticonvulsants [5,6]. There are recent reports on the relationship between the structure and antimicrobial activity of the transition metal zinc(II) and nickel(II) complexes with multidentate thiosemicarbazone and semicarbazone ligands [7-10].

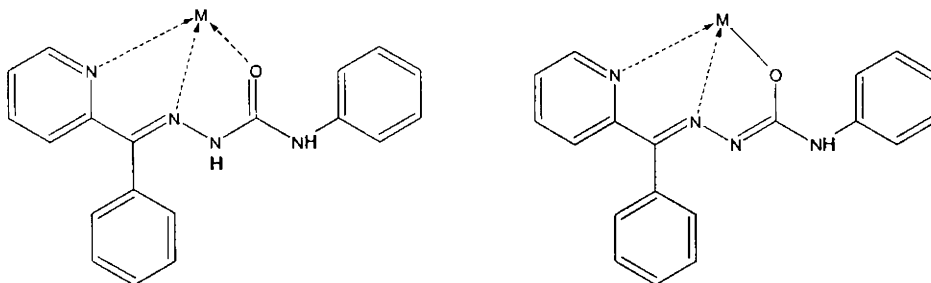
Aryl semicarbazones have documented increasing advances in antiseptic drug design and were found to act by blocking the voltage-gated sodium ion channels. It is reported that [11] aryl semicarbazones were devoid of sedative-hypnotic activity and exhibited anticonvulsant activity with less neurotoxicity. Aryl semicarbazones do not possess the dicarboximide group as found in conventional drugs like barbiturates,

hydantoin, oxazolidinones etc. that may be associated with toxicity and side effects.

### 1.3. Stereochemistry, bonding and nature of coordination of semicarbazones

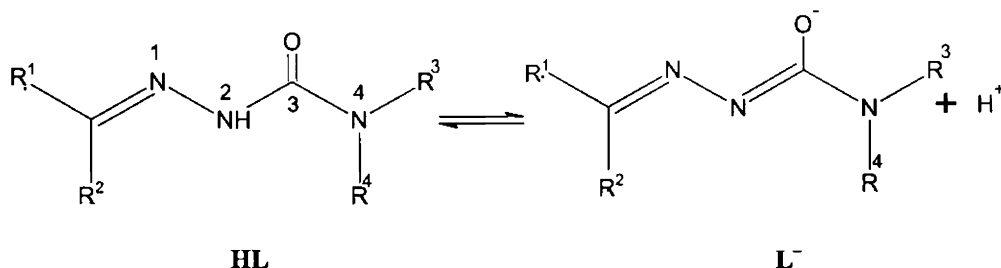
Semicarbazones are Schiff bases, usually obtained by the condensation of the semicarbazide with suitable aldehyde or ketone. Schiff bases are the key intermediates in a large number of synthetic and biological reactions. The chemistry of transition metal complexes of semicarbazones has been receiving considerable attention largely because of their pharmacological properties. Moreover, metal complexes of semicarbazones often display enhanced activities when compared to the uncomplexed semicarbazones.

The semicarbazone ligands are coordinated in different fashion and the coordination modes can be controlled chemically. The coordination mode of semicarbazones is very sensitive towards minor variations in the experimental conditions, the nature of substituents on the carbonyl compound fragment and the metal salt. The coordination mode of the N(4)-substituted semicarbazones is given below.



N,N,O – tricoordination

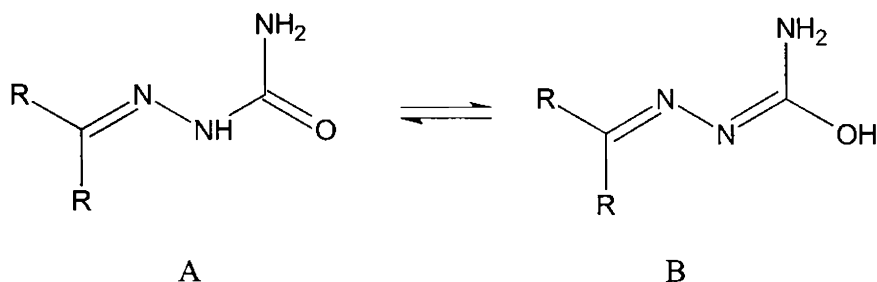
Semicarbazones are versatile ligands in both neutral (HL) and anionic ( $L^-$ ) forms (Scheme 1).



Scheme 1

The  $R^1$  and  $R^2$  groups may provide additional donor atoms and  $R^3$  and  $R^4$  are the  $N(4)$ -substituents.

Semicarbazones exist in tautomeric keto (A) and enol (B) forms [12] (Scheme 2).



Scheme 2

Keto form acts as a neutral bidentate ligand and the enol form can deprotonate and appear to serve as a monoanionic bidentate ligand in complexes. However if there is an additional coordination position in proximity to the semicarbazone part, it can act as a tridentate ligand [13].



An important feature in the chemistry of semicarbazones and their metal complexes is the acid character of the  $^2\text{NH}$ ; this allows for either neutral or anionic ligands. When coordinated as anionic ligands, the conjugation is extended to include the semicarbazone moiety (*i.e.*  $\text{C}=\text{N}-\text{N}=\text{C}(\text{O}^-)-\text{N}$ ). If  $\text{N}(2)$  is alkylated, the semicarbazone will function as the keto isomer without extended conjugation. The stereochemistries adopted by semicarbazones of transition metal complexes often depend upon the anion of the metal salt used and the nature of the  $\text{N}(4)$ -substituents [14]. Further, as indicated previously, the charge on the ligand is dictated by the keto-enol equilibrium which in turn is influenced by the solvent and pH of the preparative medium [15].

Semicarbazones have applications in analytical field also. Some of the semicarbazones produce highly colored complexes with metal ions. These complexes have been proposed as analytical reagents that can be used in selective and sensitive determinations of metal ions [16].

The coordination possibilities in the SC backbone are increased if substituents  $\text{R}^1$  and  $\text{R}^2$  include additional donor atoms and can also be modified by placing substituents on backbone donor atoms.

#### **1.4. Scope and significance of the present work**

There has been considerable interest in the studies of semicarbazones recently due to their unusual coordination modes [17] when bound to metals.

The present study employs 2-benzoylpyridine- $\text{N}(4)$ -phenyl semicarbazone ( $\text{HL}^1$ ) and 2-acetylpyridine- $\text{N}(4)$ -phenylsemicarbazone

(HL<sup>2</sup>) as principal ligands. Due to the high pharmacological potentialities and good chelating property of semicarbazones, the present work is mainly concerned with the studies on complexes of *N*(4)-substituted semicarbazones.

Thus, it is worthwhile to carry out the structural and spectral studies of heterocyclic semicarbazones with different structural features as well as their metal complexes.

Bearing in mind these findings and also to understand the coordination behavior of semicarbazones, we undertook the present work as:

1. To synthesize and physico-chemically characterize the following semicarbazone ligands:
  - a. 2-benzoylpyridine-*N*(4)-phenylsemicarbazone (HL<sup>1</sup>) and
  - b. 2-acetylpyridine-*N*(4)-phenylsemicarbazone (HL<sup>2</sup>)
2. To find optimal conditions for the synthesis of copper(II), cobalt(III), manganese(II) and zinc(II) complexes of these ligands.
3. To find the compositions and probable structures of the complexes and study their spectral properties.
4. To confirm the structures of complexes by single crystal XRD studies.
5. To understand the intermolecular interactions in the complexes.

This dissertation is divided into seven chapters.

- Chapter I titled as ‘Semicarbazones –A brief Introduction’ includes importance of coordination compounds, biological importance of semicarbazones, its mode of coordination, stereochemistry and relevance of present investigation. Brief introduction to the different analytical techniques for the characterization is also presented in this chapter.
- Chapter II deals with the procedure followed for the preparation of the ligands, and their physicochemical investigations.
- Chapters III, IV, V, VI and VII discuss the procedure followed for the preparation of the complexes of copper, cobalt, manganese and zinc and their physicochemical investigations.

### **1.5. Introduction to the relevant analytical techniques**

Several methods are available for the characterization of the ligands and their coordination compounds. They include partial elemental analysis, conductivity measurements, magnetic susceptibility studies, IR, UV-Vis, NMR and EPR spectral techniques and single crystal X-ray diffraction studies.

Some of the physicochemical methods adopted during the present investigation are discussed below.

### 1.5.1. Elemental analysis

Elemental analyses were carried out using an Elementar Vario EL III CHNS analyzer at SAIF, Cochin University of Science and Technology, Kochi, India.

### 1.5.2. Magnetic susceptibility measurements

When a substance is placed in a magnetic field of strength  $H$ , the intensity of magnetic field in the substance is greater than  $H$ . If the field of the substance is greater than  $H$ , the substance is paramagnetic and if it is less than  $H$ , the substance is diamagnetic. Paramagnetism arises as a result of unpaired electron spins in the atom.

The magnetic susceptibility and the magnetic moment are often used to describe the magnetic behaviors of substances. A magnetic dipole is a macroscopic or microscopic magnetic system in which the north and south poles are separated by a short but definite distance. In the presence of a magnetic field, magnetic dipoles within a material experience a turning effect and become partially oriented. The magnetic moment refers to the turning effect produced when a magnetic dipole is placed in a magnetic field. The fundamental unit of magnetic moment is the Bohr magneton. For isotropic substances, the magnetic susceptibility ( $\chi$ ) is defined by,

$$\chi = M/H$$

where  $M$  is the magnetic moment per unit volume (magnetization) and  $H$  is the strength of magnetic field. The molar susceptibility  $\chi_M$  is simply defined as the susceptibility per gram-mole. Hence,

$$\chi_M = \chi \times \text{molecular weight}$$

The magnetic susceptibility value calculated from magnetic measurements is the sum of paramagnetic and diamagnetic susceptibilities. To calculate the exact paramagnetic susceptibility ( $\mu_{eff}$ ), the value of diamagnetic susceptibility is subtracted from the susceptibility calculated from observed results.

When the structural formula of the complexes is correctly known, diamagnetic correction can be calculated from Pascal's constants.

The magnetic susceptibility measurements were carried out in the polycrystalline state on a Vibrating Sample Magnetometer (VSM) PAR model at 5.0 kOe field strength at room temperature at Indian Institute of Technology, Roorkee, India.

### *1.5.3. Infrared spectroscopy*

Infrared spectroscopy (IR spectroscopy) is the subset of spectroscopy that deals with the infrared part of the electromagnetic spectrum. As with all spectroscopic techniques, it can be used to identify a compound and to investigate the composition of a sample.

The vibrational states of a molecule can be probed in a variety of ways. The most direct way is infrared spectroscopy because vibrational transitions typically require an amount of energy that corresponds to the infrared region of the spectrum between 4000 and 400  $\text{cm}^{-1}$ . Radiation in this region can be utilized in structure determination in coordination chemistry by making use of the fact that interatomic bonds in ligands absorb it.

The resonant frequencies or vibrational frequencies are determined by the shape of the molecular potential energy surfaces, the masses of the atoms and, eventually by the associated vibronic coupling. In order for a vibrational mode in a molecule to be IR active, it must be associated with changes in the permanent dipole [18].

Infrared spectra were recorded on a Thermo Nicolet AVATAR 370 DTGS model FT-IR Spectrophotometer with KBr pellets at SAIF, Kochi, India.

#### *1.5.4. Electronic spectroscopy*

Electronic spectroscopy is the measurement of the wavelength and intensity of absorption of near-ultraviolet and visible light by a sample. UV-visible spectroscopy is usually applied to organic molecules and inorganic ions or complexes. The absorption of UV or visible radiation corresponds to the excitation of outer electrons. It is an analytical technique to study the electronic structure and its dynamics in atoms and molecules.

An ultraviolet-visible spectrum is essentially a graph of light absorbance versus wavelength in a range of ultraviolet or visible regions. Such a spectrum can often be produced by a more sophisticated spectrophotometer. Wavelength is often represented by the symbol  $\lambda$ . For the given substance, the wavelength at which maximum absorption in the spectrum occurs is called  $\lambda_{\text{max}}$ , pronounced "Lambda-max".

The method is most often used in a quantitative way to determine concentrations of an absorbing species in solution, using the Beer-Lambert law.

The Beer-Lambert law states that the absorbance of a solution is due to the solution's concentration. Thus UV/vis spectroscopy can be used to determine the concentration of a solution. It is necessary to know how quickly the absorbance changes with concentration.

$$A = -\log(I/I_0) = \epsilon \cdot c \cdot l$$

where  $A$  is the measured absorbance,  $I_0$  is the intensity of the incident light at a given wavelength,  $I$  is the transmitted intensity,  $l$  is the path length through the sample, and  $c$  is the concentration of the absorbing species.

Samples for UV/vis spectrophotometry are most often liquids, although the absorbance of gases and even of solids can also be measured. Samples are typically placed in a transparent cell, known as a cuvette. The best cuvettes are made of high quality quartz, although glass or plastic cuvettes are common.

There are three types of electronic transitions that can be considered for coordination compounds. These are transitions involving a)  $\pi$ ,  $\sigma$ , and  $n$  electrons of ligands, b) charge-transfer electrons and c)  $d$  and  $f$  electrons. Most absorption spectroscopy of ligands is based on  $n \rightarrow \pi^*$  and  $\pi \rightarrow \pi^*$  transitions. Many inorganic complexes show Ligand-to-Metal Charge Transfer (LMCT) transitions and Metal-to-Ligand Charge Transfer (MLCT) transitions (not as common as LMCT). Transition probability in ligand field transitions ( $d-d$  transitions) is determined by the spin selection rule and the orbital (Laporte) selection rule.

Electronic spectra were recorded on a Cary 5000, version 1.09 UV-Vis-NIR Spectrophotometer from solutions in acetonitrile.

### 1.5.5. $^1\text{H}$ NMR spectroscopy

$^1\text{H}$  NMR spectra were recorded on Bruker AMX 400 FT-NMR Spectrometer using TMS as the internal standard at Sophisticated Instrumentation Facility, Indian Institute of Science, Bangalore.

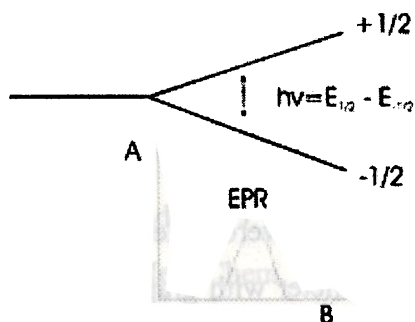
### 1.5.6. EPR spectroscopy

Electron paramagnetic resonance (EPR) is the process of resonant absorption of microwave radiation by paramagnetic ions or molecules, with at least one unpaired electron spin, in the presence of a static magnetic field. EPR was discovered by Zavoisky in 1944.

For an electron with spin,  $s = \frac{1}{2}$ , the spin angular momentum quantum number will have values  $m_s = \pm\frac{1}{2}$  which gives rise to a doubly degenerate spin energy state. In presence of an external magnetic field, the degeneracy is lifted and these electron spin states are separated. The low energy state will have the spin magnetic moment aligned with the applied field ( $m_s = -\frac{1}{2}$ ). The high-energy state will have the spin magnetic moment opposed to the applied field ( $m_s = +\frac{1}{2}$ ). A transition is induced by microwave radiation of frequency  $\nu$  such that  $\Delta E = h\nu = g\beta H$ , where  $h$  is Planck's constant,  $\beta$  is the Bohr magneton, and  $H$  is the magnitude of the applied field. The proportionality factor  $g$  is a function of the electron's environment and it is called Lande splitting factor or  $g$  factor (for the theoretical 'free' electron,  $g = 2.0023$ ). These electronic states are again split by their interaction with the spin of the nucleus (termed hyperfine coupling) into different energy states, each separated by the hyperfine coupling constant,  $A$ . Number of hyperfine lines is given by  $(2nI+1)$  where



$n$  is the number of equivalent nuclei with spin  $I$ . Further splitting of states by nearby nuclei, such as  $^{14}\text{N}$  is referred to as superhyperfine splitting [19].



EPR signals can be generated by resonant energy absorption measurements made at different electromagnetic radiation frequencies  $\nu$  in a constant external magnetic field. Measurements can be provided by changing the magnetic field  $B$  and using a constant frequency radiation. This means that an EPR spectrum is normally plotted with the magnetic field along the X-axis, with peaks at the field that cause resonance.

Symmetry can also have an effect on EPR spectra. If the spectra are obtained from frozen solutions or from a powder, where the anisotropy is not averaged away by motion of the molecule, a complex pattern can emerge. When  $g_x = g_y = g_z$  in a perfectly cubic crystal, such a  $g$  value is the isotropic one. In axial environment the  $g$  factors are anisotropic ( $g_z = g_{\parallel}$  and  $g_x, g_y = g_{\perp}$ ). For a rhombic molecular environment, three  $g$  factors are observed.

EPR spectral measurements were carried out on a Varian E-112 X-band spectrometer using TCNE as standard at SAIF, Indian Institute of Technology, Bombay, India.

### 1.5.7. Conductivity measurements

The molar conductivities [20] of the complexes in dimethylformamide (DMF) solutions ( $10^{-3}$  M) at room temperature were measured using a direct reading conductivity meter.

### 1.5.8. X-Ray crystallography

The crystallographic data were collected using Bruker Smart Apex 2 CCD area detector diffractometer with graphite monochromated MoK $\alpha$  ( $\lambda = 0.71073$  Å) radiation at the Analytical Sciences Division, Central Salt and Marine Chemicals Research Institute, Bhavanagar, Gujarat, India and also Nonius MACH3 diffractometer, equipped with graphite-monochromated MoK $\alpha$  ( $\lambda=0.71073$  Å) radiation at the National Single Crystal X-Ray Diffraction Facility, IIT, Bombay, India.

The cell refinement was done using Bruker SMART software [21] and Argus (Nonius) MACH3 software [22]. The Bruker SAINT [21] and Maxus (Nonius software) were used for data reduction [22]. The structure was solved by direct methods with the program SHELXL and SHELXS-97 and refined by full matrix least squares on  $F^2$  using SHELXL-97 [23]. The graphics used were Mercury [24] and Diamond version 3.1f [25].

**References**

1. N. Fahmi, R.V. Singh, *J. Ind. Chem. Soc.* 73 (1996) 257.
2. J.R. Dimmock, R.N. Puthucode, J.M. Smith, M. Hetherington, J.W. Quail, U. Pugazhenthii, *J. Med. Chem.* 39 (1996) 3984.
3. J.R. Dimmock, K.K. Sindhu, S.D. Tumber, S.K. Basran, M. Chen, J.W. Quail, *Eur. J. Med. Chem.* 30 (1995) 287.
4. J.R. Dimmock, S.N. Pandeya, J.W. Quail, U. Pugazhenthii, T.M. Allen, G.Y. Kao, *Eur. J. Med. Chem.* 30 (1995) 303.
5. J.R. Dimmock, K.K. Sindhu, R.S. Thayer, P. Mack, M.J. Duffy, R.S. Reid, *J. Med. Chem.* 36 (1993) 2243.
6. J.R. Dimmock, S.C. Vashishta, J.P. Stables, *Eur. J. Med. Chem.* 35 (2000) 241.
7. N.C. Kasuga, Y. Hara, C. Koumo, K. Sekino, K. Nomiya, *Acta Crystallogr., Sect. C* 55 (1999) 1264.
8. N.C. Kasuga, A. Ohashi, C. Koumo, J. Uesugi, M. Oda, K. Nomiya, *Chem. Lett.* (1997) 609.
9. N.C. Kasuga, K. Sekino, C. Koumo, N. Shimada, M. Ishikawa, K. Nomiya, *J. Inorg. Biochem.* 84 (2001) 55.
10. N.C. Kasuga, K. Sekino, M. Ishikawa, A. Honda, M. Yokoyama, S. Nakano, N. Shimada, C. Loumo K. Nomiya, *J. Inorg. Biochem.* 96 (2003) 298.
11. M. Shalini, P. Yogeewari, D. Sriram, J.P. Stables, *Biomedicine & Pharmacotherapy* 8 (Number 1) (2007).

12. A.K. Das, A. Rueda, L.R. Falvello, S.M.Peng, S. Bhattacharya, *Inorg. Chem.* 38 (1999) 4365.
13. F. Basuli, S.M. Peng, S. Bhattacharya, *Inorg. Chem.* 39 (2000) 1120.
14. M. Akkurt, S. Ozfuric, S. Ide, *Anal.Sci.* 16 (2000) 667.
15. T.A. Reena, E.B. Seena, M.R.P. Kurup, *Polyhedron* 27 (2008) 1825.
16. T. Atalay, E.G. Akgemci, *Tr. J. Chem.* 22 (1998) 123.
17. F. Basuli, M. Ruff, C.G. Pierpont, S. Bhattacharya, *Inorg. Chem.* 37 (1998) 6113.
18. A. Bozkurt, A. Rosen, H. Rosen, B. Onaral, *Biomedical Engineering Online* 4 (2005) 29.
19. T.S. Smith, R.L. Brutto, V.L. Pecoraro, *Coord. Chem. Rev.* 228 (2002) 1.
20. W.J. Geary, *Coord. Chem. Rev.* 7 (1971) 81.
21. SMART and SAINT, Area Detector Software Package and SAX Area Detector Integration Program, Bruker Analytical X-ray; Madison, WI, USA, 1997.
22. Nonius, MACH3 Software, B.V. Nonius, Delft, The Netherlands, 1997.
23. G.M. Sheldrick, *Acta Cryst.* (2008) A64, 112–122.
24. C.F. Macrae, P.R. Edgington, P. McCabe, E. Pidcock, G.P. Shields, R. Taylor, M. Towler, J. van de Streek, *J. Appl. Crystallogr.* 39 (2006) 453.

25. K. Brandenburg, Diamond Version 3.1f, Crystal Impact GbR, Bonn, Germany, 2008.

**SYNTHESES AND CHARACTERIZATION OF  
SEMICARBAZONE LIGANDS**

**2.1. Introduction**

The coordinating ability of semicarbazones to both transition and main group metallic cations is attributed to the extended delocalization of electron density over the semicarbazone skeleton, which is enhanced by substitution at *N*(4)-position. Condensation of semicarbazide with aldehydes or ketone extends the electron delocalization along azomethine bond. 2-Hydroxybenzaldehyde-*N*(4)-substituted thiosemicarbazones, as well as heterocyclic thiosemicarbazones, which derives from the presence of several potential donor atoms, their flexibility, and their ability to coordinate in either neutral or deprotonated forms, have been the subject of extensive investigations [1], because of their ability to strongly coordinate metal ions as tridentate ligands and their wide spectrum of biological applications [2]. Due to their good complexing properties, biological activity, and analytical application, semi-/thiosemi-/isothiosemicarbazides and their Schiff bases of different denticity, as well as their metal complexes, have been the subject of many studies. Apparently, the most numerous among them are the complexes with tridentate salicylaldehyde semi-/thiosemi-/isothiosemicarbazones [3].

Semicarbazones of di-2-pyridylketone [4,5] and its derivatives are classes of versatile tridentate NNO donors capable of stabilizing both higher and lower oxidation states of transition metal ions. They are capable of deprotonation at amide function to give monoanionic chelating ligands,

coordinating to a metal centre through the deprotonated ketonic oxygen, azomethine nitrogen and pyridyl nitrogen. However, the coordination chemistry of substituted or unsubstituted semicarbazones of pyridine derivatives is quite unexplored. This prompted our study into the synthesis and characterization of substituted semicarbazones using aromatic ketone and its metal complexes. Here we have synthesized the following two new ligands using 2-benzoylpyridine, 2-acetylpyridine and 4-phenylsemicarbazide.

- 2-benzoylpyridine-*N*(4)-phenylsemicarbazone (HL<sup>1</sup>)
- 2-acetylpyridine-*N*(4)-phenylsemicarbazone (HL<sup>2</sup>)

This chapter deals with the syntheses and spectral characterization of semicarbazone ligands. The IUPAC numbering scheme is not very appropriate for describing the structural data of semicarbazones because the numbering of C and N atoms on the semicarbazone chain does not run into the numbering of substituted groups. The structures of ligands prepared are given in Fig. 2.1.

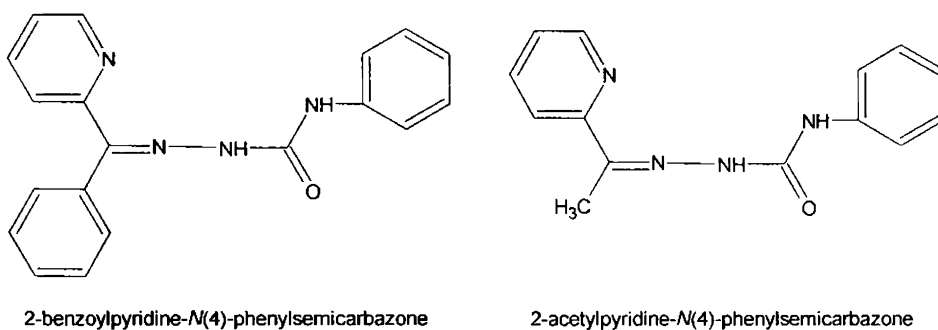


Fig. 2.1. Structures of the semicarbazones.

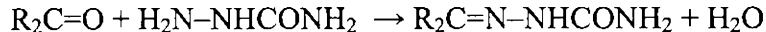
## 2.2. Experimental

### 2.2.1. Materials

2-Benzoylpyridine (Aldrich), 2-acetylpyridine (Fluka), *N*(4)-phenylsemicarbazide (Fluka) were used as received. Methanol was dried over fused CaCl<sub>2</sub> and distilled. The solvents were purified and dried by using standard methods and procedures.

### 2.2.2. Syntheses of ligands

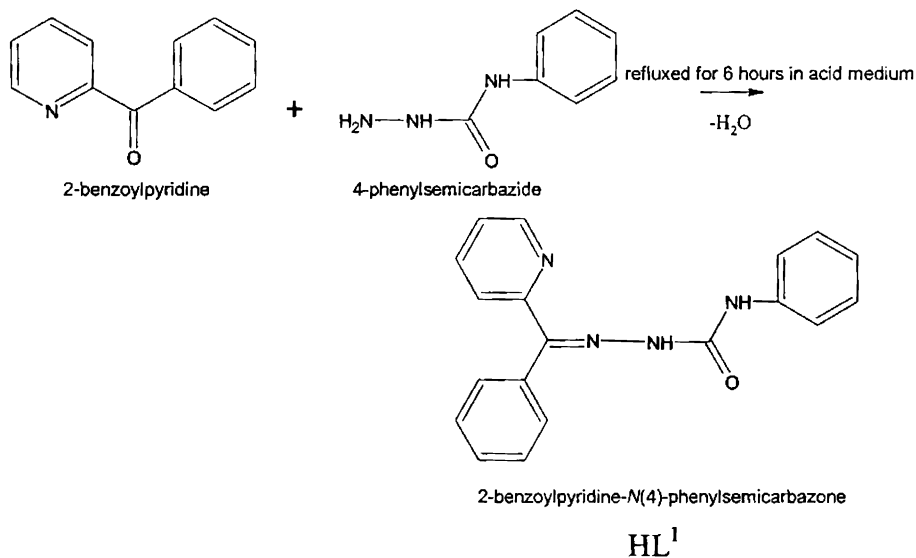
The semicarbazones are prepared by the condensation of semicarbazide with appropriate simple or substituted carbonyl compounds.



#### 2.2.2.1. Synthesis of 2-benzoylpyridine-*N*(4)-phenylsemicarbazone (*HL*<sup>1</sup>)

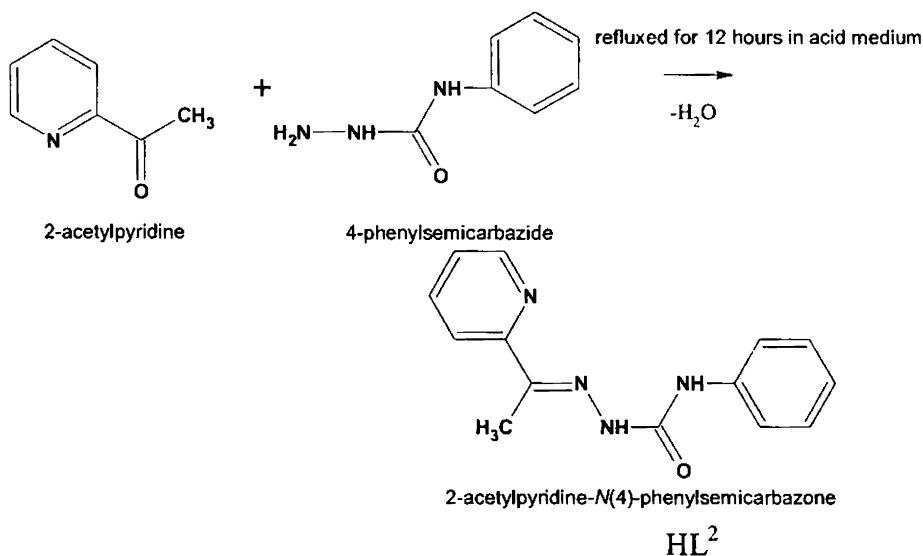
It was prepared by adapting a method reported earlier [6]. It involves the condensation of 2-benzoylpyridine and *N*(4)-phenylsemicarbazide in acid medium. A methanolic solution (50 ml) of *N*(4)-phenylsemicarbazide (1.511 g, 10 mmol) was added to a solution of 2-benzoylpyridine (1.830 g, 10 mmol) in methanol and the reaction mixture was refluxed for 30 minutes on a water bath. To this few drops of dil. acetic acid was also added to change the pH and it is again boiled for 6 hours. On cooling pale yellow crystals of the semicarbazone were separated out. It was recrystallized from methanol (yield 75%). The crystals were filtered, washed with ethanol, water and ether and dried *in vacuo* over P<sub>4</sub>O<sub>10</sub>.





#### 2.2.2.2. Synthesis of 2-acetylpyridine-N(4)-phenylsemicarbazone (HL<sup>2</sup>)

The compound (HL<sup>2</sup>) was prepared in methanol solution by condensing 2-acetylpyridine with *N*(4)-phenylsemicarbazide in acid medium. A methanolic solution (50 ml) of *N*(4)-phenylsemicarbazide (1.511 g, 10 mmol) was added to a solution of 2-acetylpyridine (1.210 g, 10 mmol) in methanol. To this, few drops of dil. acetic acid was also added to change the pH and the reaction mixture was refluxed for 12 hours on a water bath. On cooling very pale yellow crystals of the semicarbazone were separated out. It was recrystallized from methanol (yield 70%). These crystals were filtered, washed with methanol and ether and dried *in vacuo* over P<sub>4</sub>O<sub>10</sub>.



### 2.3. Characterization techniques

The ligands were characterized by using partial elemental analyses, IR, electronic and <sup>1</sup>H NMR spectra. The details regarding these techniques are given in Chapter 1.

### 2.4. Results and discussion

#### 2.4.1. Analytical data

The preparation of the semicarbazones from 4-phenylsemicarbazide in a single step involves condensation between aromatic aldehyde and NH<sub>2</sub> of the semicarbazide moiety in an acidic medium. Methanol is used as solvent and mild refluxing condition is adopted. Both the ligands HL<sup>1</sup> and

HL<sup>2</sup> are pale yellow in color. The analytical data of the ligands are presented in Table 2.1.

Table 2.1. Analytical data of the ligands

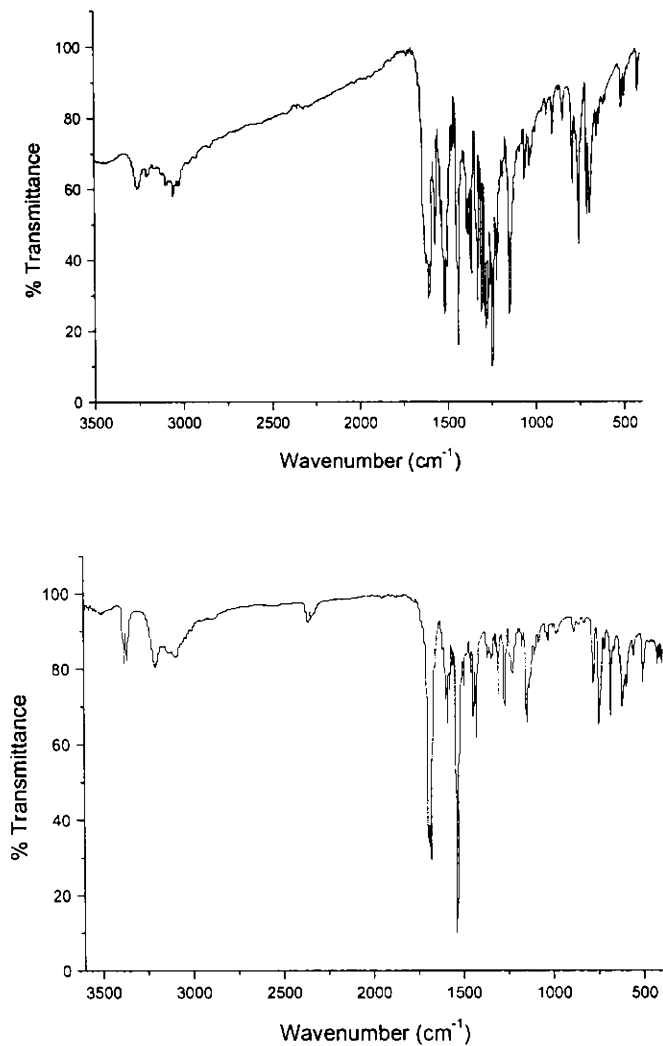
Compound	Observed (Calculated) %		
	C	H	N
HL <sup>1</sup>	72.47(72.13)	5.20 (5.10)	18.14(17.71)
HL <sup>2</sup>	66.68 (66.13)	5.58 (5.55)	22.22(22.03)

#### 2.4.2. IR spectra

The characteristic IR bands for the ligands (HL<sup>1</sup> and HL<sup>2</sup>) provide significant information regarding the various functional groups present in the ligands. Selected IR bands of the ligands are listed in Table 2.2. IR spectra of the ligands have bands in the range of 3375–3380 cm<sup>-1</sup> due to –NH groups present in the molecule. Absence of bands corresponding to enol group reveals the presence of only the keto tautomer in the solid state. The azomethine stretching vibrations, C=N<sub>azo</sub>, characteristic of a Schiff base, are observed at 1600 and 1599 cm<sup>-1</sup> for HL<sup>1</sup> and HL<sup>2</sup> respectively which are in agreement with earlier reports of *N*(4)-substituted semicarbazones [7-11]. Medium bands observed at 1132 and 1151 cm<sup>-1</sup> for HL<sup>1</sup> and HL<sup>2</sup> respectively which are assigned to hydrazinic N–N bonds [12,13]. The band corresponding to <sup>4</sup>N–H appears at 3375 cm<sup>-1</sup> for HL<sup>1</sup> and 3380 cm<sup>-1</sup> for HL<sup>2</sup>. The 1590-1400 cm<sup>-1</sup> region of the spectra is complicated by the presence of the amide bands and ring breathing vibrations of the phenyl rings. IR spectra of the ligands HL<sup>1</sup> and HL<sup>2</sup> are presented in Fig. 2.2.

Table 2.2. Selected IR bands ( $\text{cm}^{-1}$ ) of the ligands

Ligands	$\nu(\text{N-H})$	$\nu(\text{C=N})$	$\nu(\text{N-N})$	$\nu(\text{C=O})$
HL <sup>1</sup>	3375	1600	1132	1698
HL <sup>2</sup>	3380	1599	1151	1683

Fig. 2.2. IR spectra of the ligands HL<sup>1</sup> (upper) and HL<sup>2</sup> (lower).

### 2.4.3. Electronic spectra

In contrast to the infrared spectrum, the electronic spectrum is not used primarily for the identification of individual functional groups, but rather to show the relationship between functional groups, chiefly conjugation [14]. The electronic spectral data of the ligands HL<sup>1</sup> and HL<sup>2</sup> in acetonitrile are presented in Table 2.3. The spectra of ligands HL<sup>1</sup> and HL<sup>2</sup> consist of broad bands at 32890 and 33900 cm<sup>-1</sup> respectively which are due to  $n \rightarrow \pi^*$  bands of the pyridine rings. The  $\pi \rightarrow \pi^*$  transitions of the phenyl ring are observed in the 37010-37600 cm<sup>-1</sup> region [15,16]. Electronic spectra of the ligands are presented in Figs. 2.3 and 2.4.

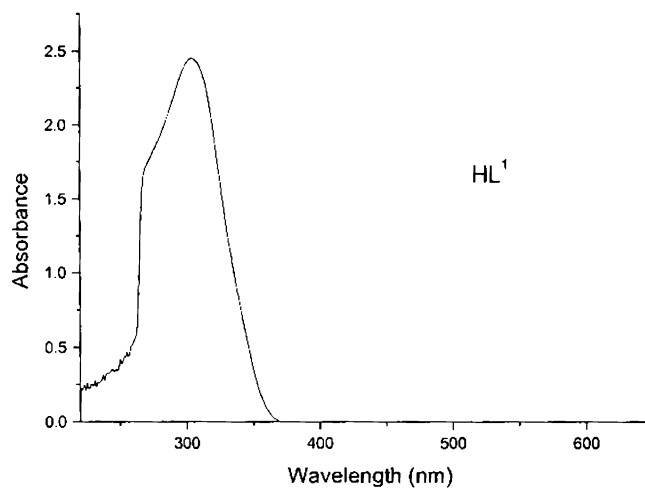
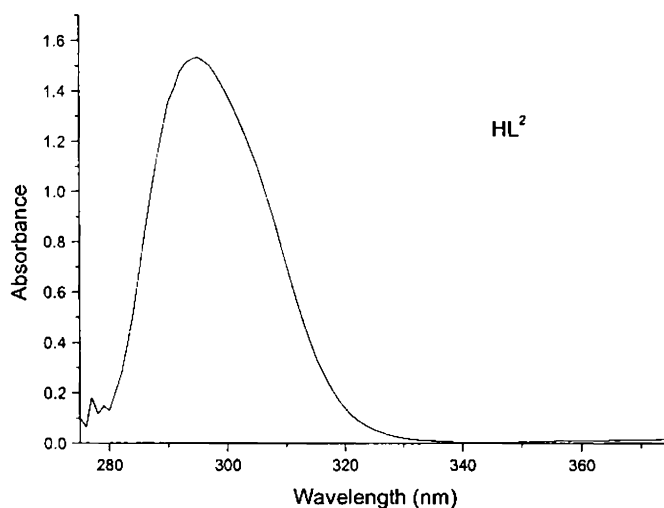


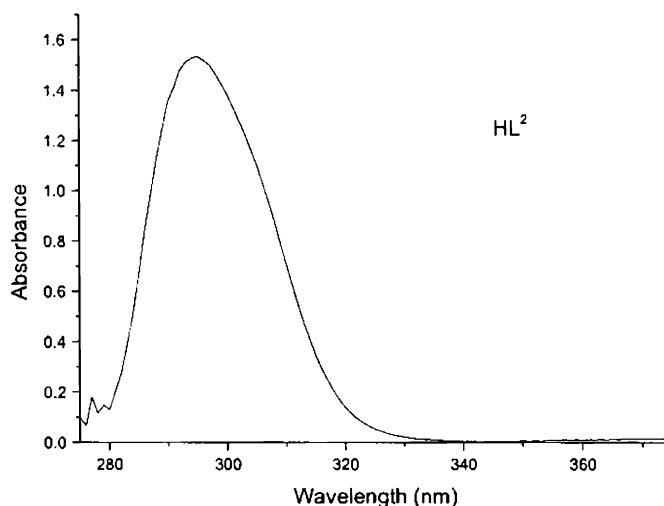
Fig. 2.3. Electronic spectrum of HL<sup>1</sup>

Fig. 2.4. Electronic spectrum of  $HL^2$ .Table 2.3. Electronic spectral assignments for the ligands (in  $cm^{-1}$ )

Ligands	$\pi \rightarrow \pi^*$	$n \rightarrow \pi^*$
$HL^1$	37590	32890
$HL^2$	37010	33900

#### 2.4.4. $^1H$ NMR spectrum of $HL^1$

Proton Magnetic Resonance spectroscopy is a helpful tool for the preparation of organic compounds in conjunction with other spectrometric information. The  $^1H$  NMR spectrum is used in identifying hydrogen atoms of the ligands and the assignments are based on the structures shown in Figs. 2.5 and 2.7. The  $^1H$  resonances are assigned on the basis of the chemical shift values and multiplicities. These give insight into the average effective magnetic fields present, interaction of the nuclear spin

Fig. 2.4. Electronic spectrum of  $HL^2$ .Table 2.3. Electronic spectral assignments for the ligands (in  $cm^{-1}$ )

Ligands	$\pi \rightarrow \pi^*$	$n \rightarrow \pi^*$
$HL^1$	37590	32890
$HL^2$	37010	33900

#### 2.4.4. $^1H$ NMR spectrum of $HL^1$

Proton Magnetic Resonance spectroscopy is a helpful tool for the preparation of organic compounds in conjugation with other spectrometric information. The  $^1H$  NMR spectrum is used in identifying hydrogen atoms of the ligands and the assignments are based on the structures shown in Figs. 2.5 and 2.7. The  $^1H$  resonances are assigned on the basis of the chemical shift values and multiplicities. These give insight into the average effective magnetic fields present, interaction of the nuclear spin

with the adjacent atoms and the number of equivalent protons. The  $^1\text{H}$  NMR spectra of the ligands are recorded in DMSO solution with TMS as internal standard.

The NMR spectrum of  $\text{HL}^1$  in  $\text{DMSO-d}_6$  shows two singlets at  $\delta = 11.7$  ppm and  $\delta = 9.20$  ppm which correspond to  $^2\text{N-H}$  and  $^4\text{N-H}$  respectively. These protons are shifted downfield because they are attached to hetero atoms which are easily subjected to hydrogen bonding and are decoupled by the electrical quadrupole effects. The downfield value of  $^4\text{N-H}$  proton is due to the deshielding effect of the phenyl group. The signal for  $^2\text{N-H}$  is more downfield because of hydrogen bonding to the oxygen of DMSO [19,20]. The downfield shifts of these protons are also assigned to their hydrogen bonding interactions with adjacent nitrogen atom of the pyridine ring. Hydrogen bonding decreases the electron density around the proton and thus moves the proton absorption to a lower field [12]. The aromatic protons of the two phenyl groups are assigned to the multiplet which appears at  $\delta$  values in the range 7-8.5 ppm [17].

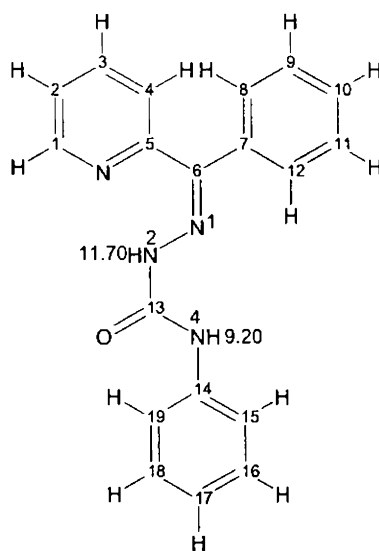


Fig. 2.5.  $^1\text{H}$  NMR Spectral assignments of  $\text{HL}^1$ .



$^1\text{H}$  NMR spectrum of HL<sup>1</sup> is presented in Fig. 2.6.

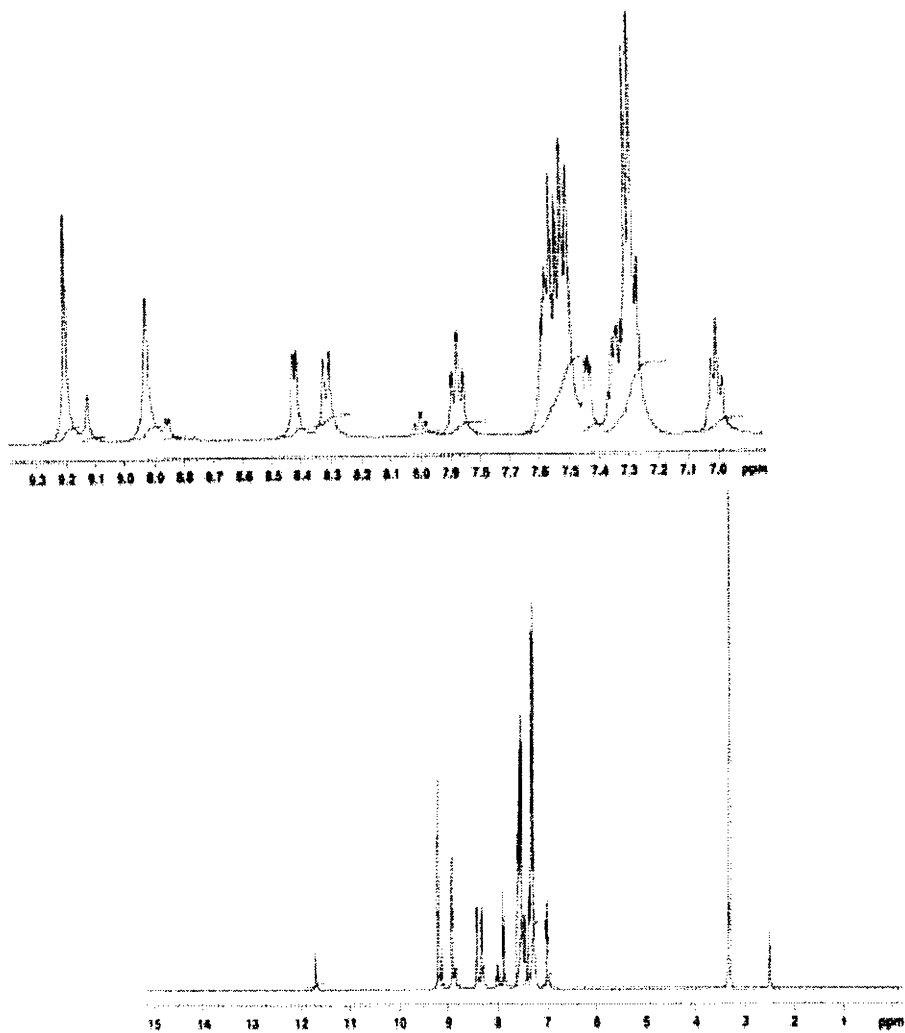


Fig. 2.6.  $^1\text{H}$  NMR spectrum of HL<sup>1</sup>.

### 2.4.5. $^1\text{H}$ NMR spectrum of $\text{HL}^2$

In the NMR spectrum of  $\text{HL}^2$ , the signal for  $^2\text{N-H}$  is observed at  $\delta = 9.94$  ppm which is due to the hydrogen bonding to the oxygen of DMSO [19,20]. The lower frequency effect of the acetyl semicarbazones is probably due to the gamma gauche effect of the methyl group. This is in accordance with the reported values for the 3- and 4-acetylpyridine semicarbazones [18]. The  $^4\text{N-H}$  is observed as a singlet at  $\delta = 8.96$  ppm. The low frequency singlet at  $\delta = 2.34$  ppm was attributed to the protons of the methyl group which are chemically and magnetically equivalent.

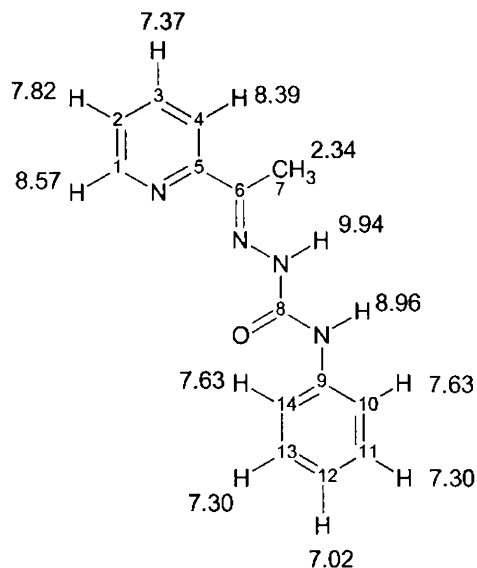


Fig. 2.7.  $^1\text{H}$  NMR Spectral assignments of  $\text{HL}^2$ .

The  $^1\text{H}$  NMR spectrum of  $\text{HL}^2$  in  $\text{DMSO-}d_6$  shows signals at  $\delta = 8.57$  (d, 1H), 7.82 (t, 1H), 7.37 (t, 1H), 8.39 (d, 1H), 2.34 (s, 3H), 9.94 (s, 1H), 8.96 (s, 1H), 7.63 (d, 2H), 7.30 (t, 2H), 7.02 (t, 1H).

$^1\text{H}$  NMR spectrum of  $\text{HL}^2$  is presented in Fig. 2.8.

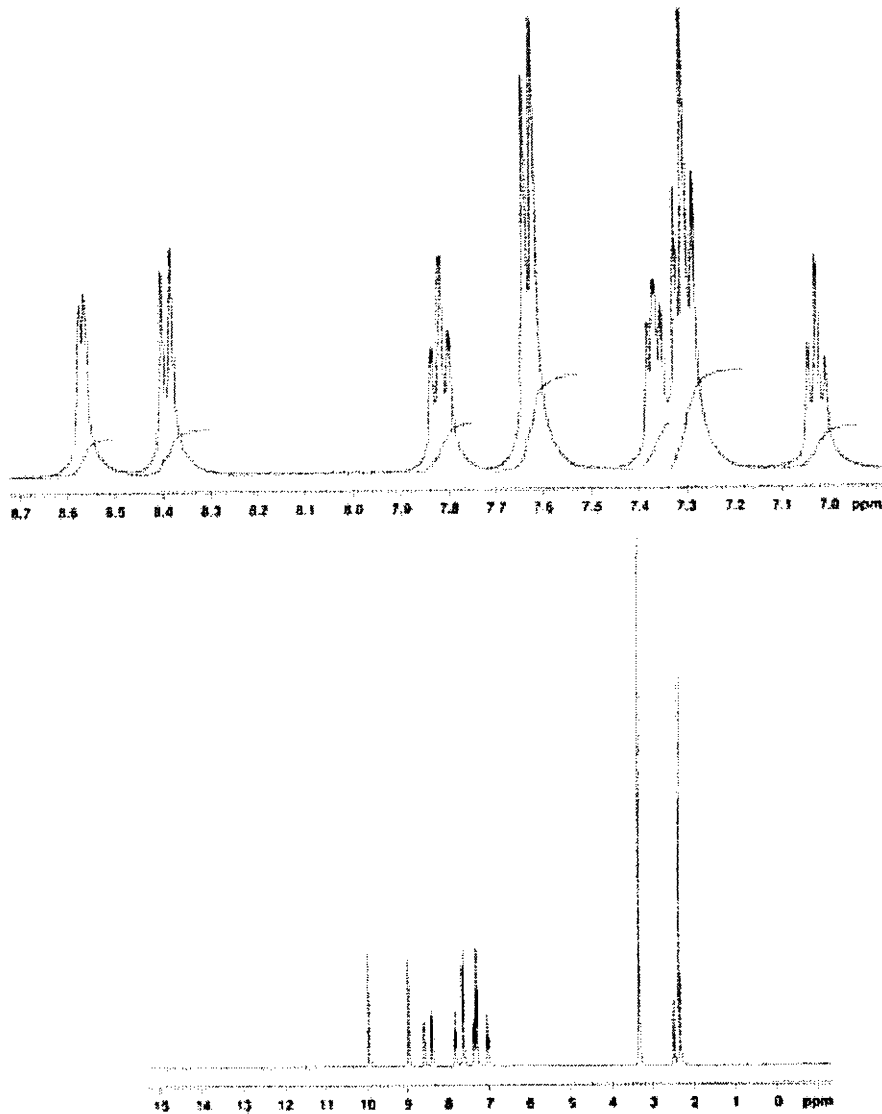


Fig. 2.8.  $^1\text{H}$  NMR spectrum of  $\text{HL}^2$ .

The proton near to the ring nitrogen viz. H(1) is observed as doublet at 8.57 ppm due to coupling with H(2) which is observed at 7.82 ppm. A triplet at 7.82 ppm corresponding to H(2) occurs due to coupling with H(1) and H(3). A doublet at 8.39 ppm corresponding to H(4) occurs due to coupling with H(3). The downfield shift occurs as this proton is near to the more electronegative nitrogen atom. The H(12) proton produces a triplet at 7.02 ppm by coupling with neighboring H(11) and H(13) protons. The aromatic protons of the phenyl group appear at  $\delta$  values in the range 7.02 - 7.63 ppm.

**References**

1. D.X. West, A.E. Liberta, S.B. Padhye, R.C. Chikate, P.B. Sonawane, A.S. Kumbhar, R.G. Yerande, *Coord. Chem. Rev.* 123 (1993) 49.
2. S.B. Padhye, G.B. Kauffman, *Coord. Chem. Rev.* 63 (1985) 127.
3. V.M. Leovac, L.S. Vojinovic, K.M. Szecsenyi, V.I. Cesljevic, J. *Serb. Chem. Soc.* 68 (2003) 919.
4. V.M. Leovac, A.F. Petrovic, *Trans. Met. Chem.* 8 (1983) 337.
5. A.F. Petrovic, M.L. Vukadin, B. Riber, *Trans. Met. Chem.* 11 (1986) 207.
6. A. Sreekanth, U.L. Kala, C.R. Nayar, M.R.P. Kurup, *Polyhedron* 23 (2004) 41.
7. T.A. Reena, E.B. Seena, M.R.P. Kurup, *Polyhedron* 27 (2008) 1825.
8. W-Y. Liu, Y-Z. Li, *Acta Ctystallogr.* E60 (2004) 694.
9. H.M. Ali, S. Puvaneswary, W.F. Basirun, S.W. Ng, *Acta Ctystallogr.* E61 (2005) 1013.
10. A.K. El-Sawaf, D.X. West, F.A. El-Saied, R.M. El-Bahnasawy, *Trans. Met. Chem.* 23 (1998) 649.
11. D.X. West, A.M. Stark, G.A. Bain, A.E. Liberta, *Trans. Met. Chem.* 21 (1996) 289.
12. R.M. Silverstein, G.C. Bassler, T.C. Morrill, *Spectrometric Identification of Organic Compounds*, 4<sup>th</sup> ed. Wiley, New York, 1981.
13. S.K. Jain, B.S. Garg, Y.K. Bhoon, D.L. Klayman, J.P. Scovill, *Spectrochim. Acta* 41A (1985) 407.
14. W. Kemp, *Organic Spectroscopy*, 3<sup>rd</sup> ed. Macmillan, Hamsphire, 1996.

15. R.P. John, A. Sreekanth, M.R.P. Kurup, A. Usman, A.R. Ibrahim, H.-K. Fun, *Spectrochim. Acta* 59A (2003) 1349.
16. D.X. West, I.S. Billeh, J.P. Jasinski, J.M. Jasinski, R.J. Butcher, *Trans. Met. Chem.* 23 (1998) 209.
17. P. Bindu, M.R.P. Kurup, *Indian J. Chem.* 36A (1997) 1094.
18. H. Beraldo, A.M. Barreto, R.P. Vieira, A.P. Rebolledo, N.L. Speziali, C.B. Pinheiro, G. Chapuis, *J. Mol. Struct.* 645 (2003) 213.
19. I.C. Mendes, L.R. Teixeira, R. Lima, H. Beraldo, N.L. Speziali, D.X. West, *J. Mol. Struct.* 559 (2001) 355.
20. W.F. Nacif, H. Beraldo, D.X. West, *Spectrochim. Acta* 57A (2001) 1847.

**SYNTHESES, STRUCTURAL AND SPECTRAL  
CHARACTERIZATION OF COPPER(II) COMPLEXES  
OF 2-BENZOYLPYRIDINE-N(4)-  
PHENYLSEMICARBAZONE**

**3.1. Introduction**

Copper is widely distributed in nature as metal, in sulphides, arsenides, chlorides, carbonates and so on [1]. Copper is one of the transition elements frequently found at the active site of proteins. The copper containing enzymes and proteins constitute an important class of biologically active compounds [2]. The biological functions of copper proteins/enzymes include electron transfer, dioxygen transport, oxygenation, oxidation, reduction, and disproportionation [3,4]. The common oxidation states of copper are I ( $d^{10}$ ), II ( $d^9$ ), and III ( $d^8$ ). Cu(I) forms mononuclear and polynuclear complexes having linear, planar, tetrahedral and distorted planar geometries. The most common oxidation state of Cu is +2, and Cu(II) complexes have been extensively studied. These complexes have trigonal planar, tetrahedral, octahedral, distorted octahedral, square planar and pentagonal bipyramidal geometries [1]. Thiosemicarbazones and semicarbazones are molecules of great interest due to their potential pharmacological properties and a wide variation in their modes of bonding and stereochemistry. Semicarbazones are also reported to possess versatile structural features [5] and very good antifungal and antibacterial properties [6,7]. A variety of semicarbazones and their metal complexes possess anti-protozoa and anti-convulsant activity also

[8]. Copper(II) complexes are interesting due to their biological applications and interesting stereochemistries. There has been considerable amount of interest in the studies of semicarbazones recently due to their unusual coordination modes when bound to metals, high pharmacological potentiality and good chelating property. Recently, copper(II) complexes of 2-hydroxyacetophenone-*N*(4)-phenylsemicarbazone have been reported from our laboratory [9].

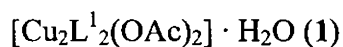
This chapter deals with the syntheses and spectral studies of nine Cu(II) complexes of 2-benzoylpyridine-*N*(4)-phenylsemicarbazone (HL<sup>1</sup>) along with the crystal structure of the compound, [Cu<sub>2</sub> L<sup>1</sup><sub>2</sub>(OAc)<sub>2</sub>] (**1a**).

## 3.2. Experimental

### 3.2.1. Materials

Details regarding the synthesis of HL<sup>1</sup> are described in Chapter 2. 4-Phenylsemicarbazide (Fluka), 2-benzoylpyridine (Aldrich), potassium thiocyanate (CDH), sodium azide (CDH), copper acetate, copper chloride, copper nitrate, copper bromide, copper perchlorate and copper sulfate (BDH) were used without further purification. All solvents obtained commercially were distilled before use.

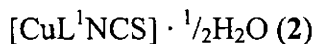
### 3.2.2. Syntheses of complexes



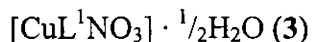
The complex [Cu<sub>2</sub>L<sup>1</sup><sub>2</sub>(OAc)<sub>2</sub>] · H<sub>2</sub>O was prepared by refluxing a hot solution of HL<sup>1</sup> (0.633 g, 2 mmol) in methanol (20 cm<sup>3</sup>) with a hot filtered



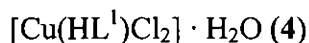
methanolic solution of  $\text{Cu}(\text{OAc})_2 \cdot \text{H}_2\text{O}$  (0.398 g, 2 mmol) for 4 hours. On cooling, the green solid separated was filtered, washed with hot water, hot methanol and ether and dried *in vacuo* over  $\text{P}_4\text{O}_{10}$ .



The complex  $[\text{CuL}^1\text{NCS}] \cdot \frac{1}{2}\text{H}_2\text{O}$  was synthesized by the following method. A hot solution of  $\text{HL}^1$  (0.633 g, 2 mmol) in methanol (20 cm<sup>3</sup>) was mixed with a hot filtered methanolic solution of potassium thiocyanate (0.194 g, 2 mmol). To this a hot filtered solution of  $\text{Cu}(\text{OAc})_2 \cdot \text{H}_2\text{O}$  (0.398 g, 2 mmol) was added with constant stirring. The mixture was then refluxed for 3 hours. The green complex separated as microcrystals was filtered and thoroughly washed with water, methanol and ether and finally dried over  $\text{P}_4\text{O}_{10}$  *in vacuo*.



The complex  $[\text{CuL}^1\text{NO}_3] \cdot \frac{1}{2}\text{H}_2\text{O}$  was prepared by refluxing a hot solution of  $\text{HL}^1$  (0.633 g, 2 mmol) in methanol (20 cm<sup>3</sup>) with a hot filtered methanolic solution of  $\text{CuNO}_3 \cdot 3\text{H}_2\text{O}$  (0.483 g, 2 mmol) for 3 hours. The green colored solid separated on cooling, was filtered, and washed with hot water, hot methanol and ether. The compound was dried over  $\text{P}_4\text{O}_{10}$  *in vacuo*.

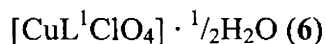


The complex  $[\text{Cu}(\text{HL}^1)\text{Cl}_2] \cdot \text{H}_2\text{O}$  was prepared by stirring a hot solution of  $\text{HL}^1$  (0.633 g, 2 mmol) in methanol (20 cm<sup>3</sup>) with a hot filtered methanolic solution of  $\text{CuCl}_2 \cdot 2\text{H}_2\text{O}$  (0.340 g, 2 mmol) for 3 hours. The

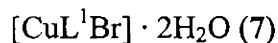
green solid separated on keeping overnight was filtered and washed with hot water, hot ethanol and ether and dried over  $P_4O_{10}$  *in vacuo*.



The complex  $[Cu_2(HL^1)_2(SO_4)_2] \cdot 4H_2O$  was prepared by refluxing a hot solution of  $HL^1$  (0.633 g, 2 mmol) in methanol (20 cm<sup>3</sup>) with a hot filtered methanolic solution of  $CuSO_4 \cdot 5H_2O$  (0.499 g, 2 mmol) for 5 hours. The pale green colored crystals, separated on keeping for a few days, were filtered and washed with hot ethanol, hot water and ether and then dried over  $P_4O_{10}$  *in vacuo*.



The complex  $[CuL^1ClO_4] \cdot \frac{1}{2}H_2O$  was prepared by stirring a hot solution of  $HL^1$  (0.633 g, 2 mmol) in methanol (20 cm<sup>3</sup>) with a hot filtered methanolic solution of copper perchlorate (0.371 g, 2 mmol) for 3 hours. The green solid separated was filtered, washed with hot water, hot ethanol, and ether and dried over  $P_4O_{10}$  *in vacuo*.



The complex  $[CuL^1Br] \cdot 2H_2O$  was synthesized by refluxing a hot solution of  $HL^1$  (0.633 g, 2 mmol) in methanol (20 cm<sup>3</sup>) with a hot filtered methanolic solution of copper bromide (0.446 g, 2 mmol) for 3 hours. The dark green colored shining compound separated on keeping the solution overnight, was collected by filtration and washed with hot water, hot methanol, and ether and dried over  $P_4O_{10}$  *in vacuo*.

$[\text{CuL}^1_2] \cdot \text{H}_2\text{O}$  (8)

The complex  $[\text{CuL}^1_2] \cdot \text{H}_2\text{O}$  was obtained when a hot solution of  $\text{HL}^1$  (0.633 g, 2 mmol) in methanol (20 cm<sup>3</sup>) was mixed a hot filtered methanolic solution of  $\text{Cu}(\text{OAc})_2 \cdot \text{H}_2\text{O}$  (0.199 g, 1 mmol) with constant stirring. The mixture was then refluxed for 3 hours. The complex separated as microcrystals was filtered and thoroughly washed with water, methanol and ether and finally dried over  $\text{P}_4\text{O}_{10}$  *in vacuo*.

$[\text{CuL}^1\text{N}_3] \cdot \text{CH}_3\text{OH}$  (9)

The complex  $[\text{CuL}^1\text{N}_3] \cdot \text{CH}_3\text{OH}$  was synthesized by the following method. A hot solution of  $\text{HL}^1$  (0.633 g, 2 mmol) in methanol (20 cm<sup>3</sup>) was mixed with a hot filtered methanolic solution of sodium azide (0.130 g, 2 mmol). To this a hot filtered solution of  $\text{Cu}(\text{OAc})_2 \cdot \text{H}_2\text{O}$  (0.398 g, 2 mmol) was added with constant stirring. The mixture was then refluxed for 3 hours. The green colored complex separated as microcrystals was filtered and thoroughly washed with water, methanol and ether and finally dried over  $\text{P}_4\text{O}_{10}$  *in vacuo*.

### 3.2.3. Analytical methods

Elemental analyses were carried out using a Vario EL III CHNS analyzer at SAIF, Kochi, India. IR spectra were recorded on a Thermo Nicolet AVATAR 370 DTGS model FT-IR Spectrophotometer with KBr pellets and ATR technique at SAIF, Kochi, India. Electronic spectra were recorded on a Cary 5000, version 1.09 UV-Vis-NIR spectrophotometer using solutions in acetonitrile. Magnetic moment measurements are carried

out in the polycrystalline state at room temperature on a PAR model 155 Vibrating Sample Magnetometer at 5 kOe field strength at the Indian Institute of Technology, Roorkee, India. EPR spectra were recorded on a Varian E-112 X-band EPR spectrometer using TCNE as a standard at SAIF, IIT, Bombay, India.

#### 3.2.4. X-Ray crystallography

Single crystals of compound  $[\text{Cu}_2\text{L}^1_2(\text{OAc})_2]$  (**1a**) suitable for X-ray diffraction studies were grown from its solution in a mixture of dimethyl formamide and methanol (1:1). A green plate like single crystal of dimension  $0.20 \times 0.14 \times 0.06 \text{ mm}^3$  was selected and mounted on a Bruker SMART APEX diffractometer, equipped with a graphite crystal, incident-beam monochromator, and a fine focus sealed tube,  $\text{MoK}\alpha$  ( $\lambda = 0.71073 \text{ \AA}$ ) X-ray source. The crystallographic data along with details of structure solution refinements are given in Table 3.1.

The unit cell dimensions were measured and the data collection was performed at 273 K. Bruker SMART software was used for data acquisition and Bruker SAINT Software for data integration [10]. Absorption corrections were carried out using SADABS based on Laue symmetry using equivalent reflections [11]. The structure was solved by direct methods and refined by full-matrix least-squares calculations with the *SHELXL -PLUS* software package (version 5.1) [12]. The graphics used was diamond version 3.1f [13]. All non-hydrogen atoms were refined anisotropically, and all hydrogen atoms were located from the difference Fourier map and refined isotropically.

Table 3.1. Crystal refinement parameters of  $[\text{Cu}_2\text{L}^1_2(\text{OAc})_2]$  (**1a**)

Empirical formula	$\text{C}_{42}\text{H}_{38}\text{Cu}_2\text{N}_{10}\text{O}_6$
Formula weight	875.86
Color	Green
Temperature (T) K	273(2) K
Wavelength (MoK $\alpha$ ) (Å)	0.71073
Crystal system	monoclinic
Space group	$P2_1/n$
Lattice constants	
a (Å)	8.6851(7)
b (Å)	16.5515(14)
c (Å)	13.6252(12)
$\alpha$ (°)	90
$\beta$ (°)	91.680(2)
$\gamma$ (°)	90
Volume V (Å <sup>3</sup> )	1957.8(3)
Z	4
Calculated density ( $\rho$ ) (Mg m <sup>-3</sup> )	1.496
Absorption coefficient, $\mu$ (mm <sup>-1</sup> )	1.151
F(000)	900
Crystal size (mm <sup>3</sup> )	0.20 x 0.14 x 0.06
$\theta$ range for data collection	1.94 to 28.28
Limiting indices	$-9 \leq h \leq 11, -21 \leq k \leq 21, -17 \leq l \leq 15$
Reflections collected	7862
Unique Reflections ( $R_{\text{int}}$ )	3556 [ $R_{\text{int}} = 0.087$ ]
Completeness to $2\theta$	28.28 70.8 %
Absorption correction	SADABS
Refinement method	Full-matrix least-squares on $F^2$
Data / restraints / parameters	3556/ 0 / 266
Goodness-of-fit on $F^2$	0.859
Final R indices [ $I > 2\sigma(I)$ ]	$R1 = 0.0741, wR2 = 0.1575$
R indices (all data)	$R1 = 0.1128, wR2 = 0.1695$
Largest difference peak and hole	0.826 and -0.421 e Å <sup>-3</sup>

### 3.3. Results and discussion

#### 3.3.1. Analytical measurements

The principal ligand  $HL^1$  was synthesized by the direct condensation of 2-benzoylpyridine with *N*(4)-phenylsemicarbazide. Ligand can exist in keto or enol form or an equilibrium mixture of the two since it has an amide  $-NH-C(=O)$  function. However, the IR spectrum of  $HL^1$  indicates that in solid state it remains in keto form. The IR spectra of complexes however, do not show any intense absorption band at  $1696\text{ cm}^{-1}$  except  $[Cu_2(HL^1)_2(SO_4)_2] \cdot 4H_2O$  and  $Cu(HL^1)Cl_2 \cdot H_2O$ , due to the carbonyl stretching of the semicarbazone moiety. This shows that in solution, it tautomerises to the enol form and coordinates to the metal in the enolate form.

The complex  $[CuL^1NCS] \cdot \frac{1}{2}H_2O$  was formed by the reaction of the ligand and potassium thiocyanate with copper acetate. The azido complex  $[CuL^1N_3] \cdot CH_3OH$  was isolated by the reaction of semicarbazone and sodium azide with copper acetate. The complexes  $[Cu_2L^1_2(OAc)_2] \cdot H_2O$ ,  $[CuL^1NO_3] \cdot \frac{1}{2}H_2O$ ,  $[Cu(HL^1)Cl_2] \cdot H_2O$ ,  $[Cu_2(HL^1)_2(SO_4)_2] \cdot 4H_2O$ ,  $[CuL^1ClO_4] \cdot \frac{1}{2}H_2O$  and  $[CuL^1Br] \cdot 2H_2O$  were formed by the reaction of the ligand with corresponding copper salts. The complex  $CuL^1_2 \cdot H_2O$  was obtained when a hot solution of  $HL^1$  was reacted with a hot filtered methanolic solution of  $Cu(OAc)_2 \cdot H_2O$ . The principal ligand  $HL^1$  undergoes deprotonation to  $L^-$  and chelates in enolate form as evidenced by the IR spectra. However, for complexes **4** and **5**, the semicarbazone remains in the neutral form.

The colors, elemental analyses, stoichiometries of HL<sup>1</sup> and its complexes are presented in Table 3.2. The complexes are soluble in methanol, ethanol, DMF, acetonitrile and DMSO. The conductivity measurements were made in DMF solutions and the values are found to be less than 20  $\Omega^{-1}\text{mol}^{-1}\text{cm}^{-1}$  and all complexes are found to be non-electrolytes [14], which indicates that the anion and the ligand are coordinated to the central copper(II).

The room temperature magnetic susceptibilities of the complexes in the polycrystalline state except complexes **1** and **5** fall in the range of 1.70-2.00 B.M., which are very close to the spin-only value of 1.73 B.M. for a typical  $S=1/2$   $d^9$  copper(II) system. The low value of complexes **1** and **5** is an evidence for their behavior as dimers.

### 3.3.2. Crystal structure of $[\text{Cu}_2\text{L}^1_2(\text{OAc})_2]$ (**1a**)

The single crystal X-ray diffraction study of the compound  $[\text{Cu}_2\text{L}^1_2(\text{OAc})_2]$  (**1a**) shows that the compound exists as oxygen bridged dimer. The molecular structure of the compound along with atom numbering scheme is given in Fig. 3.1. The asymmetric unit is formed by one half of the molecule and the other half is related by a centre of inversion in the Cu(1)-O(2)-Cu(1A)-O(2A) ring strongly bridged *via* oxygen atoms from acetate groups.

Table 3.2. Colors, elemental analyses and magnetic susceptibilities of 2-benzoylpyridine-N(4)-phenylsemicarbazone and its copper(II) complexes.

Compound	Color	Observed (Calculated) %			$\mu$ (B.M.)
		C	H	N	
HL <sup>1</sup>	Pale yellow	72.47 (72.13)	5.20 (5.10)	18.14(17.7)	-
[Cu <sub>2</sub> L <sub>2</sub> (OAc) <sub>2</sub> ] · H <sub>2</sub> O (1)	Green	56.20(56.43)	4.08(4.28)	12.67(12.54)	1.06
[CuL <sup>1</sup> NCS] · ½ H <sub>2</sub> O (2)	Green	53.72(54.97)	3.12(3.62)	15.31(15.70)	1.75
[CuL <sup>1</sup> NO <sub>3</sub> ] · ½ H <sub>2</sub> O (3)	Pale green	50.97(50.72)	3.64(3.58)	15.72(15.57)	1.87
[Cu(HL <sup>1</sup> )Cl <sub>2</sub> ] · H <sub>2</sub> O (4)	Dark green	49.25(48.68)	3.84(3.87)	11.94(11.95)	1.93
[Cu <sub>2</sub> (HL <sup>1</sup> ) <sub>2</sub> (SO <sub>4</sub> ) <sub>2</sub> ] · 4H <sub>2</sub> O (5)	Pale green	44.11(44.66)	4.42(3.75)	10.86(10.96)	1.15
[CuL <sup>1</sup> ClO <sub>4</sub> ] · ½ H <sub>2</sub> O (6)	Green	46.65(46.83)	2.96(3.31)	11.35(11.50)	1.71
[CuL <sup>1</sup> Br] · 2H <sub>2</sub> O (7)	Pale green	46.12(45.83)	3.38(3.87)	10.97(11.32)	1.76
[CuL <sup>1</sup> ] <sub>2</sub> · H <sub>2</sub> O (8)	Green	63.71(64.08)	4.02(4.53)	15.28(15.73)	1.89
[CuL <sup>1</sup> N <sub>3</sub> ] · CH <sub>3</sub> OH (9)	Dark green	52.71(53.03)	4.07(4.23)	21.85(21.65)	1.83



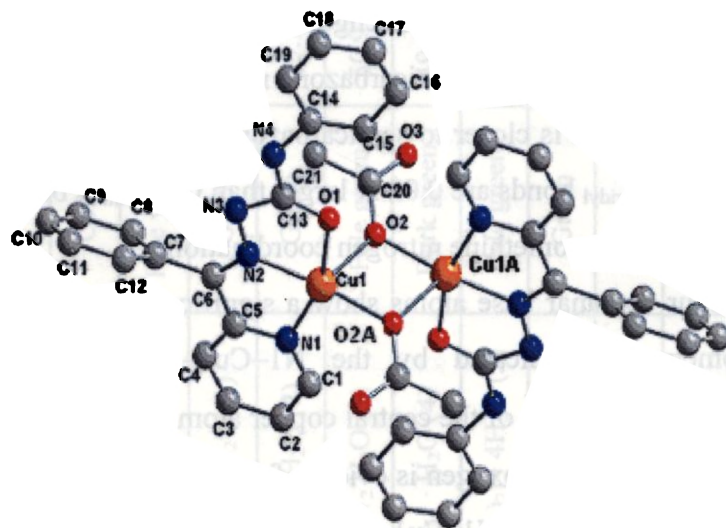
The lattice nature is monoclinic with space group  $P2_1/n$ . The structure contains two copper centers where each centre is pentacoordinated with azomethine nitrogen (N2), pyridyl nitrogen (N1) and enolate oxygen (O1) of semicarbazone moiety and oxygens (O2, O2A) from two acetate groups. The compound exhibits a distorted square pyramidal geometry with the basal plane occupied by semicarbazone ligand and the acetate oxygen (O2). Selected bond lengths (Å) and bond angles (°) of  $[\text{Cu}_2\text{L}^1_2(\text{OAc})_2]$  are shown in Table 3.3.

The oxygen (O2A) from acetate group of the adjacent monomer plugs into the axial position resulting in a dimer with a  $\text{Cu}\cdots\text{Cu}$  separation of approximately 3.422 Å. The comparison of bond distances  $\text{Cu}(1)\text{--O}(2)$  (1.945(3) Å),  $\text{Cu}(1)\text{--O}(2A)$  (2.344(4) Å),  $\text{Cu}(1A)\text{--O}(2)$  (2.346 Å) and  $\text{Cu}(1A)\text{--O}(2A)$  (1.944 Å) confirms the possibility of a bridging binuclear structure. The  $\text{Cu}\text{--N}$  and  $\text{Cu}\text{--O}$  bond lengths are smaller  $\sim 1.936$  and  $2.009$  Å indicating the domination of semicarbazone moiety in the bonding. It is found that copper atom is closer to semicarbazone moiety than the acetate group. The  $\text{Cu}\text{--N}_{\text{pyridyl}}$  bonds are  $0.09$  Å larger than  $\text{Cu}\text{--N}_{\text{imine}}$  bonds which shows the strength of azomethine nitrogen coordination.

The four coplanar base atoms show a significant distortion from a square geometry as indicated by the  $\text{N1}\text{--Cu1}\text{--O1}$  bond angle of  $159.91(17)^\circ$ . The deviation of the central copper atom from the basal plane in the direction of the axial oxygen is evident from the bond angles of  $\text{N}(2)\text{--Cu1}\text{--O}(2)$ ,  $171.06(17)$  and  $\text{N1}\text{--Cu1}\text{--O2}$ ,  $99.82(17)$ . Most of the angles involving the central copper atoms are widely different from  $90^\circ$  and  $180^\circ$ , indicating significant distortion from the square pyramidal geometry.

Table 3.3. Selected bond lengths (Å) and bond angles (°) of  $[\text{Cu}_2\text{L}^1_2(\text{OAc})_2]$  (**1a**)

Cu(1)–N(1)	2.024(4)
Cu(1)–N(2)	1.938(4)
Cu(1)–O(1)	2.010(4)
Cu(1)–O(2)	1.945(3)
Cu(1)–O(2A)	2.344(4)
C(13)–O(1)	1.261(7)
C(6)–N(2)	1.306(6)
C(13)–N(3)	1.363(6)
Cu(1)⋯Cu(1A)	3.422
N(1)–Cu(1)–N(2)	80.86(18)
N(2)–Cu(1)–O(1)	79.05(16)
N(1)–Cu(1)–O(1)	159.91(17)
N(1)–Cu(1)–O(2)	99.82(17)
N(1)–Cu(1)–O(2A)	92.03(16)
N(2)–Cu(1)–O(2)	171.06(17)

Fig. 3.1. The molecular structure of  $[\text{Cu}_2\text{L}^1_2(\text{OAc})_2]$  (**1a**) along with the atom numbering scheme. The hydrogen atoms are omitted for clarity.

The unit cell-packing diagram of the compound **1a** viewed along the a-axis is given in Fig. 3.2.

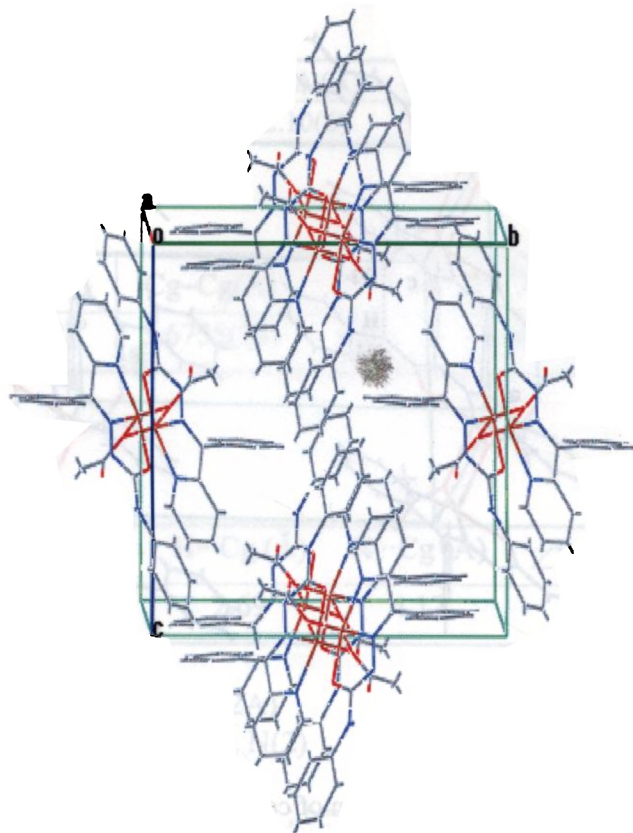


Fig. 3.2. Packing diagram of compound **1a**.

It can be observed that the molecules are packed in a 2-dimensional manner with the parallel arrangement of the rings. The adjacent units are interconnected through H-bonding interactions involving the oxygen atom of the acetate group and  $N(4)$  hydrogen of the phenyl group. Packing diagram of compound **1a** showing H-bonding is shown in Fig. 3.3.

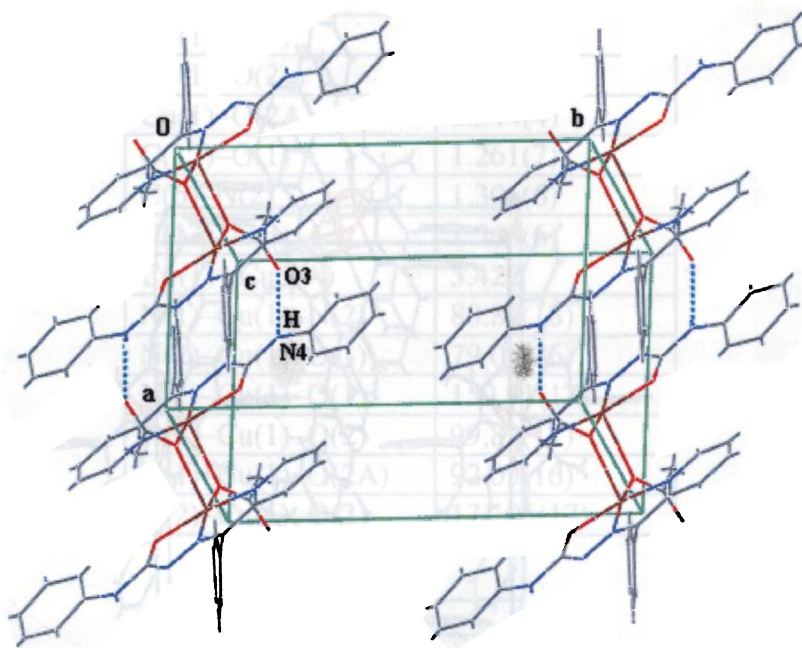


Fig. 3.3. Packing diagram of compound **1a** showing H bonding.

The H-bonding, C–H $\cdots$  $\pi$  and ring metal interactions are shown in Table 3.4. The H-bonding interaction is observed with a donor-acceptor distance of 2.852 Å. The aromatic  $\pi$ - $\pi$  stacking interactions between pyridine rings with Cg-Cg distance of 3.6755 Å (Sym. code: 2-x,-y, 1-z) reinforces crystal structure cohesion in molecular packing in the crystal lattice. The  $\pi$ - $\pi$ , C–H $\cdots$  $\pi$ , ring metal and H-bonding interactions stabilize the unit cell [15].

Table 3.4. Interaction parameters of compound 1a.

Hydrogen bonding interactions.

D-H...A	D-H (Å)	H...A (Å)	D...A (Å)	∠D-H...A(°)
N(4)-H(104) ...N(3A) <sup>a</sup>	0.76(6)	2.10(6)	2.852(7)	169(6)

[ $\pi$ ... $\pi$  Interactions]

Cg(I)-Res(I) ··· Cg(J)	Cg-Cg(Å)	$\alpha$ (°)	$\beta$ (°)	$\gamma$ (°)
Cg(2) - [1] ··· Cg(2) <sup>b</sup>	3.6755(25)	0.02	18.68	18.68

C-H... $\pi$  interactions

X-H(I) ...Cg(J)	H...Cg (Å)	X...Cg (Å)	∠X-H...Cg(°)
C(21)-H(21)B[1]...Cg(2) <sup>c</sup>	2.69	4.17	138

Cg (1) = Cu(1), O(2), Cu(1A), O(2A)

Cg (2) = Cu(1), O(1), C(13), N(3), N(2)

Equivalent position codes: a = 2-x, -y, 1-z ; b = 2-x, -y, 1-z ; c = 1-x,-y,1-z

D, donor; A, acceptor; Cg, centroid;  $\alpha$ , dihedral angles between planes I and J;  $\beta$ , angle Cg(I) and Cg(J).

The trigonality index  $\tau$  is calculated using the equation  $\tau = (\beta - \alpha)/60$  [15] (for perfect square pyramidal and trigonal bipyramidal geometries the values of  $\tau$  are zero and unity respectively). The value of  $\tau$  for the molecule is 0.185, which shows the distorted square pyramidal geometry.

### 3.3.3. IR spectra

The tentative assignments of the significant IR spectral bands of HL<sup>1</sup> and its copper(II) complexes useful for determining the ligand's mode of coordination are presented in Table 3.5. The  $\nu(\text{C}=\text{N})$  band of the semicarbazone at  $1600\text{ cm}^{-1}$  undergoes a negative shift of wavenumber in the complexes indicating coordination *via* azomethine nitrogen [16,17]. This is confirmed by the bands in the range  $410\text{-}440\text{ cm}^{-1}$ , which have been assigned to the  $\nu(\text{Cu}-\text{N})$  band [18-20]. A strong band found at  $1132\text{ cm}^{-1}$  is assigned to the  $\nu(\text{N}-\text{N})$  band of the semicarbazone.

The increase in  $\nu(\text{N}-\text{N})$  value in the spectra of complexes is due to the increase in double bond character, off-setting the loss of electron density *via* donation to the metal and is a confirmation of the coordination of the ligand through the azomethine nitrogen. The IR spectra of complexes are presented in Figs. 3.4-3.12.

The appearance of bands in the  $1510\text{-}1560\text{ cm}^{-1}$  range in complexes is due to the stretching vibration of the newly formed C=N bond as a result of enolization of the principal ligand except in complexes 4 and 5. The  $\nu(\text{N}-\text{H})$  band of semicarbazone disappears in complexes except in  $[\text{Cu}_2(\text{HL}^1)_2(\text{SO}_4)_2] \cdot 4\text{H}_2\text{O}$  and  $[\text{Cu}(\text{HL}^1)\text{Cl}_2] \cdot \text{H}_2\text{O}$  also indicating the enolization and deprotonation of HL<sup>1</sup> followed by coordination of the enolate to Cu. This is further supported by the appearance of a new peak in the range  $500\text{-}540\text{ cm}^{-1}$  indicating  $\nu(\text{Cu}-\text{O})$ . Based on the above spectral evidences, it is confirmed that the ligand HL<sup>1</sup> is tridentate, coordinating *via* the azomethine nitrogen, the pyridyl nitrogen and keto or enolate oxygen.

Table 3.5. Infrared spectroscopic assignments ( $\text{cm}^{-1}$ ) for the 2-benzoyl pyridine-*N*(4)-phenylsemicarbazone and its copper(II) complexes

Compound	$\nu(\text{NH})$	$\nu(\text{C}=\text{N})$	$\nu(\text{N}-\text{N})$	$\nu(\text{C}=\text{O})$	$\nu(\text{Cu}-\text{N})$	$\nu(\text{C}=\text{N})^a$	$\nu(\text{Cu}-\text{O})$
HL <sup>1</sup>	3375	1600	1132	1698	-	-	-
$[\text{Cu}_2\text{L}_2\text{OAc}_2] \cdot \frac{1}{2}\text{H}_2\text{O}$ (1)	-	1568	1145	-	416	1520	508
$[\text{CuL}^1\text{NCS}] \cdot \frac{1}{2}\text{H}_2\text{O}$ (2)	-	1595	1158	-	420	1554	510
$[\text{CuL}^1\text{NO}_3] \cdot \frac{1}{2}\text{H}_2\text{O}$ (3)	-	1593	1213	-	418	1546	529
$[\text{Cu}(\text{HL}^1)\text{Cl}_2] \cdot \text{H}_2\text{O}$ (4)	3068	1596	1213	1641	415	-	503
$[\text{Cu}_2(\text{HL}^1)_2(\text{SO}_4)_2] \cdot 4\text{H}_2\text{O}$ (5)	3199	1595	1213	1627	415	-	507
$[\text{CuL}^1\text{ClO}_4] \cdot \frac{1}{2}\text{H}_2\text{O}$ (6)	-	1592	1212	-	410	1538	534
$[\text{CuL}^1\text{Br}] \cdot 2\text{H}_2\text{O}$ (7)	-	1594	1211	-	436	1536	508
$[\text{CuL}^1_3] \cdot \text{H}_2\text{O}$ (8)	-	1569	1146	-	412	1516	510
$[\text{CuL}^1\text{N}_3] \cdot \text{CH}_3\text{OH}$ (9)	-	1564	1213	-	420	1517	506

<sup>a</sup> indicates newly formed C=N

In the thiocyanato complex, a very strong band at  $2112\text{ cm}^{-1}$ , a medium band at  $902\text{ cm}^{-1}$  and a strong band at  $453\text{ cm}^{-1}$  are assigned to  $\nu(\text{CN})$ ,  $\nu(\text{CS})$  and  $\delta(\text{NCS})$  modes of the NCS group, respectively. The intensity and position of these bands indicate the unidentate coordination of the thiocyanate group through the nitrogen [21,22]. In the nitrate complex, the three bands observed at  $1448$ ,  $1354$  and  $1130\text{ cm}^{-1}$  indicate the  $\nu_4$ ,  $\nu_1$  and  $\nu_2$  modes of the nitrate group. The fact that the nitrate group is terminally bonded is understood from the separation of  $94\text{ cm}^{-1}$  between the two highest frequency bands just mentioned above [18].

In the azido complex, the strong band observed at  $2054\text{ cm}^{-1}$  is assigned to the azido group indicative of azide coordination [22]. The perchlorate complex showed single broad bands at  $1121\text{ cm}^{-1}$  and  $1033\text{ cm}^{-1}$  and a strong band at  $623\text{ cm}^{-1}$  and a weak band at  $923\text{ cm}^{-1}$  indicating the presence of coordinated perchlorate [23]. The coordination is confirmed by a  $\nu(\text{Cu-O})$  band at  $534\text{ cm}^{-1}$ . The band at  $1121\text{ cm}^{-1}$  is assignable to  $\nu_3(\text{ClO}_4)$  and the band at  $623$  assignable to  $\nu_4(\text{ClO}_4)$  [24].

For the sulfato complex, strong bands at  $1142$  and  $1055\text{ cm}^{-1}$  are assignable to  $\nu_3$  of the monocoordinated sulfato group. Medium bands at  $976\text{ cm}^{-1}$  ( $\nu_1$ ) and  $650\text{ cm}^{-1}$  ( $\nu_4$ ) confirm the unidentate behaviour of sulfato group [21].

Thus it is seen that the principal ligand  $\text{HL}^1$  acts as a monoanionic tridentate ligand in complexes  $[\text{Cu}_2\text{L}^1_2(\text{OAc})_2] \cdot \text{H}_2\text{O}$ ,  $[\text{CuL}^1\text{NCS}] \cdot \frac{1}{2}\text{H}_2\text{O}$ ,  $[\text{CuL}^1\text{NO}_3] \cdot \frac{1}{2}\text{H}_2\text{O}$ ,  $[\text{CuL}^1\text{ClO}_4] \cdot \frac{1}{2}\text{H}_2\text{O}$ ,  $[\text{CuL}^1\text{Br}] \cdot 2\text{H}_2\text{O}$ ,  $[\text{CuL}^1_2] \cdot \text{H}_2\text{O}$  and  $[\text{CuL}^1\text{N}_3] \cdot \text{CH}_3\text{OH}$ .



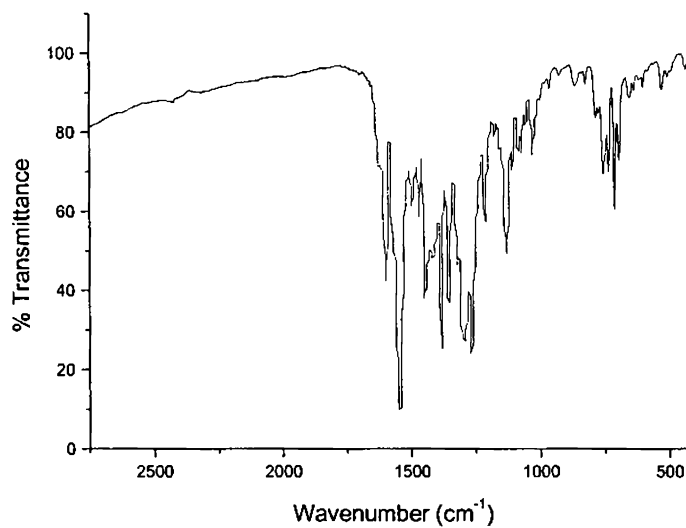


Fig. 3.4. IR spectrum of  $[\text{Cu}_2\text{L}_2(\text{OAc})_2] \cdot \text{H}_2\text{O}$  (1).

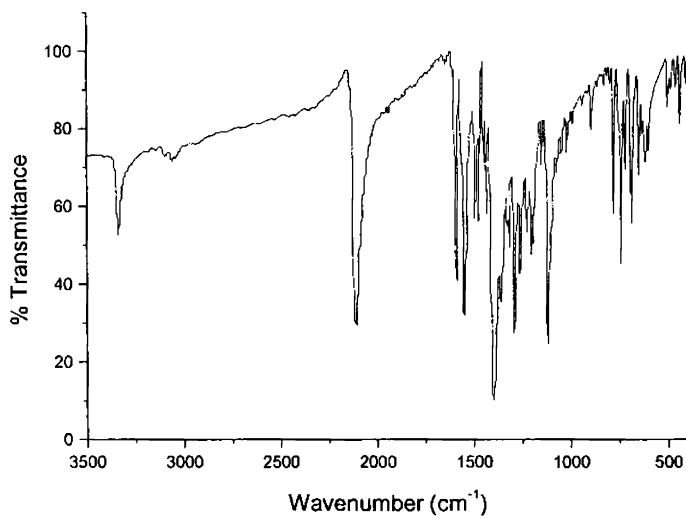


Fig. 3.5. IR spectrum of  $[\text{CuL}^1\text{NCS}] \cdot \frac{1}{2}\text{H}_2\text{O}$  (2).

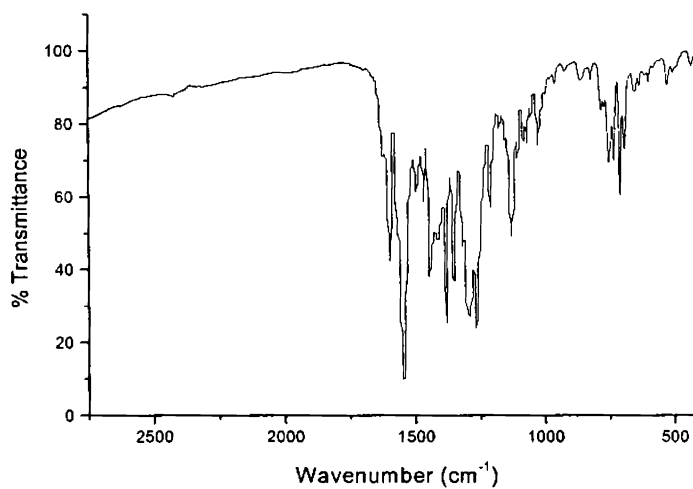


Fig. 3.6. IR spectrum of  $[\text{CuL}^1\text{NO}_3] \cdot \frac{1}{2}\text{H}_2\text{O}$  (3).

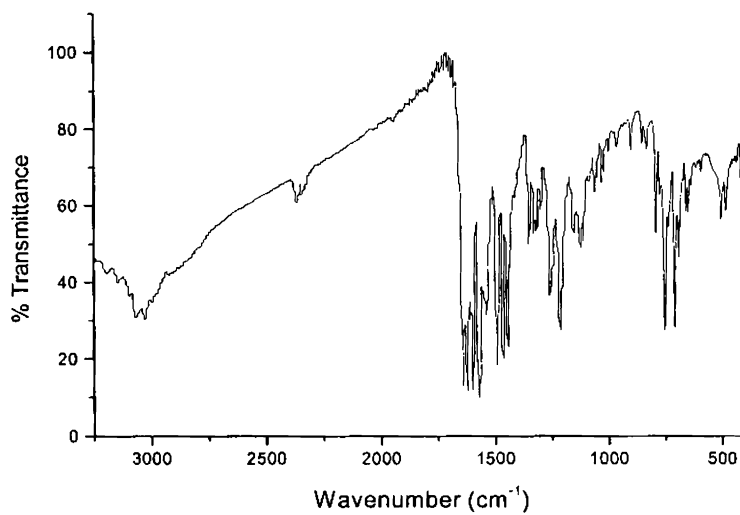


Fig. 3.7. IR spectrum of  $[\text{Cu}(\text{HL}^1)\text{Cl}_2] \cdot \text{H}_2\text{O}$  (4).

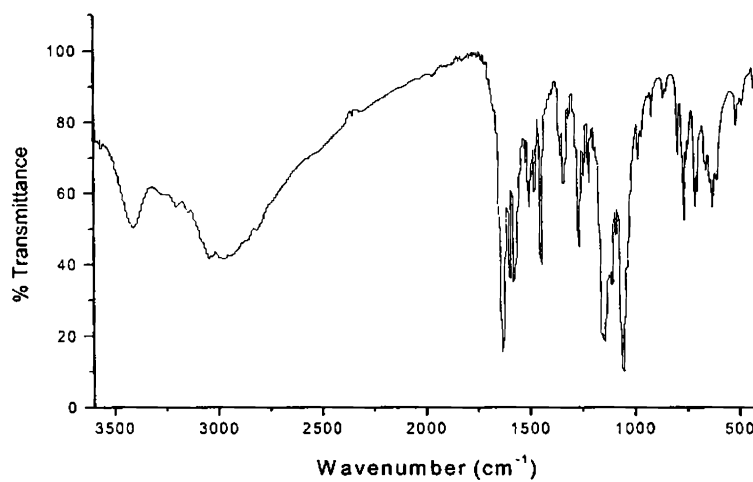


Fig. 3.8. IR spectrum of  $[\text{Cu}_2(\text{HL}^1)_2(\text{SO}_4)_2] \cdot 4\text{H}_2\text{O}$  (5).

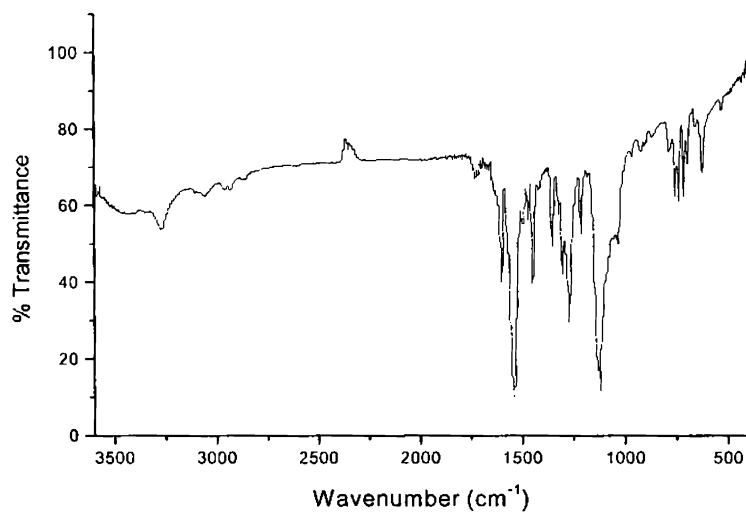
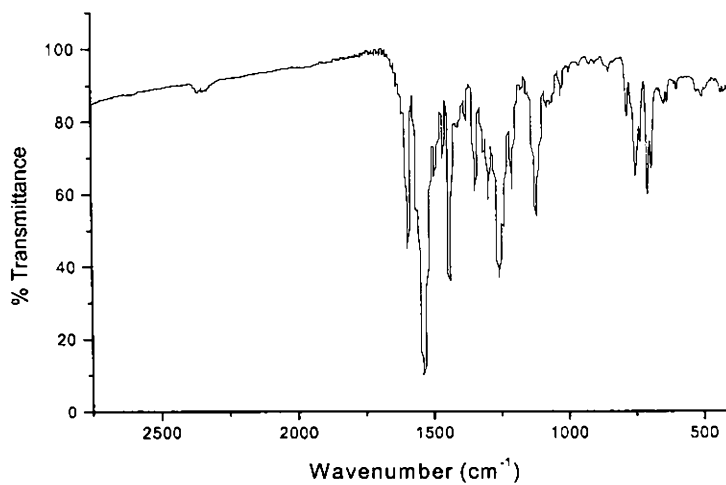
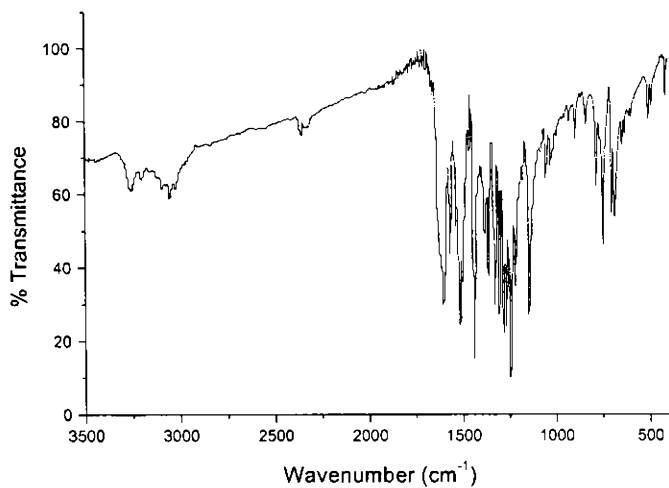


Fig. 3.9. IR spectrum of  $[\text{CuL}^1\text{ClO}_4] \cdot \frac{1}{2}\text{H}_2\text{O}$  (6).

Fig. 3.10. IR spectrum of  $[\text{CuL}^1\text{Br}] \cdot 2\text{H}_2\text{O}$  (7).Fig. 3.11. IR spectrum of  $[\text{CuL}^2] \cdot \text{H}_2\text{O}$  (8).

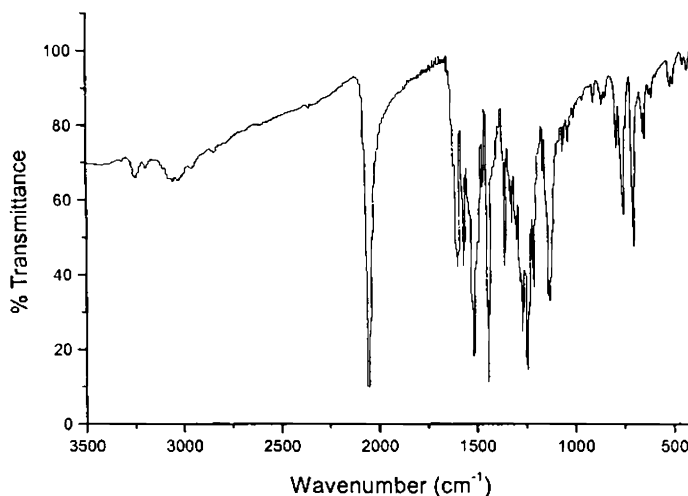


Fig. 3.12. IR spectrum of  $[\text{CuL}^1\text{N}_3] \cdot \text{CH}_3\text{OH}$  (9).

### 3.3.4. Electronic spectra

The variety of colors among transition metal complexes arises from the electronic transition between energy levels whose spacing corresponds to the wavelengths available in visible light. In complexes, these transitions are frequently referred to as *d-d* transitions because they involve the molecular orbitals that are mainly metal *d* in character [25]. Since this spacing depends on factors such as the geometry of the complex, the nature of the ligands present, and the oxidation state of the central metal atom, the electronic spectra of complexes can provide valuable information relating to bonding and structure [26].

Obviously, the colors produced are related to the magnitude of the spacing between the energy levels. Charge transfer transitions are transitions in which an electron is transferred from one atom or group in the

molecule to another atom or group. Such transitions are of high intensity and usually occur at the ultraviolet or the near ultraviolet i.e. at the high-energy end of the visible spectrum. Since a charge transfer transition originates from the redox character of the metal ion and the ligand, it is of two distinct types, namely ligand to metal and metal to ligand [27].

The band  $n \rightarrow \pi^*$  which is found at  $32890 \text{ cm}^{-1}$  in the spectrum of uncomplexed semicarbazone was slightly shifted on complexation. This is an indication of the enolization followed by the deprotonation of the ligand during complexation. The significant electronic absorption bands in the spectra of the ligand and all the complexes recorded in acetonitrile solution are presented in Table 3.6.

An absorption band observed at  $37410 \text{ cm}^{-1}$  in the spectrum of the ligand may be due to  $\pi \rightarrow \pi^*$  transition. The electronic spectra of Cu(II) complexes consists of bands in the region  $31000\text{-}33000 \text{ cm}^{-1}$  which are assigned to  $n \rightarrow \pi^*$  band of the pyridine ring. The semicarbazone and copper(II) complexes have two bands; one centered at  $37000 \text{ cm}^{-1}$  and another at  $32000 \text{ cm}^{-1}$ . These bands are assigned to  $\pi \rightarrow \pi^*$  and  $n \rightarrow \pi^*$  transitions of phenyl rings and semicarbazide moiety respectively [27,28]. The charge transfer bands were observed around  $23000$  to  $25000 \text{ cm}^{-1}$ , and its broadness can be explained as due to the combination of  $O \rightarrow Cu$  and  $N \rightarrow Cu$  LMCT transitions [29].

Compound	$d \rightarrow d$	LMCT	$n \rightarrow \pi^*$	$\pi \rightarrow \pi^*$
HL <sup>1</sup>	-	-	32890	37410
[Cu <sub>2</sub> L <sup>1</sup> (OAc) <sub>2</sub> ] · H <sub>2</sub> O (1)	14330	23970	31750	37590
[CuL <sup>1</sup> NCS] · 1/2 H <sub>2</sub> O (2)	14390	23870	31850	37590
[CuL <sup>1</sup> NO <sub>3</sub> ] · 1/2 H <sub>2</sub> O (3)	17210	23950	32000	37170
[Cu(HL <sup>1</sup> )Cl <sub>2</sub> ] · H <sub>2</sub> O (4)	17430	24700	31060	36630
[Cu <sub>2</sub> (HL <sup>1</sup> ) <sub>2</sub> (SO <sub>4</sub> ) <sub>2</sub> ] · 4H <sub>2</sub> O (5)	14440	24040	32000	37340
[CuL <sup>1</sup> ClO <sub>4</sub> ] · 1/2 H <sub>2</sub> O (6)	15580	23870	31750	37340
[CuL <sup>1</sup> Br] · 2H <sub>2</sub> O (7)	16130	23980	31970	34480
[Cu(L <sup>1</sup> ) <sub>2</sub> ] · H <sub>2</sub> O (8)	15690	23910	30860	35740
[CuL <sup>1</sup> N <sub>3</sub> ] · CH <sub>3</sub> OH (9)	16060	23920	31350	37590

For Cu(II) complexes, there are three spin allowed transitions,  $A_{1g} \leftarrow B_{1g}$ ,  $B_{2g} \leftarrow B_{1g}$  and  $E_g \leftarrow B_{1g}$ . But it is very difficult to resolve them into separate bands due to the very low energy difference between these bands. All the complexes gave *d-d* bands in the 14000-18000  $\text{cm}^{-1}$  range [30-32].

The electronic spectra of some of the copper(II) complexes of HL<sup>1</sup> are shown in Figs. 3.13.-3.18.

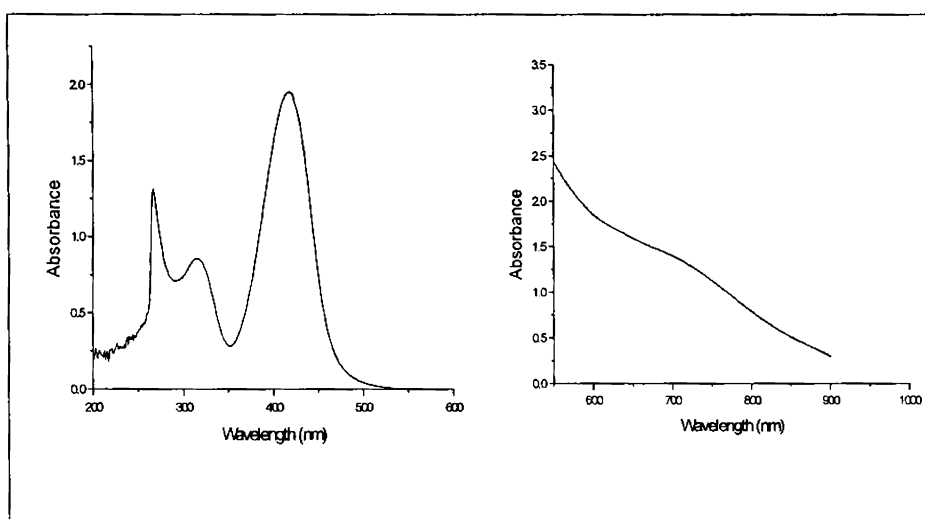


Fig. 3.13. Electronic spectra of compound 1.

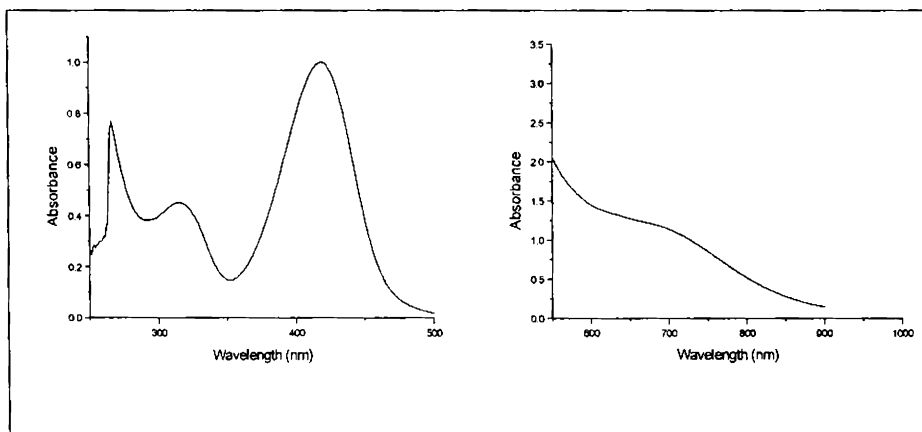


Fig. 3.14. Electronic spectra of compound 2.



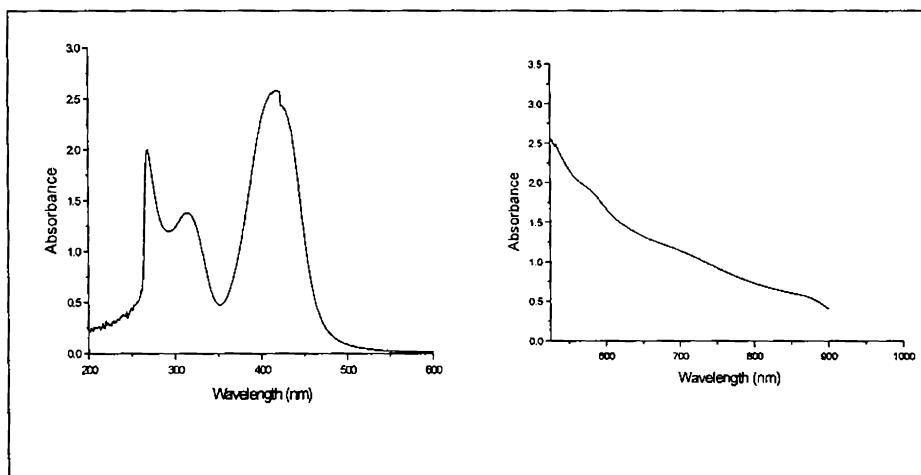


Fig. 3.15. Electronic spectra of compound 3.

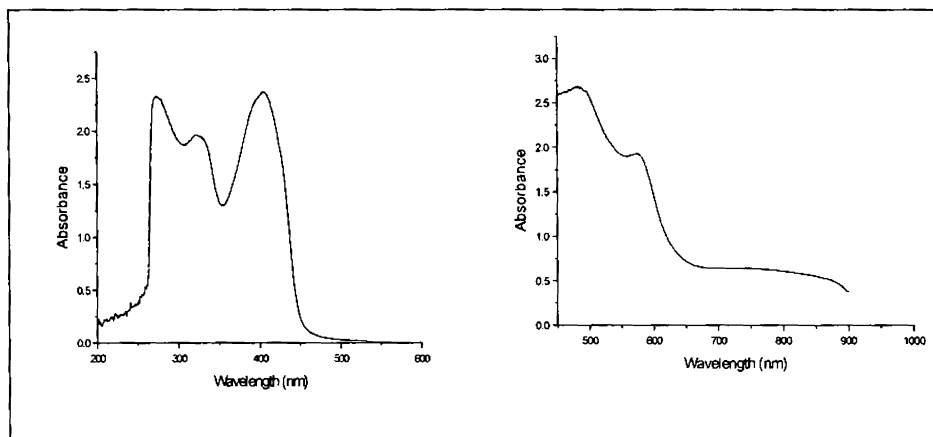


Fig. 3.16. Electronic spectra of compound 4.

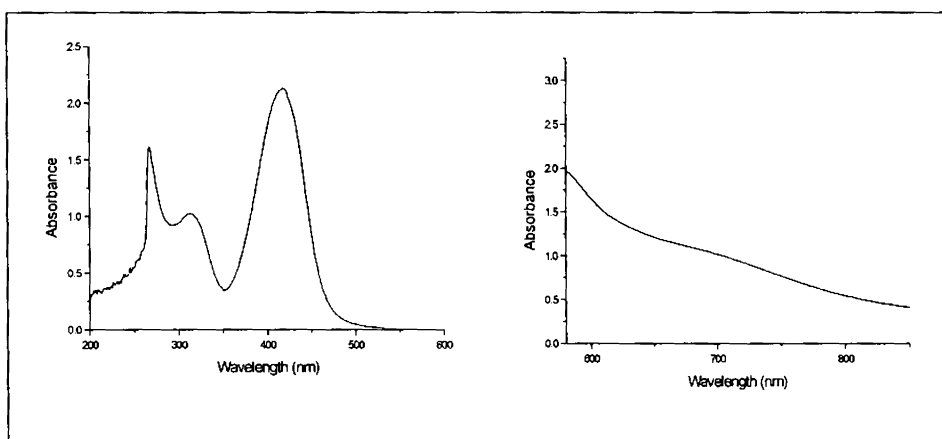


Fig. 3.17. Electronic spectra of compound 5.

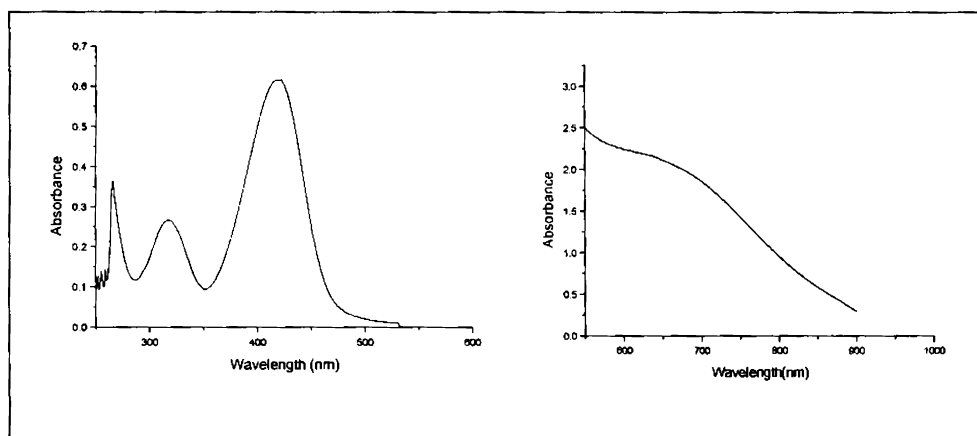


Fig. 3.18. Electronic spectra of compound 9.

### 3.3.5. Electron paramagnetic resonance spectra

The EPR spectra of the polycrystalline samples at 298 K and DMF solution at 77 K were recorded in the X-band, using 100-kHz modulation;  $g$  factors were quoted relative to the standard marker TCNE ( $g = 2.00277$ ). The EPR parameters of the copper(II) complexes are presented in the Table 3.7.

EPR spectral studies are used for predicting the geometrical arrangement of ligand around copper(II) ion. The relation between geometry of copper(II) ion in a complex and EPR spectra were studied extensively by Hathaway and co-workers [34].

Table 3.7 Spin Hamiltonian and bonding parameters of copper(II) complexes of 2-benzoylpyridine-*N*(4)-phenylsemicarbazone

	1	2	3	4	5	6	7	8	9
Polycrystalline (298 K)									
$g_{\parallel}$	2.206			2.204	2.216		2.262	2.134	2.165
$g_{\perp}$	2.084			2.074	2.062		2.084	2.047	2.045
$g_{iso} g_{av}$	2.145	2.141	2.076	2.139	2.139	2.012	2.148	2.076	2.085
$G$	2.452			2.702	2.625		3.256	3.110	3.672
DMF (77 K)									
$g_{\parallel}$	2.192	2.210	2.210	2.213	2.212(g <sub>1</sub> )	2.218	2.208	2.154	2.168
$g_{\perp}$	2.050	2.056	2.063	2.059	2.084(g <sub>1</sub> )2.074(g <sub>2</sub> )	2.056	2.074	2.048	2.054
$A_{\parallel}/A_{\perp}$	188.3	196.6	193.3	191.6	193.3	196.6	187.75	187.7	186.6
$\alpha^2$	0.7690	0.8170	0.8059	0.8017	0.8077	0.8142	0.7400	0.7822	0.7382
$\beta^2$	0.8894	0.8776	0.9265	0.908	0.8815	0.8631	0.8468	0.8048	0.8481
$\gamma^2$	0.8890	0.9473	0.9391	0.9462	0.9263	0.8890	0.9516	0.9085	0.9476
$K_{\parallel}$	0.6840	0.7179	0.7467	0.728	0.7128	0.7038	0.6266	0.6295	0.6261
$K_{\perp}$	0.6837	0.774	0.7569	0.7586	0.7485	0.7134	0.7338	0.7106	0.6995

 $A$  values in  $10^4 \text{ cm}^{-1}$

The EPR spectra of the complexes recorded in polycrystalline state at room temperature provide information about the coordination environment around copper(II) in these complexes.

The EPR spectra of the compound **1** in polycrystalline form at 298 K and in DMF solution at 77 K are given in Figs. 3.19 and 3.20 respectively.

The spectrum of compound **1** in polycrystalline state at 298 K is axial with  $g_{\parallel}$  and  $g_{\perp}$  values as 2.206 and 2.084 respectively.

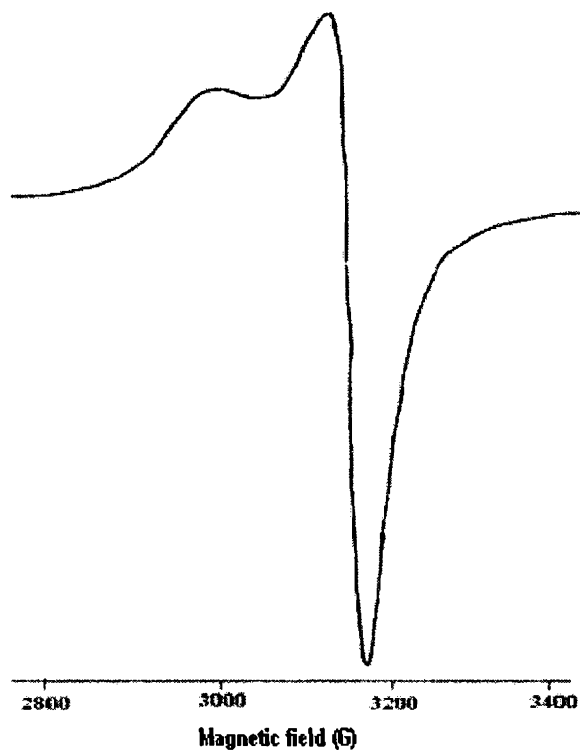


Fig. 3.19. EPR spectrum of  $[\text{Cu}_2(\text{L}^1)_2(\text{OAc})_2] \cdot \text{H}_2\text{O}$  (**1**) in polycrystalline at 298 K

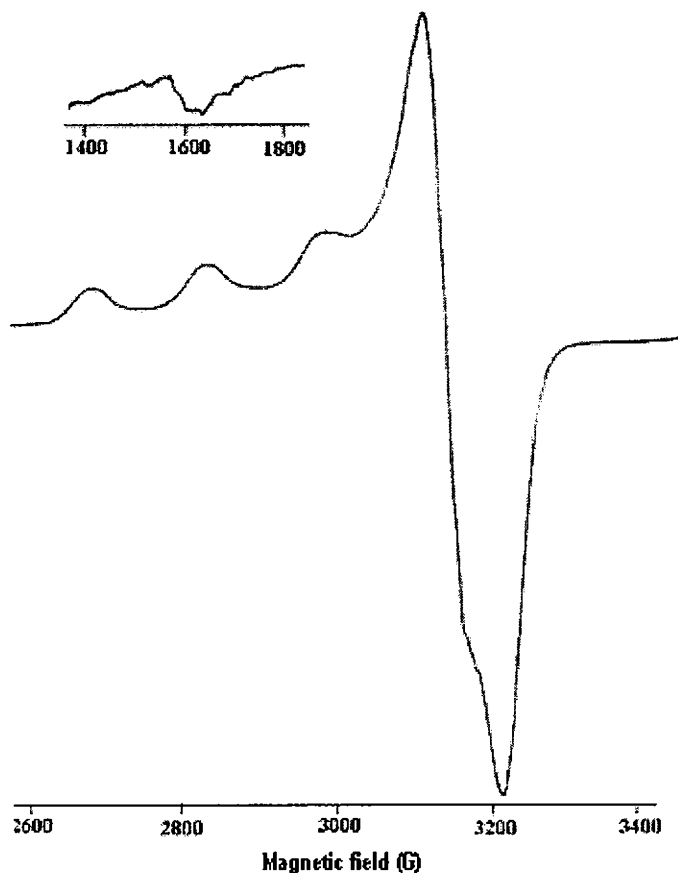


Fig. 3.20. EPR spectrum of  $[\text{Cu}_2(\text{L}^1)_2(\text{OAc})_2] \cdot \text{H}_2\text{O}$  (**1**) in DMF at 77 K.

The EPR spectrum of compound **1** in DMF at 77 K is axial with well defined  $g_{\parallel}$  and  $g_{\perp}$  values.

The solution EPR spectra of compounds  $[\text{Cu}_2\text{L}^1_2(\text{OAc})_2] \cdot \text{H}_2\text{O}$  (**1**) (Fig. 3.20) and  $[\text{Cu}_2(\text{HL}^1)_2(\text{SO}_4)_2] \cdot 4\text{H}_2\text{O}$  (**5**) (Fig. 3.28) at 77 K, exhibited a half field signal ( $g = 4.133$  and  $4.162$ ), which indicate that indeed a weak interaction between two Cu(II) ions within this compound is present [33].

The EPR spectra of the compound **2** in polycrystalline form at 298 K and in DMF solution at 77 K are given in Figs. 3.21 and 3.22 respectively.

The EPR spectrum of the compound **2** in polycrystalline state at 298 K is an axial spectrum with  $g_{\parallel}$  and  $g_{\perp}$  values as 2.141 and 2.058 respectively.

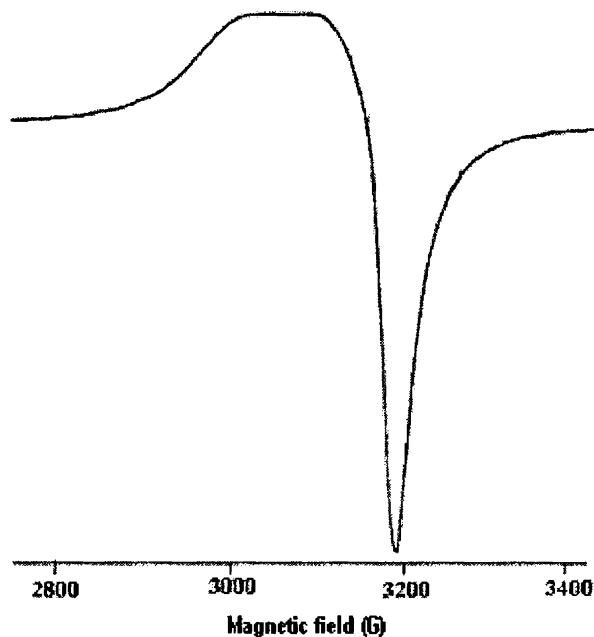


Fig. 3.21. EPR spectrum of  $[\text{CuL}^1\text{NCS}] \cdot \frac{1}{2} \text{H}_2\text{O}$  (**2**) in polycrystalline at 298 K.

The EPR spectra of compounds **3** and **6** in the polycrystalline state at 298 K showed only one broad signal at  $g_{\text{iso}} = 2.076$  and 2.012 respectively. Such isotropic spectra, consisting of a broad signal and hence only one  $g$  value arise from extensive exchange coupling through misalignment of local molecular axes between different molecules in the unit cell and enhanced spin lattice relaxation. These types of spectra unfortunately give no information on the electronic ground state of the Cu(II) ion present in the complexes.

All other compounds in the polycrystalline state show typical axial spectra with well-defined  $g_{\parallel}$  and  $g_{\perp}$  values. The variations in  $g$  values indicate that the geometry of the compounds is affected by the nature of the coordinating ligands. The spectra are often broad because of the broadening resulting from the fast spin lattice relaxation time and exchange coupling.

The EPR spectrum of compound **2** in DMF at 77 K showed a typical axial one with well defined  $g_{\parallel}$  and  $g_{\perp}$  values.

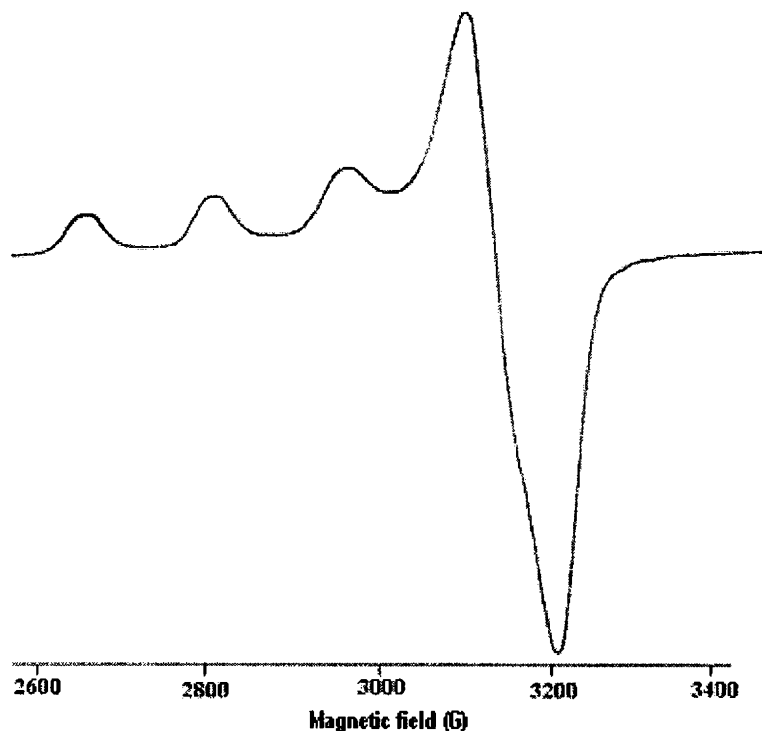


Fig. 3.22. EPR spectrum of  $[\text{CuL}^1\text{NCS}] \cdot \frac{1}{2} \text{H}_2\text{O}$  (**2**) in DMF at 77 K.

The EPR spectra of the compound **3** in polycrystalline form at 298 K and in DMF solution at 77 K are given in Figs. 3.23 and 3.24

respectively. The EPR spectrum in polycrystalline at 298 K is isotropic with  $g_{\text{iso}} = 2.076$ .

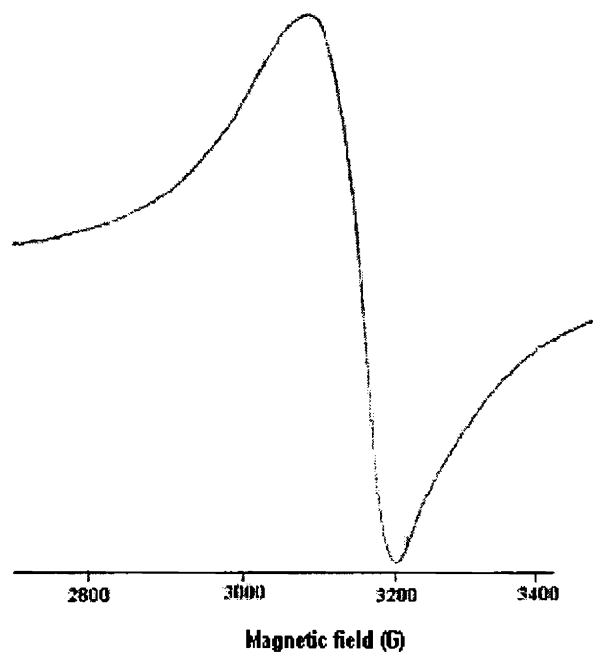


Fig. 3.23. EPR spectrum of  $[\text{CuL}^1\text{NO}_3] \cdot \frac{1}{2} \text{H}_2\text{O}$  (**3**) in polycrystalline at 298 K.

The EPR spectrum of **3** in DMF solution at 77 K is axial with  $g_{\parallel}$  and  $g_{\perp}$  values as 2.210 and 2.063. The spectrum gives five superhyperfine splittings in the perpendicular region which may be due to the coordination of azomethine nitrogen from the semicarbazone moiety.



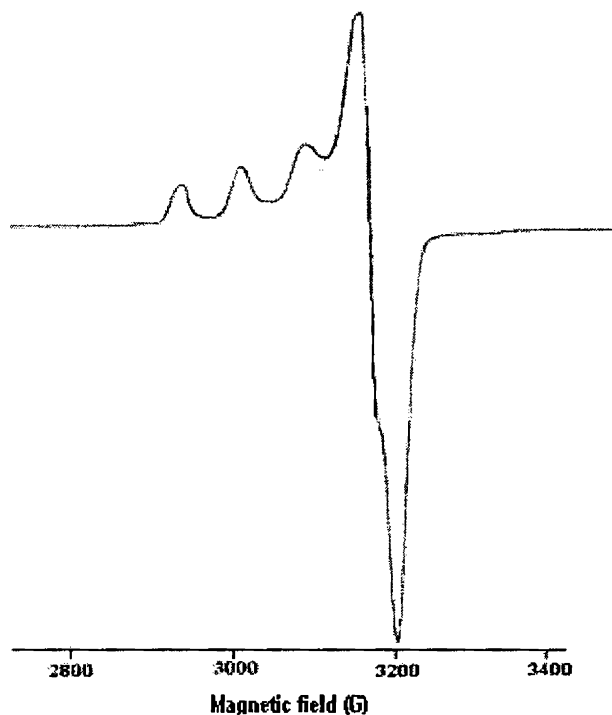


Fig. 3.24. EPR spectrum of  $[\text{CuL}(\text{NO}_3)] \cdot \frac{1}{2} \text{H}_2\text{O}$  (3) in DMF at 77 K.

The EPR spectra of the compound 4 in polycrystalline form at 298 K and in DMF solution at 77 K are given in Figs. 3.25 and 3.26 respectively.

The EPR spectrum in polycrystalline state at 298 K is axial with  $g_{\parallel}$  and  $g_{\perp}$  values as 2.204 and 2.074 respectively. The EPR spectrum in DMF solution at 77 K is axial in nature with  $g_{\parallel}$  and  $g_{\perp}$  values as 2.213 and 2.059 respectively.

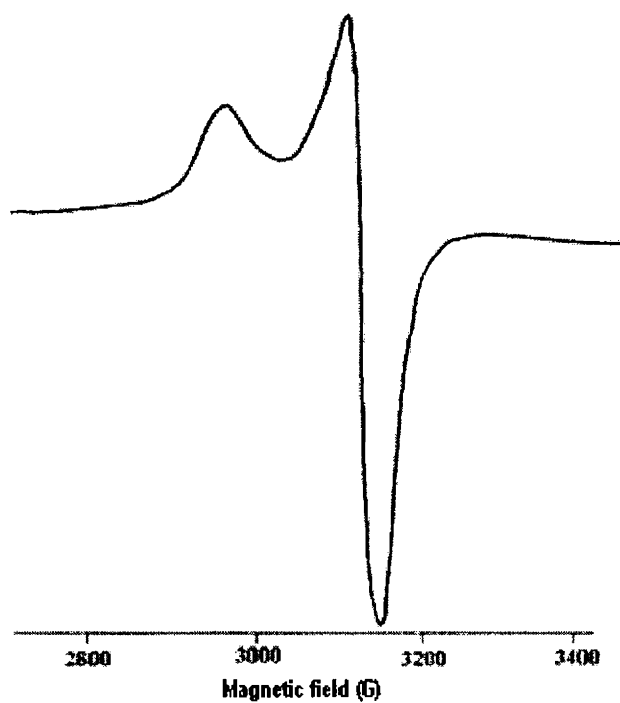


Fig. 3.25. EPR spectrum of  $[\text{Cu}(\text{HL}^1)\text{Cl}_2] \cdot \text{H}_2\text{O}$  (4) in polycrystalline at 298 K.

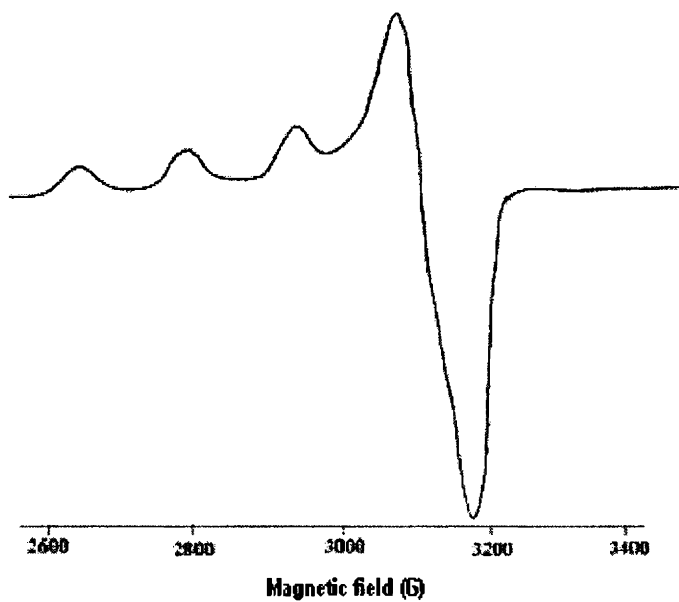


Fig. 3.26. EPR spectrum of  $[\text{Cu}(\text{HL}^1)\text{Cl}_2] \cdot \text{H}_2\text{O}$  (4) in DMF at 77 K.

The EPR spectra of the compound **5** in polycrystalline form at 298 K and in DMF solution at 77 K are given in Figs. 3.27 and 3.28 respectively.

The EPR spectrum of the compound **5** in polycrystalline form at 298 K is an axial one with  $g_{\parallel}$  and  $g_{\perp}$  values as 2.216 and 2.062 respectively. The EPR spectrum in DMF solution at 77 K is a rhombic one with  $g_1$ ,  $g_2$  and  $g_3$  values as 2.084, 2.074 and 2.212 respectively. It is observed that the  $g_3$  value of this complex is less than 2.3 and so it is possible to assign considerable covalent character to the M–L bonds [18, 26].

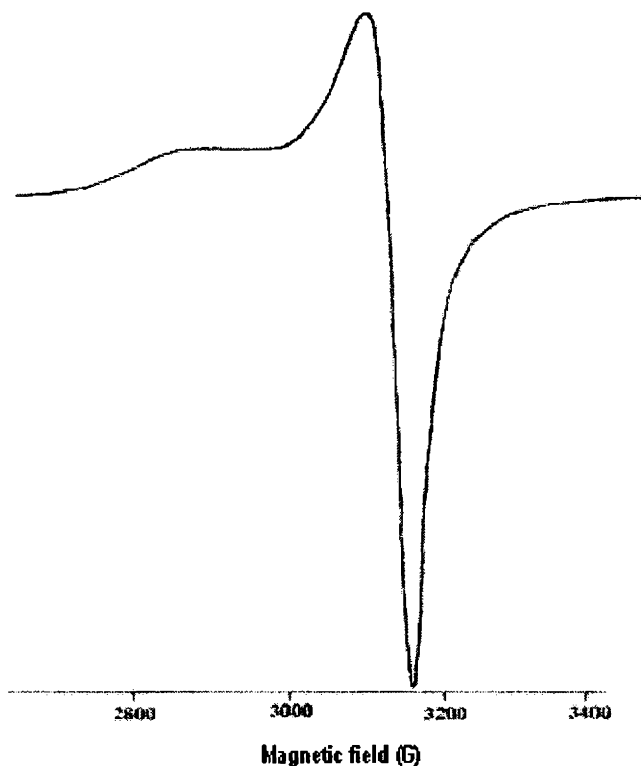


Fig.3.27. EPR spectrum of  $[\text{Cu}_2(\text{HL}^1)_2(\text{SO}_4)_2 \cdot 4\text{H}_2\text{O}$  (**5**) in polycrystalline state at 298 K.

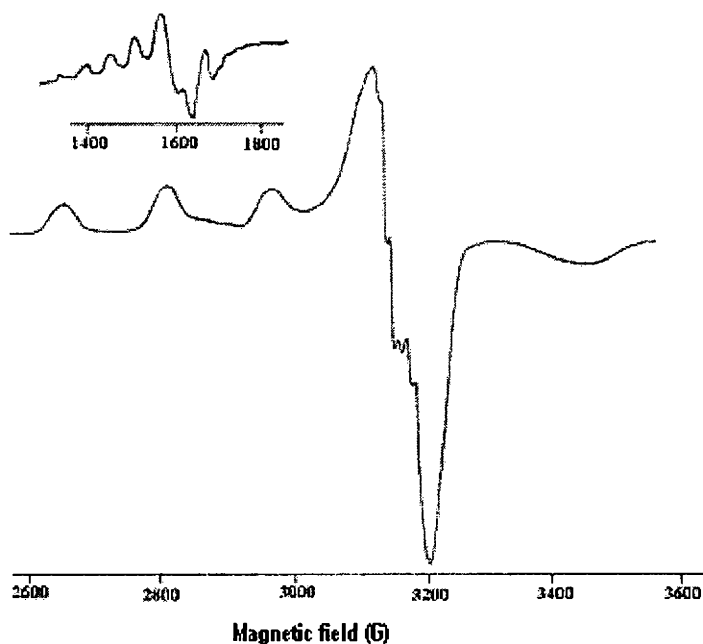


Fig. 3.28. EPR spectrum of  $[\text{Cu}_2(\text{HL}^1)_2(\text{SO}_4)_2] \cdot 4\text{H}_2\text{O}$  (**5**) in DMF at 77 K.

In this compound, the half field resonance exhibited (Fig. 3.28) a well resolved seven line hyperfine structure with an average hyperfine splitting of  $A = 83.3$  G, indicating strong antiferromagnetic coupling between the two copper(II) centers [27]. The hyperfine coupling constant observed on the parallel component complex **5** ( $A_{\parallel} = 83.3$  G) is nearly half of that observed for the corresponding mononuclear complexes ( $A_{\parallel} = 196$  G) which confirms the formation of binuclear complex from its monomers.

The EPR spectra of the compound **6** in polycrystalline form at 298 K and in DMF solution at 77 K are given in Figs. 3.29 and 3.30 respectively.

The EPR spectrum in polycrystalline state at 298 K is an isotropic in nature with  $g_{\text{iso}}$  value as 2.012. It gives an axial spectrum in DMF solution at 77 K with  $g_{\parallel}$  and  $g_{\perp}$  values as 2.218 and 2.056 respectively. The

spectrum gives five superhyperfine splittings in the perpendicular region which may be due to the coordination of azomethine nitrogen from the semicarbazone moiety.

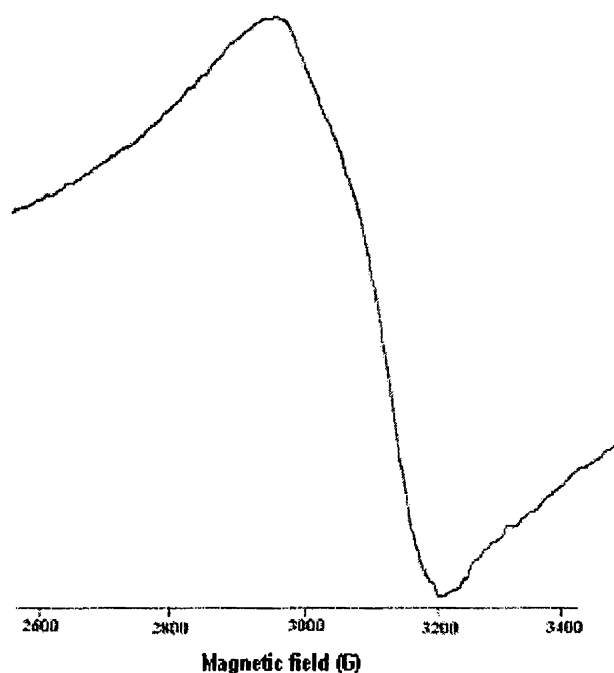


Fig. 3.29. EPR spectrum of  $[\text{Cu}(\text{L}^1)\text{ClO}_4] \cdot \frac{1}{2}\text{H}_2\text{O}$  (6) in polycrystalline at 298 K.

The EPR spectra of complexes  $[\text{CuL}^1\text{ClO}_4] \cdot \frac{1}{2}\text{H}_2\text{O}$  (6),  $[\text{CuL}^1\text{Br}] \cdot 2\text{H}_2\text{O}$  (7),  $[\text{CuL}^1_2] \cdot \text{H}_2\text{O}$  (8) and  $[\text{CuL}^1\text{N}_3] \cdot \text{CH}_3\text{OH}$  (9) show four hyperfine lines with five nitrogen superhyperfine lines on the high field copper hyperfine splitting component, which arises from the coupling of the electron spin with the nuclear spin of the two coordinating nitrogen atoms. The spectral features of all the complexes clearly show four fairly resolved hyperfine lines ( $^{35}\text{Cu}$ ,  $I=3/2$ ) corresponding to  $-3/2, -1/2, 1/2, 3/2$  transitions ( $\Delta M_s = \pm 1$ ). In the parallel region, three of the four copper

hyperfine lines are moderately resolved while perpendicular features overlap the fourth one.

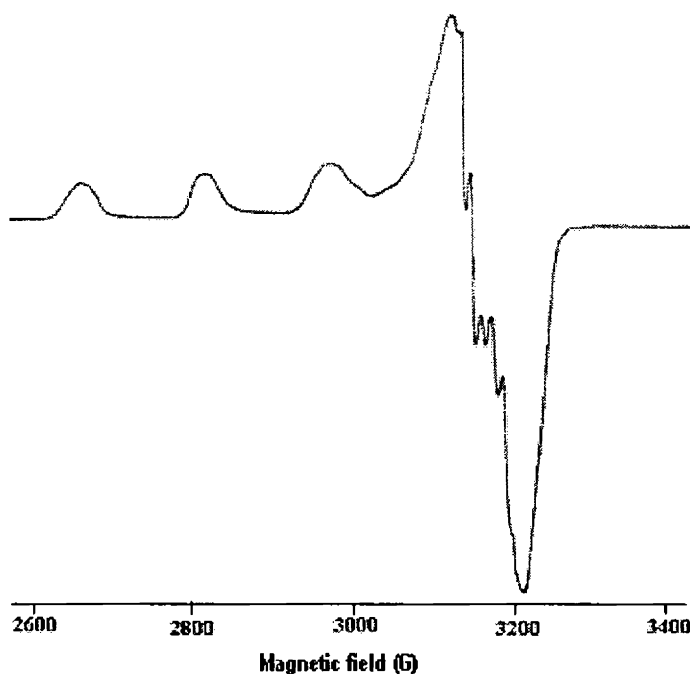


Fig. 3.30. EPR spectrum of  $[\text{Cu}(\text{L}^1)\text{ClO}_4] \cdot \frac{1}{2} \text{H}_2\text{O}$  (6) in DMF at 77 K.

The EPR spectra of the compound 7 in polycrystalline form at 298 K and in DMF solution at 77 K are given in Figs. 3.31 and 3.32. respectively.

The EPR spectrum in polycrystalline state at 298 K is axial in nature with  $g_{\parallel}$  and  $g_{\perp}$  values as 2.262 and 2.084 respectively. The EPR spectrum in DMF solution at 77 K is also axial one with  $g_{\parallel}$  and  $g_{\perp}$  values as 2.208 and 2.074 respectively. The spectrum gives five superhyperfine splittings in the perpendicular region which may be due to the coordination of azomethine nitrogen from the semicarbazone moiety.

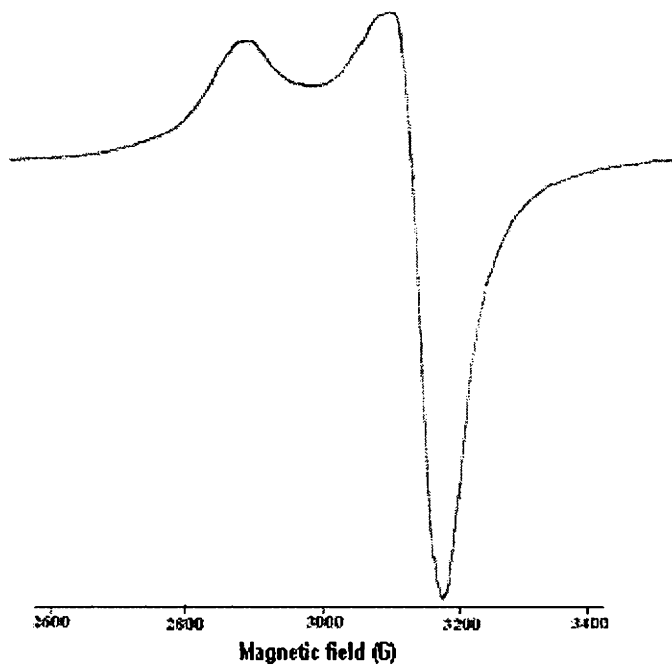


Fig. 3.31. EPR spectrum of  $[\text{CuL}^1\text{Br}] \cdot 2\text{H}_2\text{O}$  (7) in polycrystalline at 298 K.

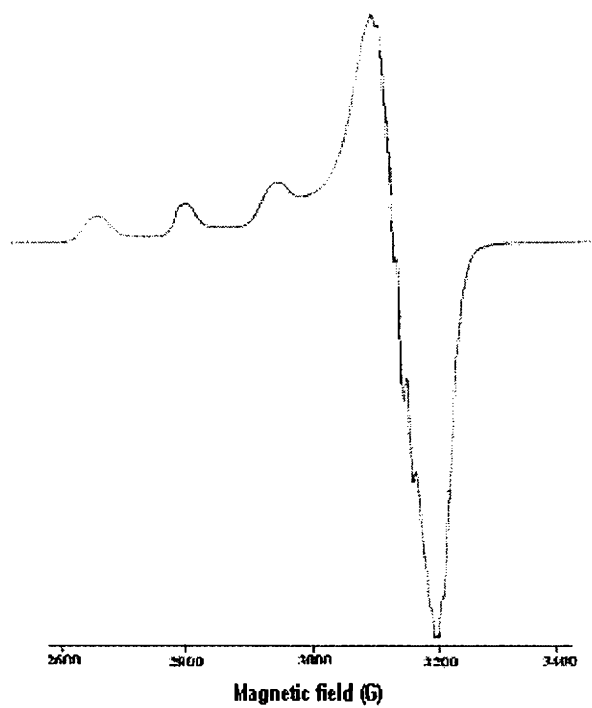


Fig. 3.32. EPR spectrum of  $[\text{CuL}^1\text{Br}] \cdot 2\text{H}_2\text{O}$  (7) in DMF at 77 K.

The EPR spectra of the compound **8** in polycrystalline form at 298 K and in DMF solution at 77 K are given in Figs. 3.33 and 3.34, respectively.

The EPR spectrum in polycrystalline state at 298 K is axial with  $g_{\parallel}$  and  $g_{\perp}$  values as 2.134 and 2.047 respectively.

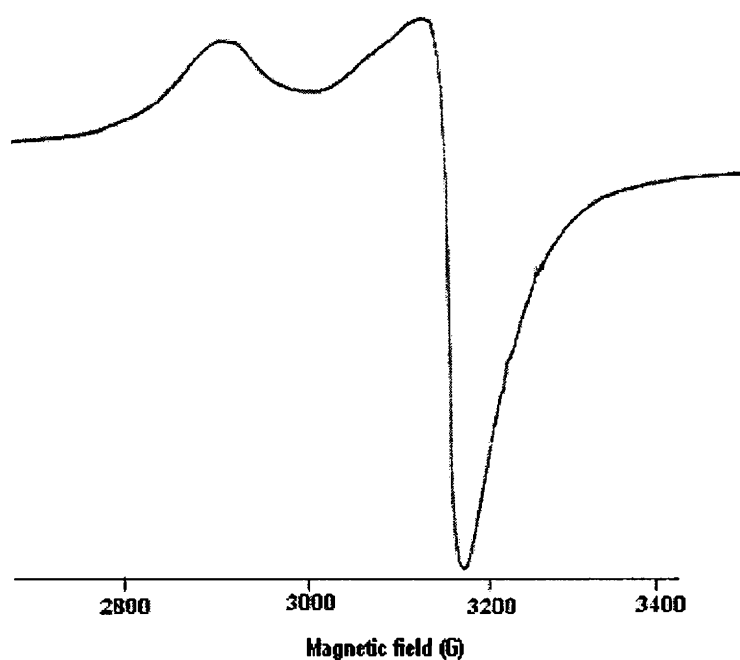


Fig. 3.33. EPR spectrum of  $[\text{CuL}_2] \cdot \text{H}_2\text{O}$  (**8**) in polycrystalline at 298 K.

The EPR spectrum in DMF solution at 77 K is also axial with  $g_{\parallel}$  and  $g_{\perp}$  values as 2.154 and 2.048 respectively. The spectrum gives five superhyperfine splittings in the perpendicular region which may be due to the coordination of azomethine nitrogen from the semicarbazone moiety.



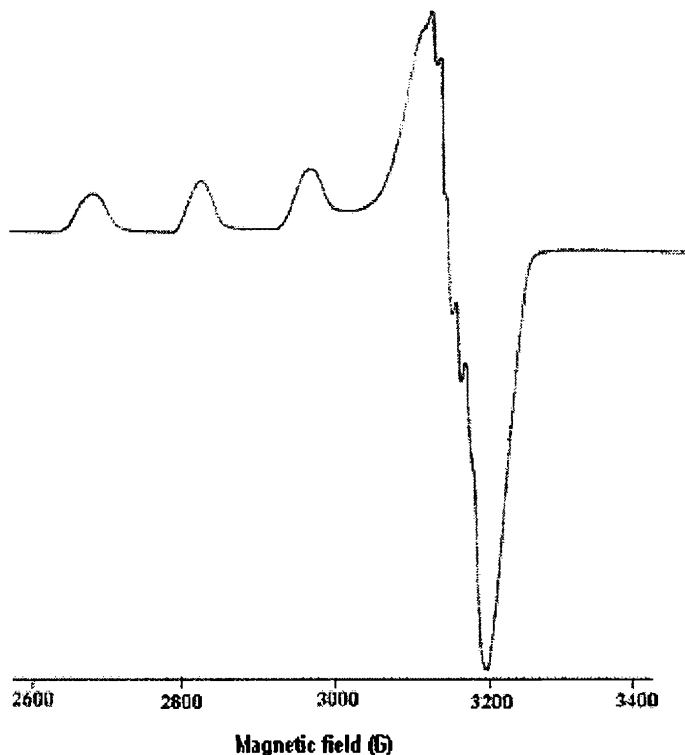


Fig. 3.34. EPR spectrum of  $[\text{CuL}_2] \cdot \text{H}_2\text{O}$  (**8**) in DMF at 77 K.

The EPR spectra of the compound **9** in polycrystalline form at 298 K and in DMF solution at 77 K are given in Figs. 3.35 and 3.36, respectively.

The EPR spectrum in polycrystalline at 298 K is axial with  $g_{\parallel}$  and  $g_{\perp}$  values as 2.165 and 2.045 respectively. The EPR spectrum in DMF solution at 77 K is also axial with  $g_{\parallel}$  and  $g_{\perp}$  values as 2.168 and 2.054 respectively. The above spectrum gives five superhyperfine splitting lines in the perpendicular region which may be due to the coordination of azomethine nitrogen and nitrogen from the equatorial azido group.

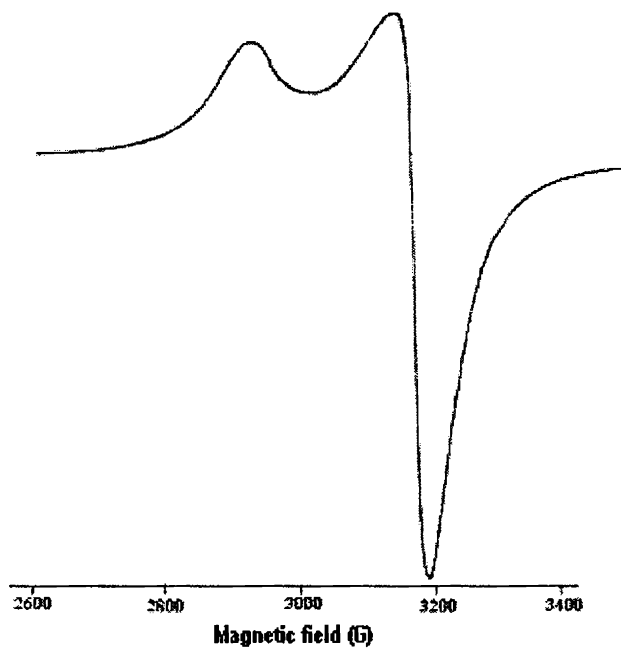


Fig. 3.35. EPR spectrum of  $[\text{CuL}^1\text{N}_3] \cdot \text{CH}_3\text{OH}$  (9) in polycrystalline at 298 K.

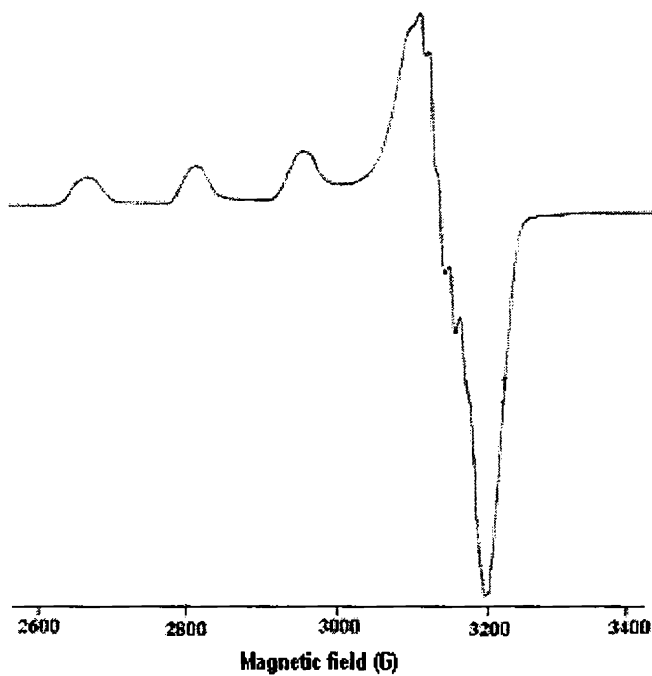


Fig. 3.36. EPR spectrum of  $[\text{CuL}^1\text{N}_3] \cdot \text{CH}_3\text{OH}$  (9) in DMF at 77 K.

The  $g_{\parallel}$  values of all the compounds are found to be almost the same, which indicate that the bonding is dominated by the semicarbazone moiety. The geometric parameter  $G$ , which is a measure of exchange interaction between the copper centers in the polycrystalline compound, is calculated and the value of  $G$  is found to be in the range 2.3-3.7. It is perceived that, if  $G > 4$ , the exchange interaction is negligible and vice versa in the complexes. The  $G$  values indicate that the exchange interactions are strong in all these complexes. In all the complexes,  $g_{\parallel} > g_{\perp} > 2.0023$  is consistent with a  $d_x^2 - y^2$  ground state in a square planar or square pyramidal geometry [34].

In the spectra of all compounds in DMF solution at 77 K, four well-resolved hyperfine lines corresponding to coupling of the electron spin with the nuclear spin ( $^{63,65}\text{Cu}$ ,  $I = 3/2$ ) are obtained in the parallel region.

In polynuclear copper(II) complexes, due to Cu—Cu dipolar interaction, the zero field splitting parameter,  $D$  gives rise to transitions corresponding to  $\Delta M_s = \pm 2$ . In the X-band spectra,  $\Delta M_s = \pm 1$  transitions are associated with fields of *ca.* 3000 Gauss, while the  $\Delta M_s = \pm 2$  transition generate a transition at the half field value of *ca.* 1500 Gauss and the presence of this half field band is a useful criterion for dipolar interaction from the presence of some binuclear (or polynuclear) complex formation.

The EPR parameters  $g_{\parallel}$ ,  $g_{\perp}$ ,  $g_{av}$ ,  $A_{\parallel}(\text{Cu})$  and  $A_{\perp}(\text{Cu})$  and the energy values of the  $d-d$  transition were used to evaluate the bonding parameters  $\alpha^2$ ,  $\beta^2$  and  $\gamma^2$  which may be regarded as measures of the covalency of the in-plane  $\sigma$ -bonds, in-plane  $\pi$ -bonds, and out-of-plane  $\pi$ -bonds respectively.

The value of in-plane  $\sigma$ -bonding parameter  $\alpha^2$  was calculated using the expression:

$$\alpha^2 = -A_{\parallel} / 0.036 + (g_{\parallel} - 2.0023) + 3/7(g_{\perp} - 2.0023) + 0.04 \quad [35]$$

The orbital reduction factors,  $K_{\parallel} = \alpha^2 \beta^2$  and  $K_{\perp} = \alpha^2 \gamma^2$  were calculated using the following expressions [36]:

$$K_{\parallel}^2 = (g_{\parallel} - 2.0023) E_{d-d} / 8\lambda_0$$

$$K_{\perp}^2 = (g_{\perp} - 2.0023) E_{d-d} / 2\lambda_0$$

where  $\lambda_0$  is the spin-orbit coupling constant with a value of  $-828 \text{ cm}^{-1}$  for copper(II)  $d^9$  system. According to Hathaway [34], for pure  $\sigma$ -bonding,  $K_{\parallel} \approx K_{\perp} \approx 0.77$ , and for in-plane  $\pi$ -bonding,  $K_{\parallel} < K_{\perp}$ ; while for out-of-plane  $\pi$  bonding,  $K_{\perp} < K_{\parallel}$ . In all the complexes, it is observed that  $K_{\parallel} < K_{\perp}$  which indicates the presence of significant in-plane  $\pi$ -bonding. This is further confirmed by the bonding parameters  $\alpha^2$ ,  $\beta^2$  and  $\gamma^2$ , which are less than 1.0 expected of the purely ionic character of the bonds, and decreases with the increasing covalent nature of the bonding.

**References**

1. F.A. Cotton, G. Wilkinson, C.A. Murillo, M. Bochmann, *Advanced Inorganic Chemistry*, 6<sup>th</sup> ed., Wiley, New York, 1999.
2. R.N. Mukherjee, *Indian J. Chem.* 42A (2003) 2175.
3. R.N. Mukherjee, *Comprehensive Coordination Chemistry-II: From Biology to Nanotechnology*, 5 (2003).
4. R.H. Holm, P. Kennepohl, E.I. Solomon, *Chem. Rev.* 96 (1996) and references therein.
5. M. Akkurt, S. Ozfuric, S. Ide, *Anal. Sci.* 16 (2000) 667.
6. J.R. Dimmock, R.N. Puthucode, J.M. Smith, M. Hetherington, J.W. Quil, U. Pugazhenti, *J. Med. Chem.* 39 (1996) 3984.
7. J.R. Dimmock, K.K. Sidhu, S.D. Thumber, S.K. Basran, M. Chen, J.W. Quil, *Eur. J. Chem.* 30 (1995) 287.
8. H. Beraldo, D. Gaminob, *Mini Rev. Med. Chem.* 4 (2004) 31.
9. U.L. Kala, S. Suma, M.R.P. Kurup, Suja Krishnan, R.P. John, *Polyhedron* 26 (2007) 1427.
10. SMART and SAINT, Area Detector Software Package and SAX Area Detector Integration Program, Bruker Analytical X-ray; Madison, WI, USA, 1997.
11. *SADABS, Area Detector Absorption Correction Program*; Bruker Analytical X-ray; Madison, WI, 1997.
12. G.M. Sheldrick, *Acta Cryst.* (2008) A64, 112–122.
13. K. Brandenburg, *Diamond Version 3.1f*, Crystal Impact GbR, Bonn, Germany, 2008.

14. W.J. Geary, *Coord. Chem. Rev.* 7 (1971) 81.
15. A.W. Addison, J.N. Rao, J. Reedijk, G.C. Vershoor, *J. Chem. Soc., Dalton Trans.* (1984) 1349.
16. M. Joseph, V. Suni, M.R.P. Kurup, M. Nethaji, A. Kishore, S.G. Bhat, *Polyhedron* 23 (2004) 3069.
17. K. Nakamoto, *Infrared and Raman Spectra of Inorganic and Coordination Compounds, Part B*, 5<sup>th</sup> edition, Wiley, New York, 1997.
18. A. Sreekanth, M.R.P. Kurup, *Polyhedron* 22 (2003) 3321.
19. E.B. Seena, M.R.P. Kurup, *Acta Cryst. C* 62 (2006) 486.
20. U.L. Kala, *in* Synthesis, spectral and magnetic studies on some transition metal complexes, Ph.D thesis, Kerala University, Kerala, 2007.
21. R.A. Bailey, S.L. Kozak, T.W. Michelson, W.N. Mills, *Coord. Chem. Rev.* 6 (1971) 407.
22. R. Raina, T.S. Srivastava, *Indian J. Chem. A* 22 (1983) 701.
23. B.J. Hathaway, A.E. Uderchill, *J. Chem. Soc.* (1961) 3091.
24. R.P. John, A. Sreekanth, M.R.P. Kurup, H.-K. Fun, *Polyhedron* 24 (2005) 601.
25. J.R. Wasson, C. Trapp, *J. Phys. Chem.* 73 (1969) 3763.
26. M.J. Bew, B.J. Hathaway, R.R. Faraday, *J. Chem. Soc., Dalton Trans.* (1972) 1229.
27. R.L. Dutta, A. Syamal, *Elements of Magnetochemistry*, 2<sup>nd</sup> ed., East-west press, New Delhi, 1993.
28. C.R.K. Rao, P.S. Zacharias, *Polyhedron* 16 (1997) 1201.
29. H. Sacconi, G.Speroni, *J. Am Chem. Soc.* 87 (1965) 3102.

30. R.P. John, A. Sreekanth, V. Rajakannan, T.A. Ajith, M.R.P. Kurup, *Polyhedron* 23 (2004) 2549.
31. M. Joseph, M. Kuriakose, M.R.P. Kurup, E. Suresh, A. Kishore, G. Bhat, *Polyhedron* 25 (2006) 61.
32. B.N. Bessy Raj, M.R.P. Kurup, E. Suresh, *Spectrochim. Acta Section A* 71 (2008) 1253.
33. V. Philip, V. Suni, M.R.P. Kurup, M. Nethaji, *Polyhedron* 24 (2005) 1133.
34. B.J. Hathaway, in: G. Wilkinson, R.D. Gillard, J. A. McCleverty (Eds.), *Comprehensive Coordination Chemistry*, vol. 5, Pergamon, Oxford, 1987, p. 533.
35. A.H. Maki, B.R. McGarvey, *J. Chem. Phys.* 29 (1958) 31.
36. B.N. Figgis, *Introduction to ligand Fields*, Interscience, New York 1996, p 295.

SYNTHESES, STRUCTURAL AND SPECTRAL  
CHARACTERIZATION OF COPPER(II) COMPLEXES  
OF 2-ACETILPYRIDINE-  
*N*(4)-PHENYLSEMICARBAZONE

4.1. Introduction

The coordination chemistry involving heterocyclic thiosemicarbazones and semicarbazones have been an interesting research area in the last 30 years because of their well-documented biological activities. Complexation of semicarbazone ligands with metal ions has been found to produce synergistic effects on the antiproliferative activities of the parent ligands. Semicarbazones are also reported to possess versatile structural features and chelating behavior [1] and possess a broad spectrum of potentially useful chemotherapeutic activities ranging from antifungal, antibacterial, anti-inflammatory and antiviral properties [2,3]. A variety of semicarbazones and their metal complexes possess anti-protozoa and anti-convulsant activity also [4].

There has been considerable amount of interest in the studies of semicarbazones recently due to their unusual coordination modes when bound to metals, high pharmacological potentiality and good chelating property. Metal complexes of thiosemicarbazones of 2-acetylpyridine are extensively studied [5-10], but those of *N*(4)-substituted semicarbazones of 2-acetylpyridine have received much less attention, though there are some reports on the studies of metal complexes of 2-hydroxyacetophenone-*N*(4)-



phenylsemicarbazone [11,12]. The structural and spectral studies of cadmium(II) complexes of di-2-pyridylketone-*N*(4)-phenylsemicarbazone [13] have been reported from our laboratory.

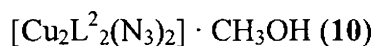
This chapter deals with the syntheses and spectral studies of 2-acetylpyridine-*N*(4)-phenylsemicarbazone ( $HL^2$ ) and its nine Cu(II) complexes along with the crystal structure of the compound,  $[Cu_2L^2_2(\mu-N_3)_2]$  (**10a**).

## 4.2. Experimental

### 4.2.1. Materials

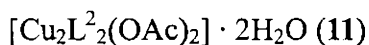
Details regarding the synthesis of  $HL^2$  are described in Chapter 2. 4-Phenylsemicarbazide (Fluka), 2-acetylpyridine (Fluka), potassium thiocyanate (CDH), sodium azide (CDH), copper acetate, copper chloride, copper nitrate, copper bromide, copper perchlorate and copper sulfate (BDH) were used without further purification. All solvents obtained commercially were distilled before use.

### 4.2.2. Syntheses of complexes

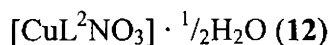


The complex  $[Cu_2L^2_2(N_3)_2] \cdot CH_3OH$  (**10**) was synthesized by the following method. A hot solution of  $HL^2$  (0.508 g, 2 mmol) in methanol (20 cm<sup>3</sup>) was mixed with a hot filtered methanolic solution of sodium azide (0.130 g, 2 mmol). To this, a hot filtered solution of  $Cu(OAc)_2 \cdot H_2O$

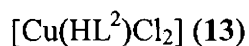
(0.398 g, 2 mmol) was added with constant stirring. The mixture was then refluxed for 3 hours. The complex separated as microcrystals was filtered and thoroughly washed with water, methanol and ether and finally dried over  $P_4O_{10}$  *in vacuo*.



The complex  $[Cu_2L^2_2(OAc)_2] \cdot 2H_2O$  (11) was prepared by refluxing a hot solution of  $HL^2$  (0.508 g, 2 mmol) in methanol (20 cm<sup>3</sup>) with a hot filtered methanolic solution of  $Cu(OAc)_2 \cdot H_2O$  (0.398 g, 2 mmol) for 4 hours. The green complex separated as microcrystals was filtered and thoroughly washed with water, methanol and ether and finally dried over  $P_4O_{10}$  *in vacuo*.

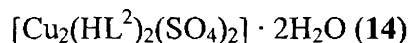


The complex  $[CuL^2NO_3] \cdot \frac{1}{2}H_2O$  (12) was prepared by refluxing a hot solution of  $HL^2$  (0.508 g, 2 mmol) in methanol (20 cm<sup>3</sup>) with a hot filtered methanolic solution of  $CuNO_3 \cdot 3H_2O$  (0.483 g, 2 mmol) for 3 hours. The green colored solid, separated on cooling, was filtered, and washed with hot water, hot methanol and ether. The compound was dried over  $P_4O_{10}$  *in vacuo*.



The complex  $[Cu(HL^2)Cl_2]$  (13) was prepared by stirring a hot solution of  $HL^2$  (0.508 g, 2 mmol) in methanol (20 cm<sup>3</sup>) with a hot filtered methanolic solution of  $CuCl_2 \cdot 2H_2O$  (0.340 g, 2 mmol) for 5 hours. The

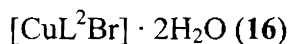
green solid separated on keeping overnight, was filtered and washed with hot water, hot ethanol and ether and dried over  $P_4O_{10}$  *in vacuo*.



The complex  $[Cu_2(HL^2)_2(SO_4)_2] \cdot 2H_2O$  (14) was prepared by refluxing a hot solution of  $HL^2$  (0.508 g, 2 mmol) in methanol (20 cm<sup>3</sup>) with a hot filtered methanolic solution of  $CuSO_4 \cdot 5H_2O$  (0.499 g, 2 mmol) for 6 hours. The pale green colored crystals, separated on keeping for a few days, were filtered and washed with hot ethanol, hot water and ether and then dried over  $P_4O_{10}$  *in vacuo*.

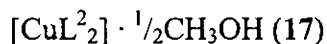


The complex  $[CuL^2ClO_4]$  (15) was prepared by stirring a hot solution of  $HL^2$  (0.508 g, 2 mmol) in methanol (20 cm<sup>3</sup>) with a hot filtered methanolic solution of copper perchlorate (0.371 g, 2 mmol) for 4 hours. The green solid separated, was filtered, washed with hot water, hot methanol, and ether and dried over  $P_4O_{10}$  *in vacuo*.

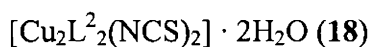


The complex  $[CuL^2Br] \cdot 2H_2O$  (16) was synthesized by refluxing a hot solution of  $HL^2$  (0.508 g, 2 mmol) in methanol (20 cm<sup>3</sup>) with a hot filtered methanolic solution of copper bromide (0.446 g, 2 mmol) for 3 hours. The dark green colored shining crystals, separated on keeping the

solution overnight, were collected by filtration and washed with hot water, hot methanol, and ether and dried over P<sub>4</sub>O<sub>10</sub> *in vacuo*.



The complex  $[\text{CuL}^2_2] \cdot \frac{1}{2}\text{CH}_3\text{OH}$  (17) was obtained when a hot solution of HL<sup>2</sup> (0.508 g, 2 mmol) in methanol (20 cm<sup>3</sup>) was mixed a hot filtered methanolic solution of Cu(OAc)<sub>2</sub> · H<sub>2</sub>O (0.199 g, 1 mmol) with constant stirring and then refluxed for 3 hours. The complex separated as microcrystals was filtered and thoroughly washed with water, methanol and ether and finally dried over P<sub>4</sub>O<sub>10</sub> *in vacuo*.



The complex  $[\text{Cu}_2\text{L}^2_2(\text{NCS})_2] \cdot 2\text{H}_2\text{O}$  (18) was synthesized by the following method. A hot solution of HL<sup>2</sup> (0.508 g, 2 mmol) in methanol (20 cm<sup>3</sup>) was mixed with a hot filtered methanolic solution of potassium thiocyanate (0.194 g, 2 mmol). To this a hot filtered solution of Cu(OAc)<sub>2</sub> · H<sub>2</sub>O (0.398 g, 2 mmol) was added with constant stirring. The mixture was then refluxed for 3 hours. The complex separated as microcrystals was filtered and thoroughly washed with water, methanol and ether and finally dried over P<sub>4</sub>O<sub>10</sub> *in vacuo*.

#### **4.2.3. Analytical methods**

Elemental analyses were carried out using a Vario EL III CHNS analyzer at SAIF, Kochi, India. IR spectra were recorded on a Thermo Nicolet AVATAR 370 DTGS model FT-IR Spectrophotometer with KBr pellets and ATR technique at SAIF, Kochi, India. Electronic spectra were

recorded on a Cary 5000, version 1.09 UV-Vis-NIR spectrophotometer using solutions in acetonitrile. Magnetic moment measurements are carried out in the polycrystalline state at room temperature on a PAR model 155 Vibrating Sample Magnetometer at 5 kOe field strength at the Indian Institute of Technology, Roorkee, India. EPR spectra were recorded on a Varian E-112 X-band EPR spectrometer using TCNE as a standard at SAIF, IIT, Bombay, India.

#### 4.2.4. X-Ray crystallography

Single crystals of compound  $[\text{Cu}_2\text{L}_2(\mu\text{-N}_3)_2]$  (**10a**) suitable for X-ray diffraction studies were grown from its solution in a mixture of methanol and ethanol (1:1). A dark blue monoclinic single crystal of dimension  $0.28 \times 0.20 \times 0.20 \text{ mm}^3$  was selected and mounted on a Nonius MACH3 diffractometer, equipped with a graphite crystal, incident-beam monochromator, and a fine focus sealed tube,  $\text{MoK}\alpha$  ( $\lambda = 0.71073 \text{ \AA}$ ) X-ray source.

The unit cell dimensions were measured and the data collection was performed at 293 K. The intensity data were collected by the  $\omega/\theta$ -scan mode within  $2.04^\circ < \theta < 24.97^\circ$  for hkl ( $-26 \leq h \leq 26$ ,  $-8 \leq k \leq 0$ ,  $-23 \leq l \leq 0$ ). The cell refinement was done using the Argus (Nonius, MACH3 software) [14]. The Maxus (Nonius software) were used for data reduction. The structure was solved by direct methods with the program SHELXS-97 and refined by full matrix least squares on  $F^2$  using SHELXL-97 [15]. The graphics used were Mercury and Diamond [16,17]. All non-hydrogen atoms were refined anisotropically, and all hydrogen atoms were located from the difference Fourier map and refined isotropically.

### 4.3. Results and discussion

#### 4.3.1. Analytical measurements

The principal ligand  $HL^2$  was synthesized by the direct condensation of 2-acetylpyridine with *N*(4)-phenylsemicarbazide. Ligand can exist in keto or enol form or an equilibrium mixture of the two since it has an amide  $-NH-C(=O)$  function. However, the presence of a band at  $1683\text{ cm}^{-1}$  in the IR spectrum of  $HL^2$  indicates that in the solid state it remains in keto form. The IR spectra of complexes, however, do not show any intense absorption band around  $1683\text{ cm}^{-1}$  except  $[Cu_2(HL^2)_2(SO_4)_2] \cdot 2H_2O$  and  $Cu(HL^2)Cl_2$ , due to the carbonyl stretching of the semicarbazone moiety. This shows that in solution, it tautomerises to the enol form and coordinates to the metal in the enolate form.

The complexes  $[Cu_2L^2_2(N_3)_2] \cdot CH_3OH$  and  $[Cu_2L^2_2(NCS)_2] \cdot 2H_2O$  were readily formed by the reaction of the ligand and sodium azide or potassium thiocyanate with copper acetate. The complexes  $[Cu_2L^2_2(OAc)_2] \cdot 2H_2O$ ,  $[CuL^2NO_3] \cdot \frac{1}{2}H_2O$ ,  $[Cu(HL^2)Cl_2]$ ,  $[Cu_2(HL^2)_2(SO_4)_2] \cdot 2H_2O$ ,  $[CuL^2ClO_4]$  and  $[CuL^2Br] \cdot 2H_2O$  were formed by the reaction of the ligand with corresponding copper salts. The complex  $CuL^2_2 \cdot \frac{1}{2}CH_3OH$  was obtained when a hot solution of  $HL^2$  was reacted with a hot filtered methanolic solution of  $Cu(OAc)_2 \cdot H_2O$  in the ratio 2:1. The principal ligand  $HL^2$  undergoes deprotonation to  $L^-$  and chelates in enolate form as evidenced by the IR spectra.

The complexes are soluble in methanol, ethanol, DMF and acetonitrile. The conductivity measurements were made in DMF solutions

and the values are found to be less than  $20 \Omega^{-1}\text{mol}^{-1}\text{cm}^{-1}$  for all the complexes and are found to be non-electrolytes [18], which indicates that the anion and the ligand are coordinated to the central copper(II).

The colors, elemental analyses, stoichiometries of  $\text{HL}^2$  and its complexes are presented in Table 4.1.

Table 4.1. Colors, elemental analyses and magnetic susceptibility of 2-acetylpyridine-*N*(4)-phenylsemicarbazone and its copper(II) complexes.

Compound	Color	Observed (Calculated) %			$\mu(\text{B.M.})$
		C	H	N	
$\text{HL}^2$	Pale yellow	66.68 (66.13)	5.58 (5.55)	22.22 (22.03)	-
$[\text{Cu}_2\text{L}_2^2(\text{N}_3)_2] \cdot \text{CH}_3\text{OH}$ (10)	Green	46.44 (46.46)	3.81 (4.03)	25.83 (26.16)	1.04
$[\text{Cu}_2\text{L}_2^2(\text{OAc})_2] \cdot 2\text{H}_2\text{O}$ (11)	Green	48.65 (48.79)	4.96 (4.61)	14.35 (14.22)	1.13
$[\text{CuL}^2\text{NO}_3] \cdot \frac{1}{2}\text{H}_2\text{O}$ (12)	Pale green	42.72 (43.36)	3.40 (3.64)	18.26 (18.06)	1.68
$[\text{Cu}(\text{HL}^2)\text{Cl}_2]$ (13)	Dark green	43.16 (43.26)	3.74 (3.63)	14.33 (14.41)	1.97
$[\text{Cu}_2(\text{HL}^2)_2(\text{SO}_4)_2] \cdot 2\text{H}_2\text{O}$ (14)	Pale green	38.62 (38.84)	3.84 (3.96)	12.53 (12.94)	1.12
$[\text{CuL}^2\text{ClO}_4]$ (15)	Green	40.83 (40.39)	3.64 (3.15)	12.96 (13.46)	1.71
$[\text{CuL}^2\text{Br}] \cdot 2\text{H}_2\text{O}$ (16)	Pale green	38.31 (38.86)	4.22 (3.96)	12.56 (12.95)	1.72
$[\text{CuL}^2] \cdot \frac{1}{2}\text{CH}_3\text{OH}$ (17)	Green	58.71 (58.40)	4.37 (4.82)	19.85 (19.12)	1.86
$[\text{Cu}_2\text{L}_2^2(\text{NCS})_2] \cdot \text{H}_2\text{O}$ (18)	Dark green	45.92 (45.85)	3.91 (3.85)	17.59 (17.82)	1.16

The room temperature magnetic susceptibilities of the complexes in the polycrystalline state formulated with one metal centre except complexes

**10**, **11**, **14** and **18** fall in the range of 1.60-2.00 B.M., which are very close to the spin-only value of 1.73 B.M. for a typical  $S=1/2$   $d^9$  copper(II) system. The magnetic susceptibilities of the polynuclear complexes **10**, **11**, **14** and **18** suggest considerable interaction between metal centers and the magnetic moments fall in the range 1.03-1.16 B.M. which makes an evidence for their behavior as dimers.

#### 4.3.2. Crystal structure of $[\text{Cu}_2\text{L}^2_2(\mu\text{-N}_3)_2]$ (**10a**)

The single crystal X-ray diffraction study of the compound  $[\text{Cu}_2\text{L}^2_2(\mu\text{-N}_3)_2]$  (**10a**) shows that the compound exists as an end-on azido bridged dimer. The molecular structure of the compound along with atom numbering scheme is given in Fig. 4.1.

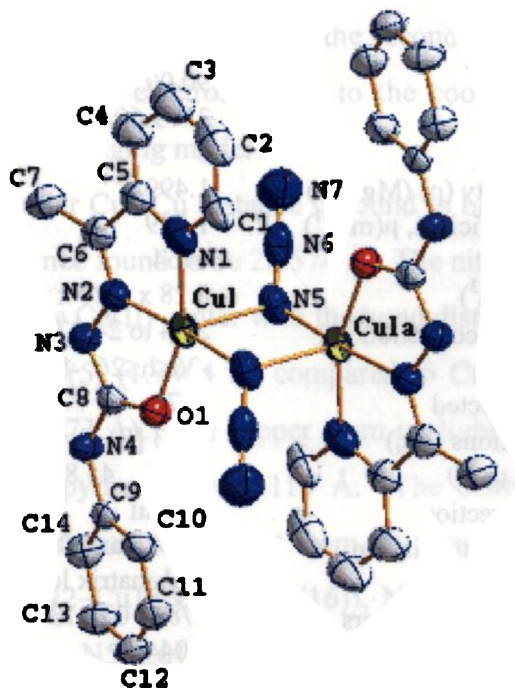


Fig. 4.1. The molecular structure of  $[\text{Cu}_2\text{L}^2_2(\mu\text{-N}_3)_2]$  (**10a**) along with the atom numbering scheme. The hydrogen atoms are omitted for clarity.



The crystallographic data along with details of structure solution refinements are given in Table 4.2.

Table 4.2. Crystal refinement parameters of  $[\text{Cu}_2\text{L}_2(\mu\text{-N}_3)_2](\mathbf{10a})$

Empirical formula	$\text{C}_{28}\text{H}_{26}\text{Cu}_2\text{N}_{14}\text{O}_2$
Formula weight	717.73
Color, habit	Dark blue
Temperature (T) K	293(2) K
Wavelength (MoK $\alpha$ ) (Å)	0.71073
Crystal system	monoclinic
Space group	$C2/c$
Lattice constants	
a (Å)	22.0626(15)
b (Å)	7.2240(5)
c (Å)	19.9780(3)
$\alpha$ (°)	90.00
$\beta$ (°)	93.056(8)
$\gamma$ (°)	90.00
Volume V (Å <sup>3</sup> )	3179.6(5)
Z	8
Calculated density ( $\rho$ ) (Mg m <sup>-3</sup> )	1.499
Absorption coefficient, $\mu$ (mm <sup>-1</sup> )	1.389
F(000)	1464
Crystal size (mm <sup>3</sup> )	0.28 x 0.20 x 0.20
$\theta$ range for data collection	2.04 to 24.97
Limiting indices	$-26 \leq h \leq 26, -8 \leq k \leq 0, -23 \leq l \leq 0$
Reflections collected	2874
Unique Reflections ( $R_{\text{int}}$ )	2783 [ $R_{\text{int}} = 0.0187$ ]
Completeness to $2\theta$	24.97 45.8%
Absorption correction	$\psi$ -scan
Max. and min. transmission	0.7687 and 0.7013
Refinement method	Full-matrix least-squares on $F^2$
Data / restraints / parameters	2783 / 0 / 213
Goodness-of-fit on $F^2$	1.044
Final R indices [ $I > 2\sigma(I)$ ]	$R1 = 0.0457, wR2 = 0.1060$
R indices (all data)	$R1 = 0.1107, wR2 = 0.1242$
Largest difference peak and hole	0.764 and -0.579 e. Å <sup>-3</sup>

The lattice nature is monoclinic with space group  $C2/c$ . Each semicarbazone unit acts as a tridentate chelate, coordinating through pyridyl nitrogen, azomethine nitrogen and the enolate oxygen to a single Cu(II) center which is involved in a  $\mu_{1,1}$ -azido bridging to an identical coordination network, thus each copper atom is in a penta-coordinate environment.

The trigonality index  $\tau$  is calculated using the equation  $\tau = (\beta - \alpha)/60$  [19] (for perfect square pyramidal and trigonal bipyramidal geometries the values of  $\tau$  are zero and unity respectively). The value of  $\tau$  for the molecule is 0.246, which shows the coordination polyhedron around each copper atom is a distorted square pyramid. The base of each distorted square pyramidal unit is occupied by N(1), N(2), N(5) and O(1) atoms, with the apical position occupied by the N(5) atom of the second azido group. Each azido ligand functions as an electron donor to the coordination network through an end-on azido bridging mode.

The intramolecular Cu...Cu distance is found to be 3.170 Å and the axial Cu(1)–N5(a) distance found to be 2.4574 Å. The nitrogen atoms N(2) and N(5) are closer to the Cu(II) center with the bond distances Cu(1)–N(2) (1.9254 Å) and Cu(1)–N(5) (1.9464 Å) compared to Cu(1)–N(1) (2.0164 Å) and Cu(1)–O(1) (1.9573 Å). The copper atom is slightly deviated from the base of the square pyramid by 0.1116 Å. The distortion from the regular square planar structure is evident from the departure of the bond angles around Cu(II) [N2–Cu1–N1 (80.42(16)), N2–Cu1–O1 (80.14(13)), O1–Cu1–N5 (96.54(13)), N5–Cu1–N1 (101.34(17))] from 90°. The found distortion may be due to the rigidity of the chelate rings formed.

Selected bond lengths (Å) and bond angles (°) of  $[\text{Cu}_2\text{L}_2^2(\mu\text{-N}_3)_2]$  are shown in Table 4.3.

Table 4.3. Selected bond lengths (Å) and bond angles (°) of  $[\text{Cu}_2\text{L}_2^2(\mu\text{-N}_3)_2]$  (**10a**)

Cu(1)–N(1)	2.016(4)
Cu(1)–N(2)	1.925(4)
Cu(1)–O(1)	1.957(3)
Cu(1)–N(5)	1.946(4)
Cu(1)–N5(a)	2.457(4)
O(1)–C(8)	1.275(5)
N(2)–N(3)	1.362(5)
N(3)–C(8)	1.363(5)
N(4)–C(8)	1.333(5)
N(2)–C(6)	1.289(5)
Cu···Cu	3.170
N(1)–Cu(1)–N(2)	80.42(16)
N(2)–Cu(1)–N(5)	174.18(15)
N(2)–Cu(1)–O(1)	80.14(13)
N(1)–Cu(1)–O(1)	159.40(15)
N(5)–Cu(1)–N(1)	101.34(17)
N(1)–Cu(1)–N5(a)	92.47(14)
N(5)–Cu(1)–N5(a)	88.62(14)

The unit cell packing diagram of the compound **10a** viewed along **b**-axis is given in Fig. 4.2.

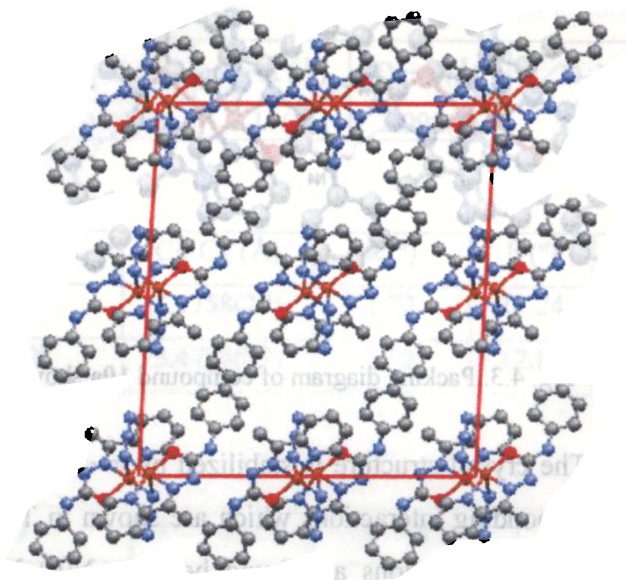


Fig. 4.2. Packing diagram of compound **10a** along **b**-axis

It can be observed that the molecules are packed in a 2-dimensional manner with the parallel arrangement of rings. The adjacent units are interconnected through H-bonding interactions involving N(4) hydrogen and N(3) with donor- acceptor distance 2.9925 Å.

Packing diagram of compound **10a** showing H-bonding is shown in Fig. 4.3.

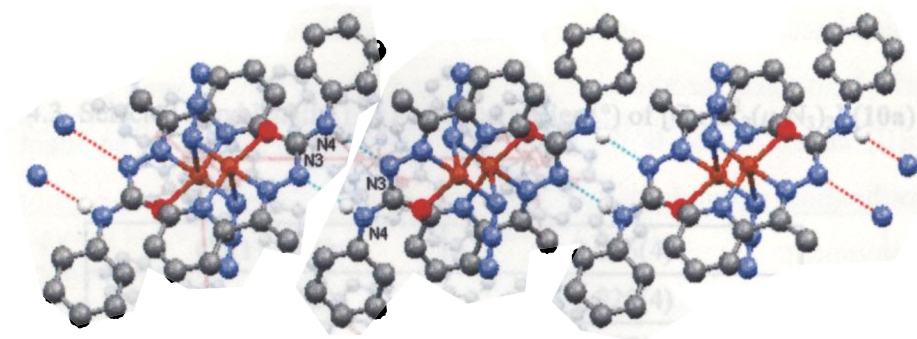


Fig. 4.3. Packing diagram of compound **10a** showing H bonding

The crystal structure is stabilized by  $\pi\cdots\pi$ , C-H $\cdots\pi$ , ring-metal and hydrogen bonding interactions which are shown in Table 4.4. Additional Y-X $\cdots\pi$  ring interactions are found between N(6)–N(7) and Cg(3) and similarly between N(6)–N(7) and Cg(4) with  $d_{\text{N}(7)\text{--Cg}} = 3.5215 \text{ \AA}$  and  $d_{\text{N}(7)\text{--Cg}} = 3.5915 \text{ \AA}$  respectively [Sym. Code: 1-x,1-y,1-z]. Ring-metal interactions Cg(3)–Cu(1)<sup>i</sup> and Cg(4)–Cu(1)<sup>i</sup> [ $i=1-x,-y,1-z$ ] are observed at a distance of 3.713 and 3.642  $\text{\AA}$  respectively. The  $\pi\cdots\pi$  interactions are rather weak, with 3.4758(27)  $\text{\AA}$  being a minimum distance between the centroids.

Table 4.4. Interaction parameters of compound 10a

Hydrogen bonding interactions.

D-H...A	D-H (Å)	H...A (Å)	D...A (Å)	∠D-H...A(°)
N(4)-H(104)...N(3A) <sup>a</sup>	0.80(4)	2.19(4)	2.992(5)	179(4)

[ $\pi$ ... $\pi$  Interactions]

Cg(I)-Res(I) ...Cg(J)	Cg-Cg (Å)	$\alpha$ (°)	$\beta$ (°)	$\gamma$ (°)
Cg(2)...[1]...Cg(4) <sup>b</sup>	3.4758(27)	1.72	11.24	12.85
Cg(4)...[1]...Cg(2) <sup>b</sup>	3.4758(27)	1.72	12.85	11.24

C-H... $\pi$  interactions

X-H(I)...Cg(J)	H...Cg (Å)	X...Cg (Å)	∠X-H...Cg (°)
C(12)-H(12)[1]...Cg(5) <sup>c</sup>	2.71	3.531(5)	148

Ring-Metal Interactions

Cg(I) Res(I) Me(J)	Cg(I)-Me(J) (Å)	$\beta$ (°)
Cg(3) [1] -> Cu(1) <sup>d</sup>	3.713	22.34
Cg(4) [1] -> Cu(1) <sup>d</sup>	3.642	18.27

N-N...  $\pi$  interactions

Y-X(I) Res(I) Cg(J)	X...Cg (Å)	∠Y-X...Cg (°)	Y...Cg (Å)
N(6)-N(7)[1] -> Cg(3) <sup>e</sup>	3.521(5)	60.5(3)	3.1219(47)
N(6)-N(7)[1] -> Cg(4) <sup>e</sup>	3.591(5)	87.0(3)	3.711(5)

Equivalent position codes: a = x,y,1/2-z; b = 1-x,-y,1-z; c = 3/2-x,1/2+y,1/2-z  
; d = 1-x,-y,1-z; e = 1-x,1-y,1-z

Cg (1) = Cu(1),N(5),Cu(1A),N(5A); Cg (2) = Cu(1),O(1),N(2),N(3),C(8)

Cg (3) = Cu(1),N(1),N(2),C(5), C(6); Cg (4) = N(1),C(1),C(2),C(3),C(4),C(5)

D, donor; A, acceptor; Cg, centroid;  $\alpha$ , dihedral angles between planes I and J;  $\beta$ , angle Cg(I) and Cg(J).

### 4.3.3. IR spectra

The tentative assignments of the IR spectral bands of HL<sup>2</sup> and its copper(II) complexes useful for determining the ligand's mode of coordination are listed in Table 4.5.

The peak at 1599 cm<sup>-1</sup> corresponding to  $\nu(\text{C}=\text{N})$  in the IR spectrum of uncomplexed semicarbazone shifts to lower wavenumbers by 10-30 cm<sup>-1</sup> in the spectra of the complexes [20].

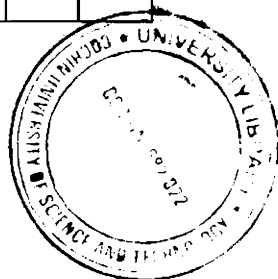
Coordination of azomethine nitrogen is confirmed with the presence of a new band at 412–453 cm<sup>-1</sup>, assignable to  $\nu(\text{Cu}-\text{N})$  for these complexes [20,21]. The occurrence of  $\nu(\text{N}-\text{N})$  at higher wavenumbers in the spectra of the complexes compared to that of the ligand confirms the coordination of the azomethine nitrogen [22]. The IR spectra of the complexes except compounds **13** and **14** show new sharp bands in the 1510-1575 cm<sup>-1</sup> range which is assigned to the newly formed C=N. This indicates that the ligand enolizes and coordinates in the enolate form [23].

The spectral band  $\nu(\text{C}=\text{O})$  of semicarbazone disappears in the complexes except **13** and **14** indicating deprotonation of NH proton and coordination *via* the enolate oxygen [24]. The presence of a new band assignable to  $\nu(\text{Cu}-\text{O})$  around 500 cm<sup>-1</sup> is another indication of the involvement of oxygen coordination. The absence of spectral bands in the region of coordinated water according to Stefov. *etal* in the spectra of complexes indicates that the water molecules are not coordinated but are present as lattice water [25,26].

Table 4.5. Infrared spectroscopic assignments ( $\text{cm}^{-1}$ ) for the 2-acetylpyridine-*N*(4)-phenylsemicarbazone and its copper(II) complexes

Compound	$\nu(\text{NH})$	$\nu(\text{C}=\text{N})$	$\nu(\text{N}-\text{N})$	$\nu(\text{C}=\text{O})$	$\nu(\text{Cu}-\text{N})$	$\nu(\text{C}=\text{N})^a$	$\nu(\text{Cu}-\text{O})$
$\text{HL}^2$	3380	1599	1151	1683	-	-	-
$[\text{Cu}_2\text{L}_2(\text{N}_3)_2] \cdot \text{CH}_3\text{OH}$ (10)	3199	1597	1176	-	453	1514	514
$[\text{Cu}_2\text{L}_2(\text{OAc})_2] \cdot 2\text{H}_2\text{O}$ (11)	3271	1573	1157	-	416	1520	511
$[\text{CuL}^2\text{NO}_3] \cdot \frac{1}{2}\text{H}_2\text{O}$ (12)	3299	1594	1153	-	417	1574	505
$[\text{Cu}(\text{HL}^2)\text{Cl}_2]$ (13)	3276	1573	1198	1652	412	-	505
$[\text{Cu}_2(\text{HL}^2)_2(\text{SO}_4)_2] \cdot 2\text{H}_2\text{O}$ (14)	3273	1597	1198	1650	415	-	505
$[\text{CuL}^2\text{ClO}_4]$ (15)	3270	1592	1212	-	417	1538	534
$[\text{CuL}^2\text{Br}] \cdot 2\text{H}_2\text{O}$ (16)	3270	1590	1197	-	412	1572	504
$[\text{CuL}^2] \cdot \frac{1}{2}\text{CH}_3\text{OH}$ (17)	3260	1569	1147	-	413	1518	512
$[\text{Cu}_2\text{L}_2(\text{NCS})_2] \cdot 2\text{H}_2\text{O}$ (18)	3381	1592	1176	-	432	1552	504

a indicates newly formed C=N





In the azido complex, strong bands observed at 2050 and 1355  $\text{cm}^{-1}$  corresponding to  $\nu_a$  and  $\nu_s$  of azido group are assigned to the coordinated azido group. The asymmetric and symmetric stretching vibrations of the acetate group appear at 1573 and 1446  $\text{cm}^{-1}$ , respectively, for complex **11** having the separation value  $\Delta\nu = 127 \text{ cm}^{-1}$  suggests the presence of chelating acetate group linked with the metal center for the complex [27]. We found that compound **12** has four strong bands at 1489, 1384, 1297 and 1020  $\text{cm}^{-1}$  corresponding to  $\nu_1$ ,  $\nu_2$ ,  $\nu_4$  and  $\nu_5$  of the nitrate group indicating the presence of a terminal monodentate coordination of the nitrate group.  $\nu_3$  and  $\nu_6$  could not be assigned due to the richness of the spectrum of the complex.

The sulfato complex has strong bands at 1115 and 1048  $\text{cm}^{-1}$ , indicating the presence of monocoordinated sulfato group. Compound **15** showed bands at 1122 and 1033, and a strong band at 623 and a weak band at 923  $\text{cm}^{-1}$  indicating the presence of coordinated perchlorate. Thiocyanato complex exhibits a strong and sharp band at 2090  $\text{cm}^{-1}$  and a weak band at 751  $\text{cm}^{-1}$  which can be attributed to  $\nu(\text{CN})$  and  $\nu(\text{CS})$  respectively. These values are typical for N bonded thiocyanate complexes. The expected region for copper-halide stretching frequencies is below 400  $\text{cm}^{-1}$  which is beyond the scan range [22,28].

Thus it is seen that the principal ligand  $\text{HL}^2$  acts as a monoanionic tridentate ligand in complexes  $[\text{Cu}_2\text{L}^2_2(\text{N}_3)_2] \cdot \text{CH}_3\text{OH}$ ,  $[\text{Cu}_2\text{L}^2_2(\text{OAc})_2] \cdot 2\text{H}_2\text{O}$ ,  $[\text{CuL}^2\text{NO}_3] \cdot \frac{1}{2}\text{H}_2\text{O}$ ,  $[\text{CuL}^2\text{ClO}_4]$ ,  $[\text{CuL}^2\text{Br}] \cdot 2\text{H}_2\text{O}$ ,  $[\text{CuL}^2_2] \cdot \frac{1}{2}\text{CH}_3\text{OH}$  and  $[\text{Cu}_2\text{L}^2_2(\text{NCS})_2] \cdot 2\text{H}_2\text{O}$ .

The IR spectra of complexes are shown in Figs. 4.4 - 4.12.

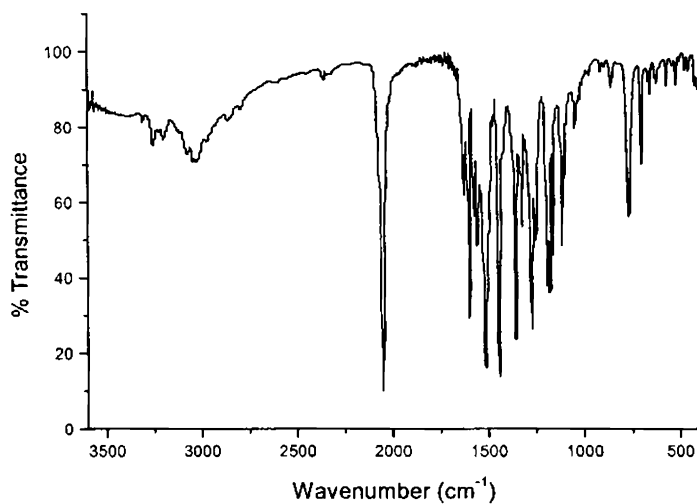


Fig. 4.4. IR spectrum of  $[\text{Cu}_2\text{L}_2(\text{N}_3)_2] \cdot \text{CH}_3\text{OH}$  (10).

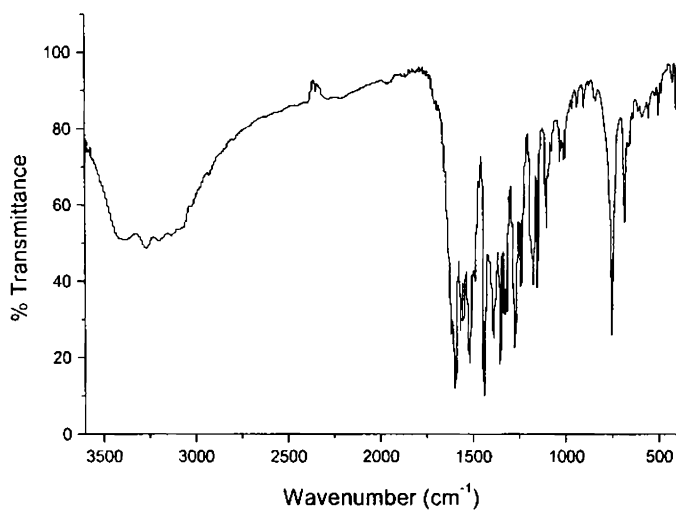


Fig. 4.5. IR spectrum of  $[\text{Cu}_2\text{L}_2(\text{OAc})_2] \cdot 2\text{H}_2\text{O}$  (11).

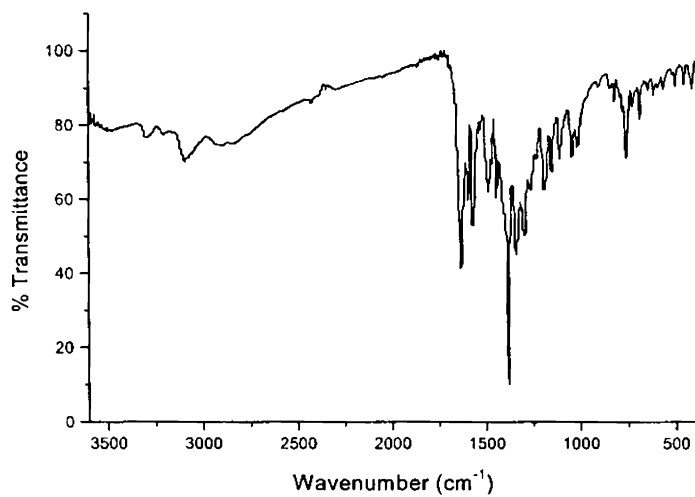


Fig. 4.6. IR spectrum of  $[\text{CuL}^2(\text{NO}_3)] \cdot \frac{1}{2}\text{H}_2\text{O}$  (12).

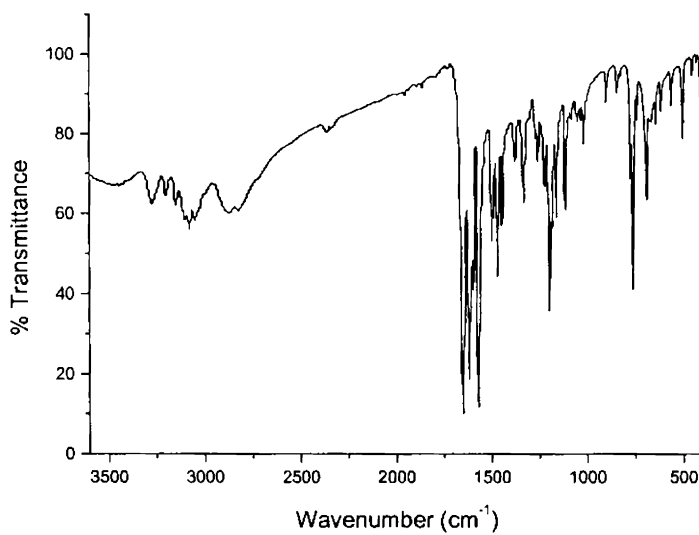


Fig. 4.7. IR spectrum of  $[\text{Cu}(\text{HL}^2)\text{Cl}_2]$  (13).

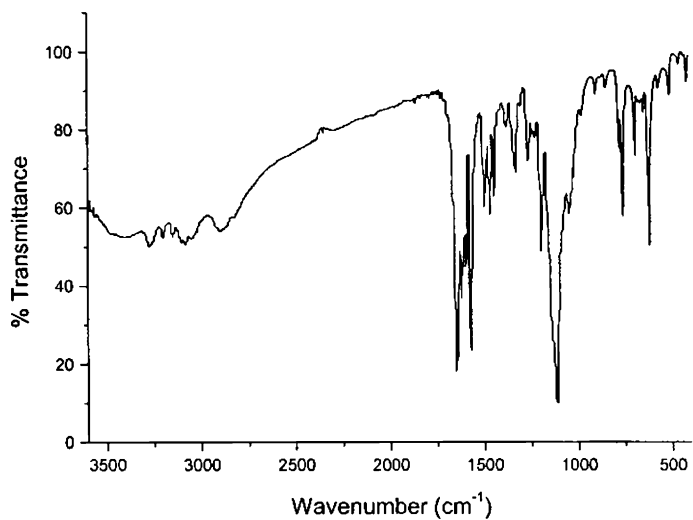


Fig. 4.8. IR spectrum of  $[\text{Cu}_2(\text{HL}^2)_2(\text{SO}_4)_2] \cdot 2\text{H}_2\text{O}$  (14).

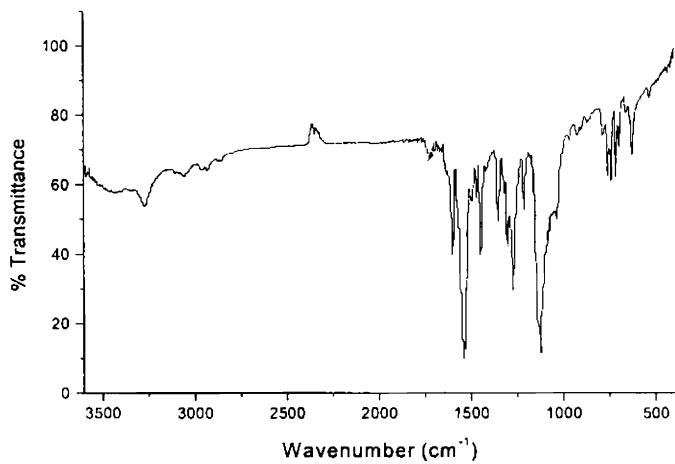


Fig. 4.9. IR spectrum of  $[\text{CuL}^2\text{ClO}_4]$  (15).

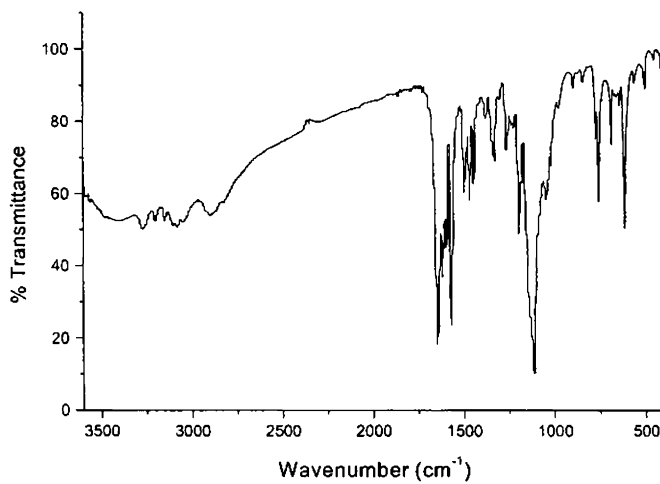


Fig. 4.10. IR spectrum of  $[\text{CuL}^2\text{Br}] \cdot 2\text{H}_2\text{O}$  (16).

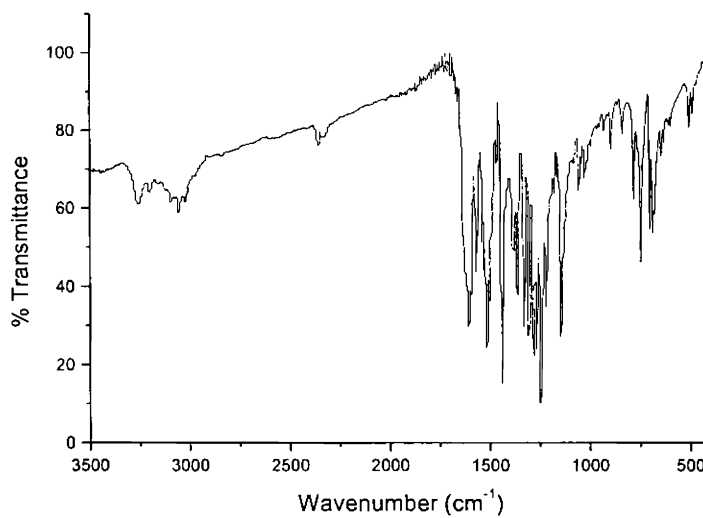


Fig. 4.11. IR spectrum of  $[\text{CuL}^2] \cdot \frac{1}{2}\text{CH}_3\text{OH}$  (17).

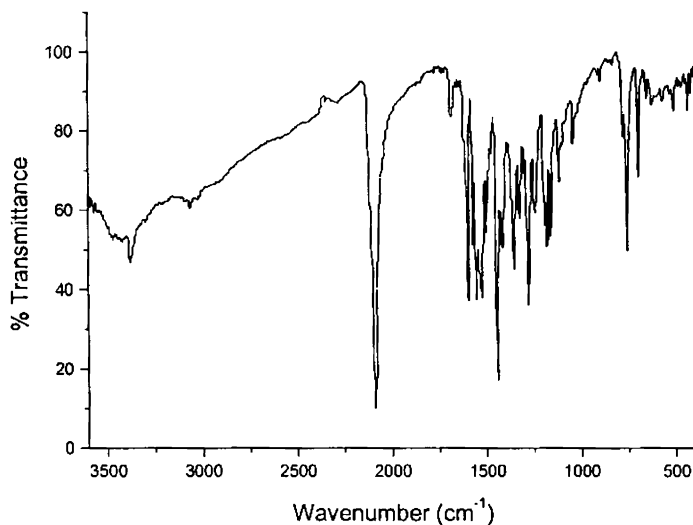


Fig. 4.12. IR spectrum of  $[\text{Cu}_2\text{L}_2^2(\text{NCS})_2] \cdot 2\text{H}_2\text{O}$  (18).

#### 4.3.4. Electronic spectra

The variety of colors among transition metal complexes arises from the electronic transition between energy levels whose spacing corresponds to the wavelengths available in visible light. In complexes, these transitions are frequently referred to as *d-d* transitions because they involve the molecular orbitals that are mainly metal *d* in character [29]. Since this spacing depends on factors such as the geometry of the complex, the nature of the ligands present, and the oxidation state of the central metal atom, the electronic spectra of complexes can provide valuable information relating to bonding and structure [30].

The electronic spectrum of HL<sup>2</sup> consists of a broad band at 33900 cm<sup>-1</sup> which is n→π\* band of the pyridine ring. The electronic spectra of Cu(II) complexes consist of bands in the region 31000-38000 cm<sup>-1</sup>. These broad bands can be regarded as a combination of n→π\* transitions and π→π\* of aromatic rings and semicarbazide moiety respectively [31]. The charge transfer bands were observed as broad bands between 24000 and 26000 cm<sup>-1</sup>, and their broadness can be explained as due to the combination of O→Cu and N→Cu LMCT transitions [32].

For copper(II) complexes, there are three spin allowed transitions, A<sub>1g</sub>←B<sub>1g</sub>, B<sub>2g</sub> ←B<sub>1g</sub> and E<sub>g</sub>←B<sub>1g</sub>. But it is very difficult to resolve the three spin allowed transitions into separate bands due to the very low energy difference between these bands. All the complexes gave *d-d* bands in the 15000-18000 cm<sup>-1</sup> range [33-35].

The band n→π\* which is found at 33900 cm<sup>-1</sup> in the spectrum of uncomplexed semicarbazone was slightly shifted on complexation. This is an indication of the enolization followed by the deprotonation of the ligand during complexation.

The significant electronic absorption bands in the spectra of the ligand and all the complexes recorded in acetonitrile solution are presented in Table 4.6.

Table 4.6. Electronic spectral assignments,  $\lambda$  ( $\text{cm}^{-1}$ ) for  $\text{HL}^2$  and its copper(II) complexes

Compound	d→d	LMCT	n→π* π→π*
$\text{HL}^2$	-	-	33900
$[\text{Cu}_2\text{L}_2(\text{N}_3)_2] \cdot \text{CH}_3\text{OH}$ (10)	17350	25290	32890
$[\text{Cu}_2\text{L}_2(\text{OAc})_2] \cdot 2\text{H}_2\text{O}$ (11)	14340	25320	32530
$[\text{CuL}^2\text{NO}_3] \cdot \frac{1}{2} \text{H}_2\text{O}$ (12)	16950	24100	34720, 32520
$[\text{Cu}(\text{HL}^2)\text{Cl}_2]$ (13)	17090	25150	32520
$[\text{Cu}_2(\text{HL}^2)_2(\text{SO}_4)_2] \cdot 2\text{H}_2\text{O}$ (14)	14470	25210	34790, 32680
$[\text{CuL}^2\text{ClO}_4]$ (15)	17450	25350	34360, 32890
$[\text{CuL}^2\text{Br}] \cdot 2\text{H}_2\text{O}$ (16)	17550	25130	31690
$[\text{CuL}^2_2] \cdot \frac{1}{2} \text{CH}_3\text{OH}$ (17)	17640	24750	37660, 32430
$[\text{Cu}_2\text{L}_2(\text{NCS})_2] \cdot 2\text{H}_2\text{O}$ (18)	16410	25250	34630, 33280

The electronic spectra of some of the copper(II) complexes of  $\text{HL}^2$  are shown in the Figs. 4.13 and 4.14.



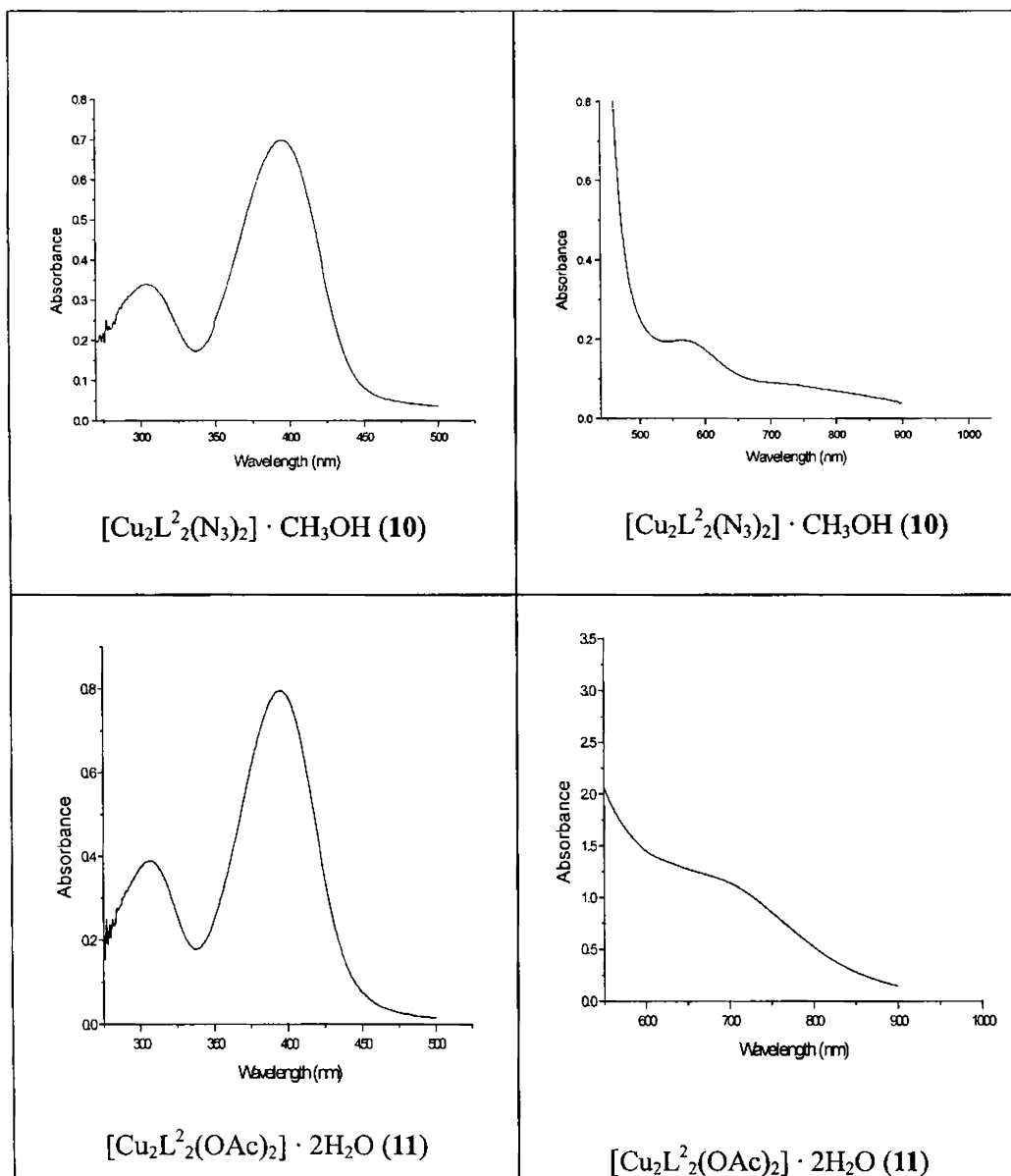


Fig. 4.13. Electronic spectra of copper(II) complexes (10 and 11).

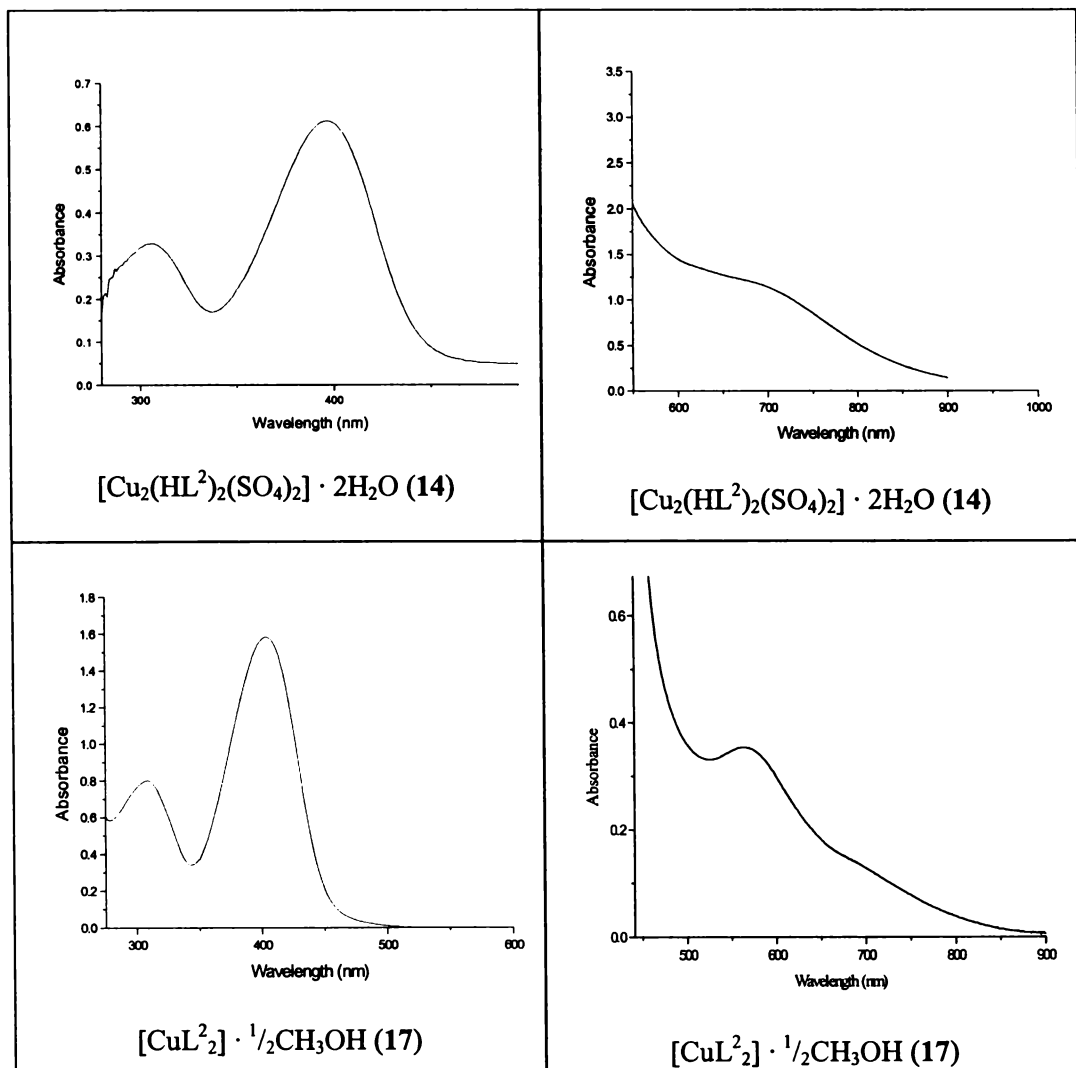


Fig. 4.14. Electronic spectra of complexes (14 and 17)

#### 4.3.5. Electron paramagnetic resonance spectra

The EPR spectra of the polycrystalline samples at 298 K and DMF solution at 77 K were recorded in the X-band, using 100-kHz modulation;  $g$  factors were quoted relative to the standard marker TCNE ( $g = 2.00277$ ). The EPR parameters of the copper(II) complexes are presented in the Table 4.7. The EPR spectra of the complexes recorded in polycrystalline state at room temperature provide information about the coordination environment around copper(II) in these complexes.

The EPR spectrum of the compound **10** in polycrystalline form at 298 K is given in Fig. 4.15.

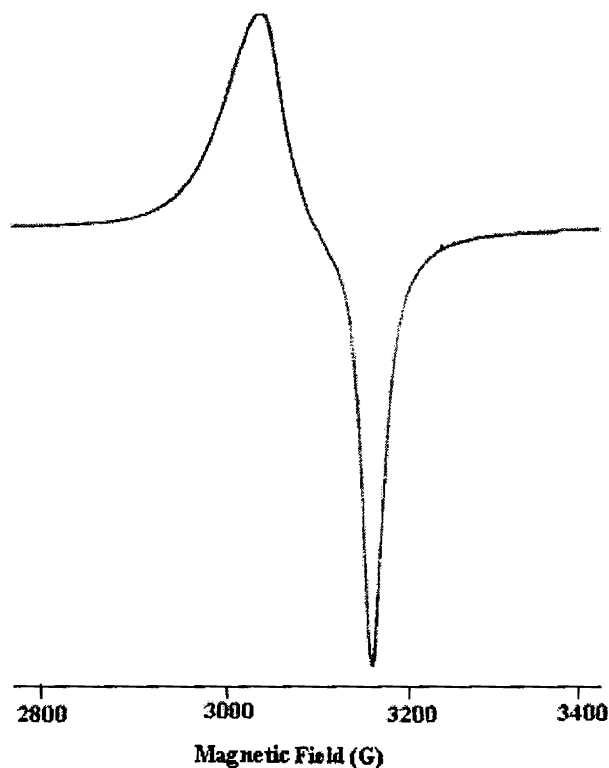


Fig. 4.15. EPR spectrum of  $[\text{Cu}_2\text{L}_2(\text{N}_3)_2] \cdot \text{CH}_3\text{OH}$  (**10**) in polycrystalline state at 298 K.

Table 4.7. Spin Hamiltonian and bonding parameters of copper(II) complexes of 2-acetylpyridine-*N*(4)-phenylsemicarbazone

	10	11	12	13	14	15	16	17	18
Polycrystalline (298 K)									
$g_{\parallel}$	2.142( $g_1$ )	2.265		2.288	2.230	2.269		2.275	
$g_{\perp}$	2.053( $g_2$ )	2.073		2.076	2.093	2.073		2.073	
$g_{\text{iso}}, g_{\text{av}}$		2.137	2.073	2.147	2.139	2.138	2.099	2.141	2.107
$G$		3.630		3.790	2.473	3.685		3.767	
DMF (77 K)									
$g_{\parallel}$	2.199	2.218	2.216	2.213	2.291	2.215	2.207	2.265	2.209
$g_{\perp}$	2.056	2.059	2.056	2.059	2.080	2.060	2.054	2.078	2.056
$A_{\parallel}/A_{\perp}$	186.7	191.6	191.6	185.0	208.3	186.7	190.0	196.7	188.3
$\alpha^2$	0.7783	0.8122	0.8089	0.7889	0.9406	0.7960	0.7942	0.8815	0.7928
$\beta^2$	0.9298	0.8923	0.9142	0.9346	0.9084	0.9404	0.9272	0.8948	0.9026
$\gamma^2$	0.9717	0.9150	0.9166	0.9696	0.9425	0.9796	0.9320	0.9607	0.9213
$K_{\parallel}$	0.7237	0.7247	0.7395	0.7373	0.8544	0.7486	0.7364	0.7888	0.7156
$K_{\perp}$	0.7563	0.7432	0.7414	0.7649	0.8865	0.7798	0.7402	0.8469	0.7295

 $A$  values in  $10^{-4} \text{ cm}^{-1}$

The EPR spectrum of **10** in the polycrystalline state at 298 K gives a near isotropic signal with two  $g$  values,  $g_1 = 2.142$  and  $g_2 = 2.053$ . This broadening of the spectrum may be due to the exchange coupling between copper centers [36]. This means that compound **10** is a dimer or polynuclear and from X-ray diffraction studies, it is confirmed that it is a dimer.

All the spectra in DMF solution at 77 K are axial with well resolved four hyperfine lines in the parallel region corresponding to coupling of the electron spin with the nuclear spin ( $^{63,65}\text{Cu}$ ,  $I = 3/2$ ).

In polynuclear copper(II) complexes, due to Cu—Cu dipolar interaction, the zero field splitting parameter,  $D$  gives rise to transitions corresponding to  $\Delta M_s = \pm 2$ . In the X-band spectra,  $\Delta M_s = \pm 1$  transitions are associated with fields of *ca.* 3000 Gauss, while the  $\Delta M_s = \pm 2$  generate a transition at the half field value of *ca.* 1500 Gauss.

The EPR spectrum of the compound **10** in DMF solution at 77 K is given in Fig, 4.16. The EPR spectrum of compound **10** in DMF at 77 K is axial with well defined  $g_{\parallel}$  and  $g_{\perp}$  values. It showed a half field signal at  $g = 4.107$  which indicates that a weak interaction between two Cu(II) ions within this compound is present. The presence of this half field band is a useful criterion for dipolar interaction from the presence of some binuclear complex formation.

The above spectrum gives five superhyperfine splitting lines in the perpendicular region which may be due to the coordination of azomethine nitrogen and nitrogen from the equatorial azido group. From the crystallographic data, it is observed that these two nitrogens are closer to

the copper centre than the other two. That is why only five superhyperfine lines are observed even if four nitrogens are coordinated to the metal.

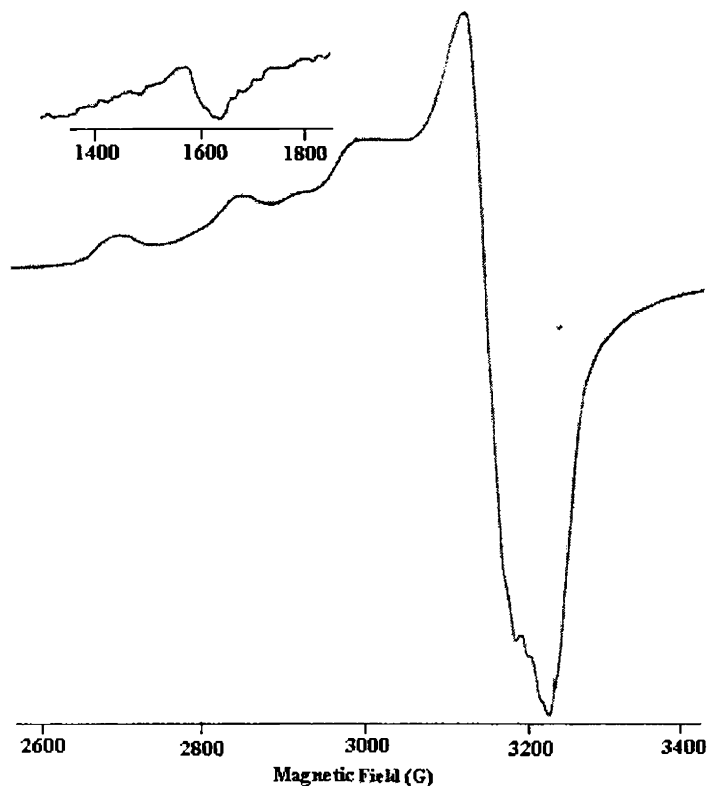


Fig. 4.16. EPR spectrum of  $[\text{Cu}_2\text{L}_2(\text{N}_3)_2] \cdot \text{CH}_3\text{OH}$  (**10**) in DMF at 77 K.

The EPR spectra of the compound **11** in polycrystalline form at 298 K and in DMF solution at 77 K are given in Figs. 4.17 and 4.18 respectively. The EPR spectrum of the compound **11** in polycrystalline state at 298 K is axial with  $g_{\parallel}$  and  $g_{\perp}$  values as 2.265 and 2.073 respectively. The spectrum exhibits a half field signal ( $g = 4.101$ ), which indicates the formation of binuclear complex [37].

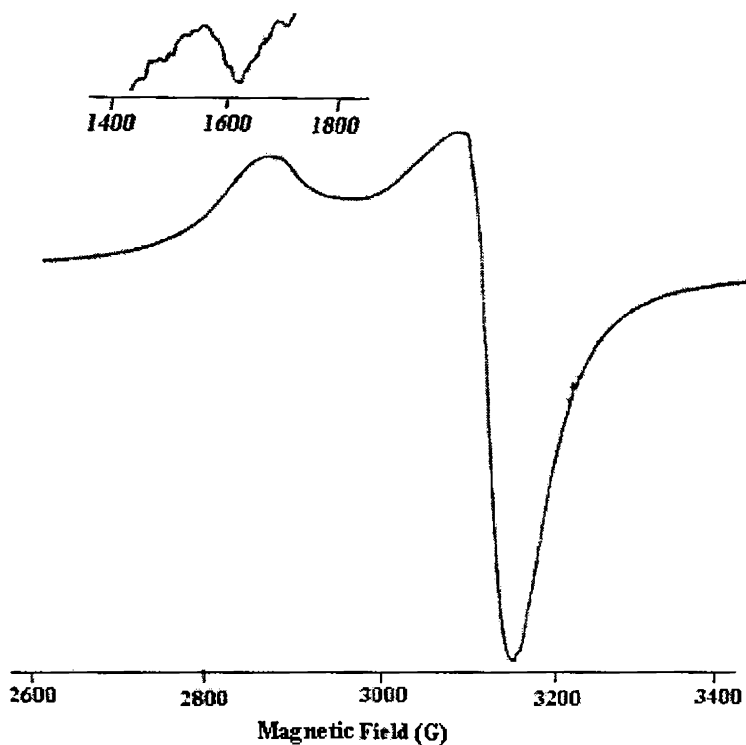


Fig. 4.17. EPR spectrum of  $[\text{Cu}_2\text{L}_2(\text{OAc})_2] \cdot 2\text{H}_2\text{O}$  (**11**) in polycrystalline at 298 K.

The EPR spectrum of compound **11** in DMF at 77 K is axial with four well resolved hyperfine splitting lines in the parallel and perpendicular regions ( $A_{\parallel} = 191.6$  and  $A_{\perp} = 33.3 \times 10^{-4} \text{ cm}^{-1}$ )

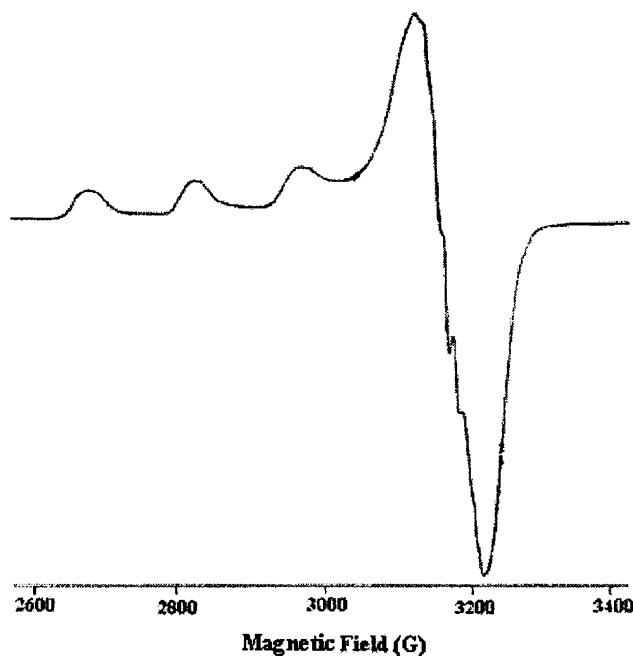


Fig. 4.18. EPR spectrum of  $[\text{Cu}_2\text{L}_2(\text{OAc})_2] \cdot 2\text{H}_2\text{O}$  (**11**) in DMF at 77 K.

The EPR spectra of compounds **12**, **16** and **18** in the polycrystalline state at 298 K (Figs. 4.19-4.21) showed only one broad signal at  $g_{\text{iso}} = 2.073$ , 2.099 and 2.107 respectively. Such isotropic spectra have only one  $g$  value which arises from extensive exchange coupling through misalignment of local molecular axes between different molecules in the unit cell and enhanced spin lattice relaxation. These types of spectra unfortunately give no information on the electronic ground state of the Cu(II) ion present in the complexes.



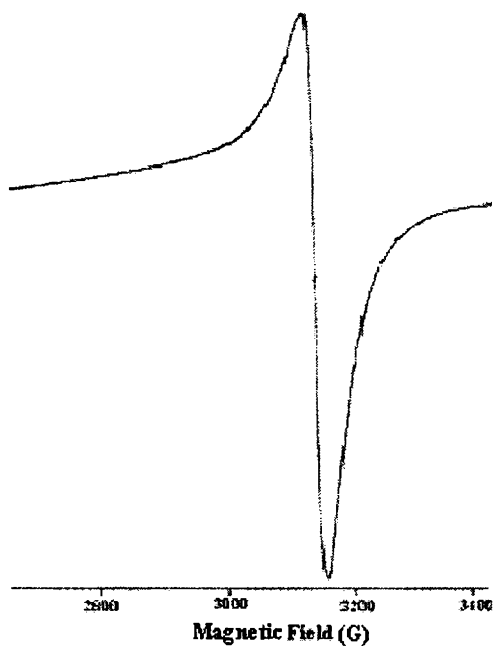


Fig. 4.19. EPR spectrum of  $[\text{CuL}^2\text{NO}_3] \cdot \frac{1}{2} \text{H}_2\text{O}$  (12) in polycrystalline state at 298 K.

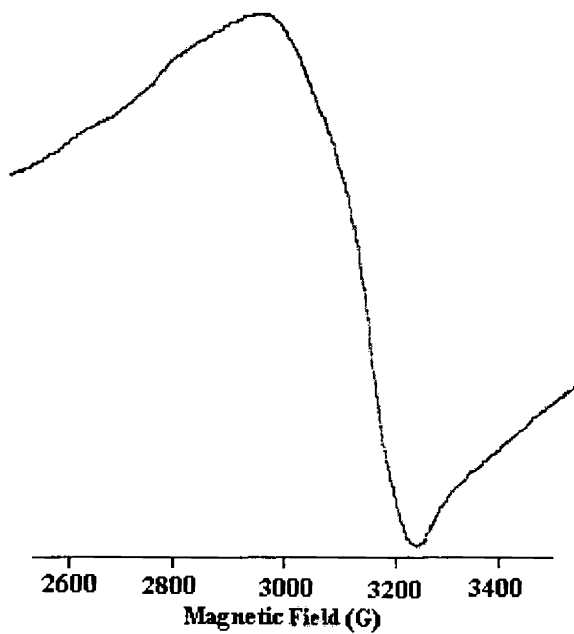


Fig. 4.20. EPR spectrum of  $[\text{CuL}^2\text{Br}] \cdot 2 \text{H}_2\text{O}$  (16) in polycrystalline state at 298 K.

In addition, the EPR spectrum of compound **18** in the polycrystalline state at 298 K, exhibits a half field signal ( $g = 4.173$ ), which indicates that indeed a weak interaction between two Cu(II) ions within this compound is present and the complex may be binuclear [37].

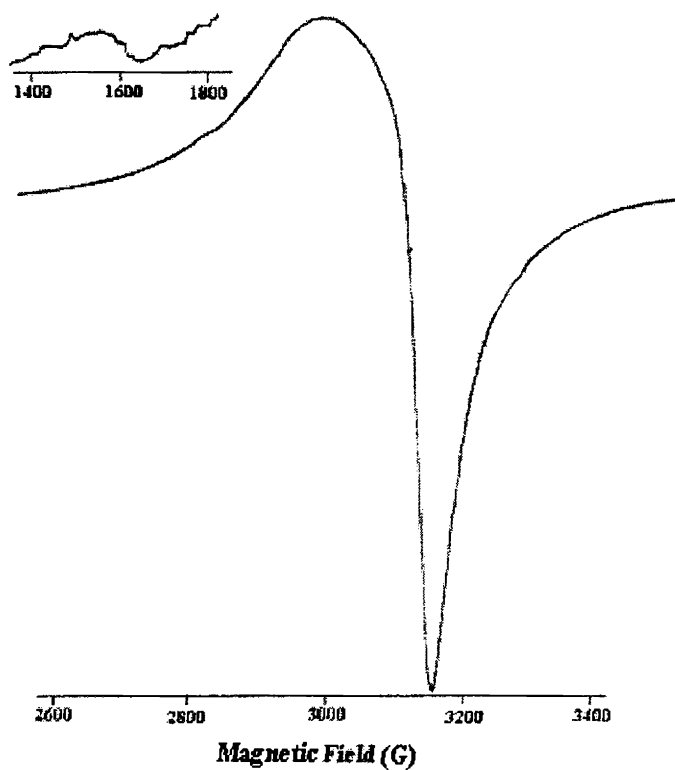


Fig. 4.21. EPR spectrum of  $[\text{Cu}_2\text{L}_2(\text{NCS})_2] \cdot 2 \text{H}_2\text{O}$  (**18**) in polycrystalline state at 298K

The EPR spectrum of the compound **12** in DMF solution at 77 K is axial (Fig. 4.22) with  $g_{\parallel}$  and  $g_{\perp}$  values as 2.216 and 2.056 respectively.

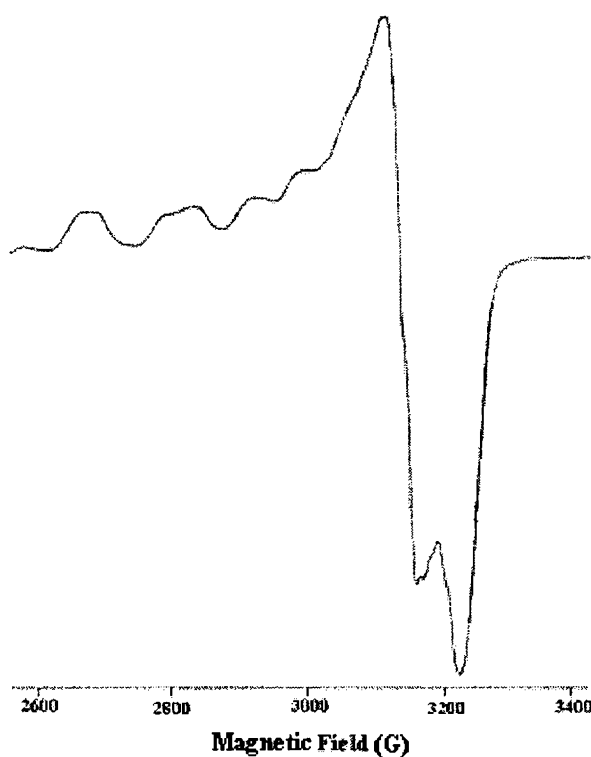


Fig. 4.22. EPR spectrum of  $[\text{CuL}^2\text{NO}_3] \cdot \frac{1}{2} \text{H}_2\text{O}$  (**12**) in DMF at 77 K.

The EPR spectrum of compound **12** in DMF at 77 K gives three superhyperfine splittings in the perpendicular region which may be due to the coordination of azomethine nitrogen from the semicarbazone moiety.

The EPR spectra of the compounds **13**, **14**, **15** and **17** in polycrystalline form at 298 K are axial in nature (Figs. 4.23-4.26). The EPR spectrum of compound **14** in the polycrystalline state at 298 K, exhibited a half field signal ( $g = 4.107$ ) [37].

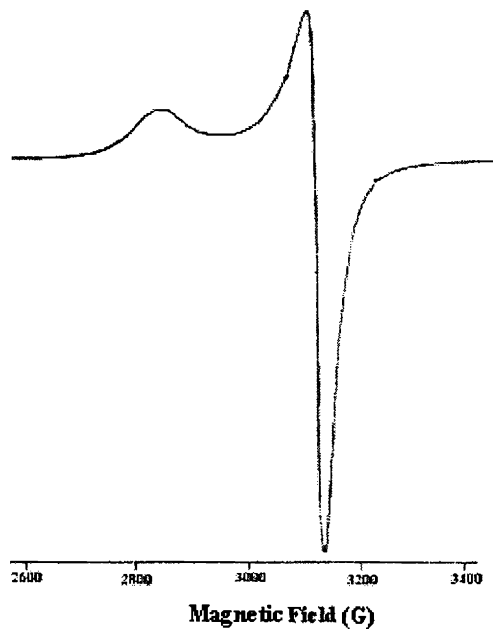


Fig. 4.23. EPR spectrum of  $[\text{Cu}(\text{HL}^2)\text{Cl}_2]$  (**13**) in polycrystalline state at 298 K.

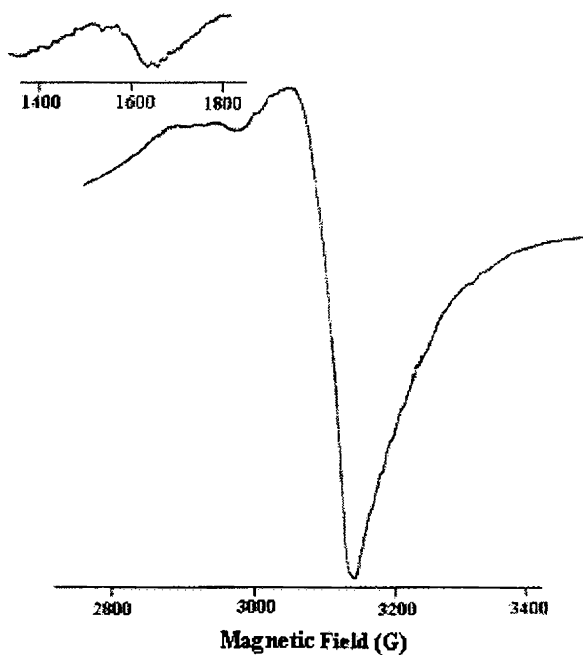


Fig. 4.24. EPR spectrum of  $[\text{Cu}_2(\text{HL}^2)_2(\text{SO}_4)_2] \cdot 2\text{H}_2\text{O}$  (**14**) in polycrystalline state at 298 K.

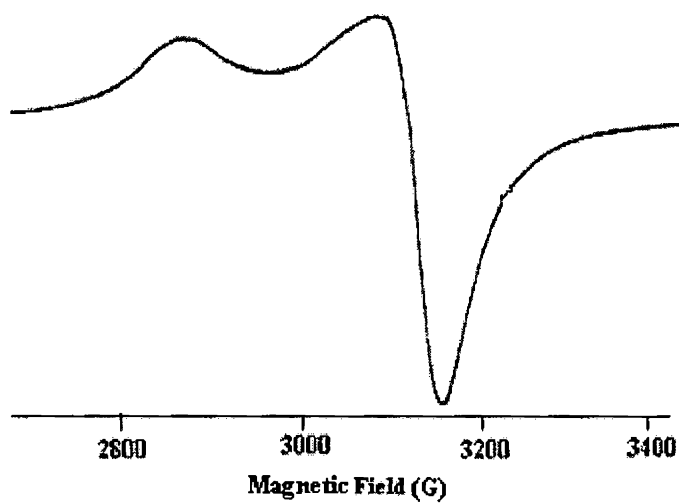


Fig. 4.25. EPR spectrum of  $[\text{CuL}^2\text{ClO}_4]$  (15) in polycrystalline state at 298 K.

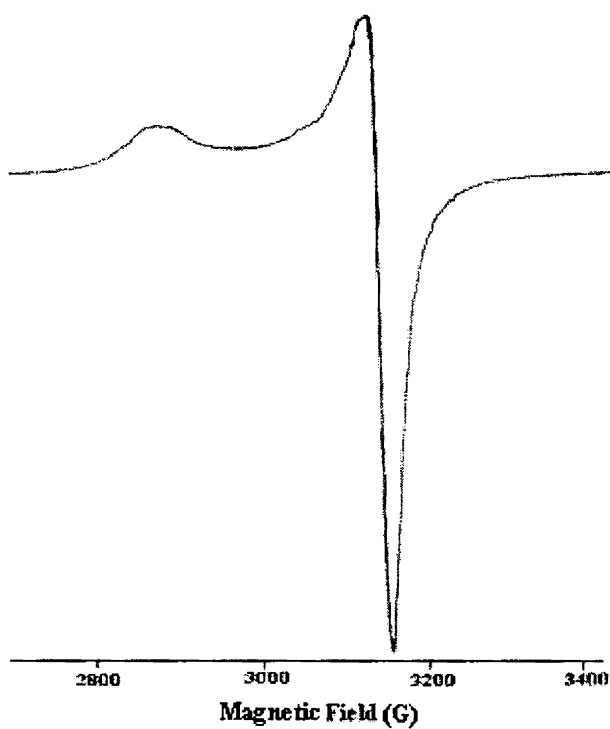


Fig. 4.26. EPR spectrum of  $[\text{CuL}^2_2] \cdot \frac{1}{2} \text{CH}_3\text{OH}$  (17) in polycrystalline state at 298 K.

The EPR spectrum of compound **13** in DMF at 77 K gives more than five superhyperfine splitting in the perpendicular region (Fig. 4.27). This means that chlorine as well as nitrogen from semicarbazone moiety is coordinated to the metal centre.

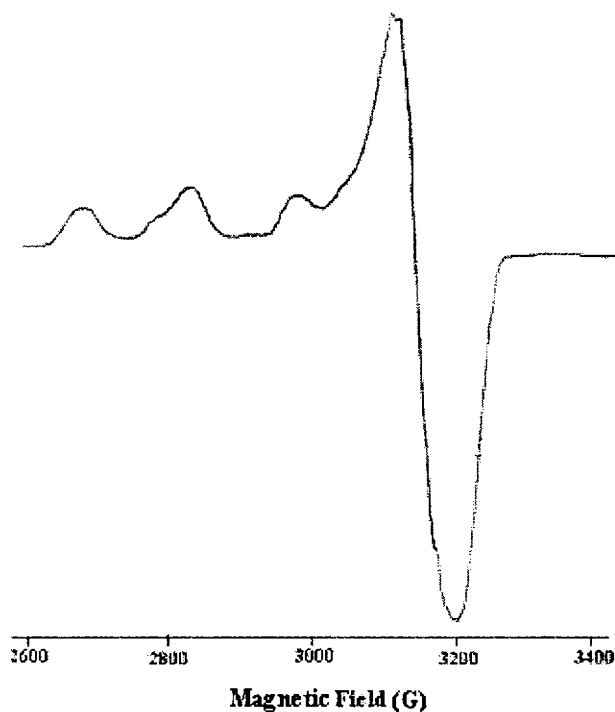


Fig. 4.27. EPR spectrum of  $[\text{Cu}(\text{HL}^2)\text{Cl}_2]$  (**13**) in DMF at 77 K.

The EPR spectrum of compound **14** in DMF at 77 K gives three superhyperfine splitting in the perpendicular region which may be due to the coordination of azomethine nitrogen from the semicarbazone moiety (Fig. 4.28).

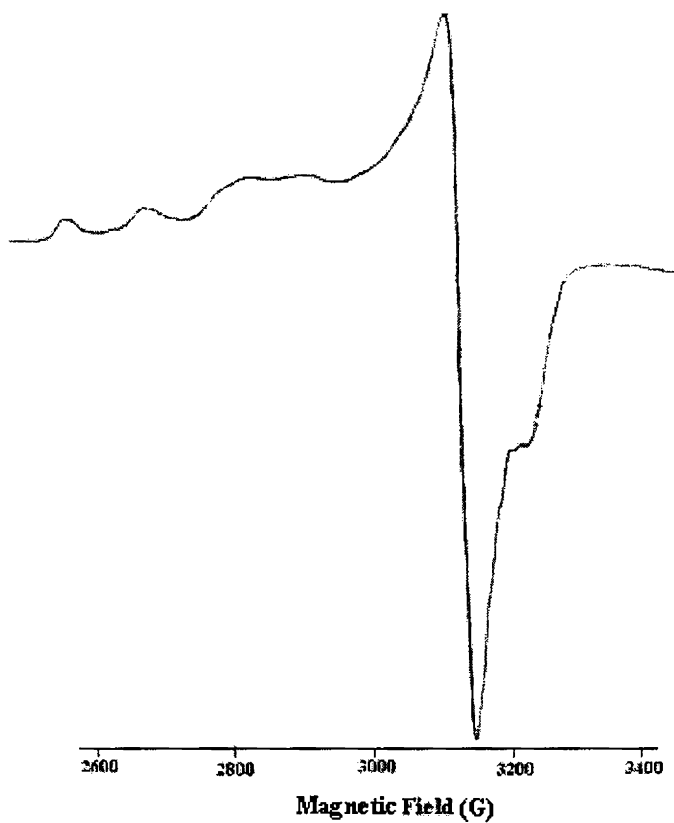


Fig. 4.28. EPR spectrum of  $[\text{Cu}_2(\text{HL}^2)_2(\text{SO}_4)_2] \cdot 2 \text{H}_2\text{O}$  (**14**) in DMF at 77 K.

The EPR spectra of **15** and **16** in DMF solution at 77 K are axial in nature with four well resolved hyperfine splitting lines in the parallel and perpendicular region (Figs. 4.29 and 4.30).

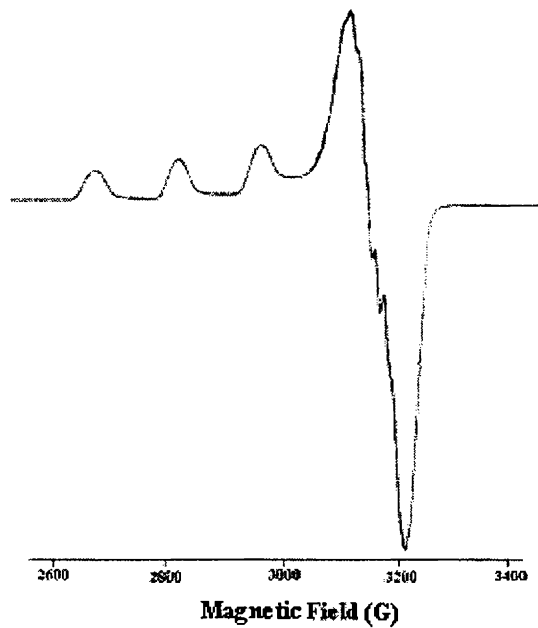


Fig. 4.29. EPR spectrum of  $[\text{CuL}^2\text{ClO}_4]$  (**15**) in DMF at 77 K.

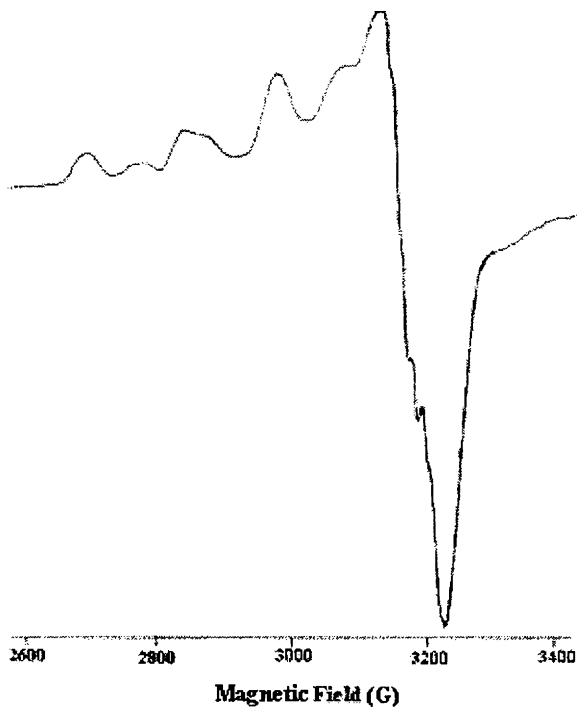


Fig. 4.30. EPR spectrum of  $[\text{CuL}^2\text{Br}] \cdot 2 \text{H}_2\text{O}$  (**16**) in DMF at 77 K.



The EPR spectrum of **17** in DMF solution at 77 K is also axial with  $g_{\parallel}$  and  $g_{\perp}$  values as 2.265 and 2.078 respectively (Fig. 4.31). The spectrum gives five superhyperfine splitting in the perpendicular region which may be due to the coordination of azomethine nitrogen from each ligand moiety.

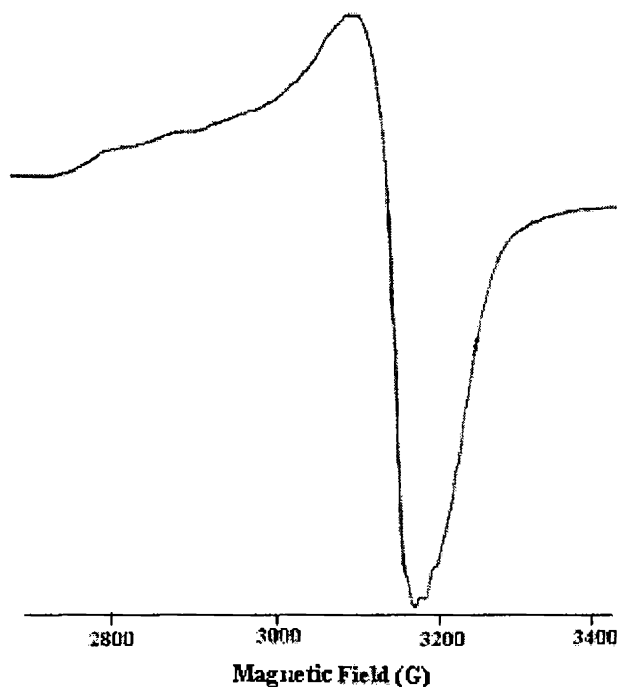


Fig. 4.31. EPR spectrum of  $[\text{CuL}_2] \cdot \frac{1}{2} \text{CH}_3\text{OH}$  (**17**) in DMF at 77 K.

The EPR spectrum of compound **18** in DMF solution at 77 K is axial (Fig. 4.32) with  $g_{\parallel}$  and  $g_{\perp}$  values as 2.209 and 2.056 respectively. The spectrum shows four hyperfine splitting lines both in the parallel and perpendicular region and no superhyperfine splitting is observed in this case.

The geometric parameter  $G$ , which is a measure of exchange interaction between the copper centers in the polycrystalline compound, is calculated and the value of  $G$  is found to be in the range 2.4-3.8. It is perceived that, if  $G > 4$ , the exchange interaction is negligible and vice versa in the complexes. The  $G$  values indicate that the exchange interactions are strong in all these complexes. In all the complexes,  $g_{\parallel} > g_{\perp} > 2.0023$  is consistent with a  $d_{x^2-y^2}$  ground state in a square planar or square pyramidal geometry [36].

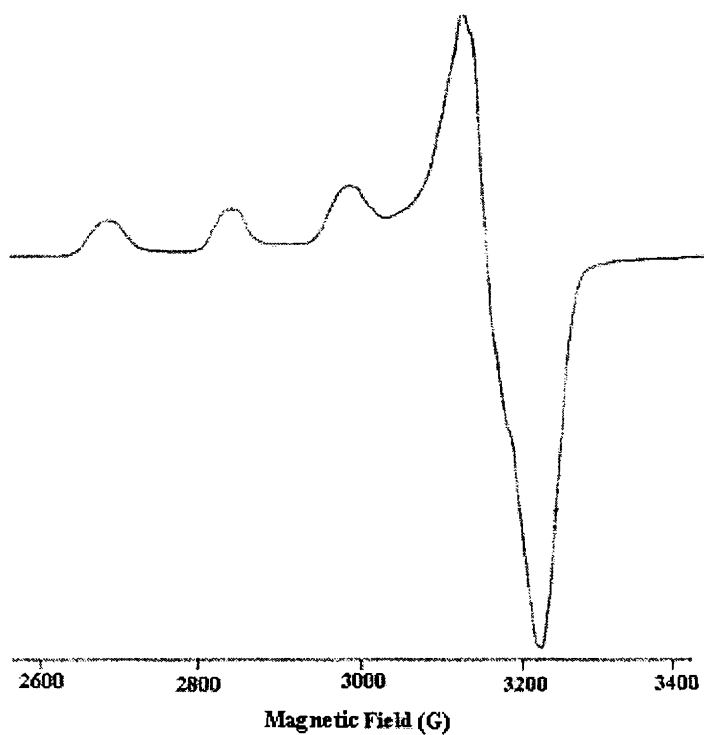


Fig. 4.32. EPR spectrum of  $[\text{Cu}_2\text{L}_2(\text{NCS})_2] \cdot 2 \text{H}_2\text{O}$  (**18**) in DMF at 77 K.

The variations in  $g$  values indicate that the geometry of the compounds is affected by the nature of the coordinating ligands. The  $g_{\parallel}$

values of all the compounds are found to be almost the same, which indicate that the bonding is dominated by the semicarbazone moiety. The  $g_{\parallel} > g_{\perp}$  values accounts to the distorted square pyramidal structure and rules out the possibility of a trigonal bipyramidal structure which would be expected to have  $g_{\perp} > g_{\parallel}$ . The fact that the  $g_{\parallel}$  values are less than 2.3 is an indication of significant covalent character to the M–L bond [23,29].

The EPR parameters  $g_{\parallel}$ ,  $g_{\perp}$ ,  $g_{av}$ ,  $A_{\parallel}(\text{Cu})$  and  $A_{\perp}(\text{Cu})$  and the energy values of the  $d-d$  transition were used to evaluate the bonding parameters  $\alpha^2$ ,  $\beta^2$  and  $\gamma^2$  which may be regarded as measures of the covalency of the in-plane  $\sigma$ -bonds, in-plane  $\pi$ -bonds, and out-of-plane  $\pi$ -bonds respectively. The value of in-plane sigma bonding parameter  $\alpha^2$  was calculated using the expression:

$$\alpha^2 = -A_{\parallel} / 0.036 + (g_{\parallel} - 2.0023) + 3/7(g_{\perp} - 2.0023) + 0.04 \quad [38]$$

The orbital reduction factors,  $K_{\parallel} = \alpha^2 \beta^2$  and  $K_{\perp} = \alpha^2 \gamma^2$  were calculated using the following expressions [39]:

$$K_{\parallel}^2 = (g_{\parallel} - 2.0023) E_{d-d} / 8\lambda_0$$

$$K_{\perp}^2 = (g_{\perp} - 2.0023) E_{d-d} / 2\lambda_0$$

where  $\lambda_0$  is the spin-orbit coupling constant with a value of  $-828 \text{ cm}^{-1}$  for copper(II)  $d^9$  system. According to Hathaway [37], for pure  $\sigma$ -bonding,  $K_{\parallel} \approx K_{\perp} \approx 0.77$ , and for in-plane  $\pi$ -bonding,  $K_{\parallel} < K_{\perp}$ ; while for out-of-plane  $\pi$ -bonding,  $K_{\perp} < K_{\parallel}$ . In all the complexes, it is observed that  $K_{\parallel} < K_{\perp}$  which indicates the presence of significant in-plane  $\pi$ -bonding. This is further confirmed by the bonding parameters  $\alpha^2$ ,  $\beta^2$  and  $\gamma^2$ , which are less than 1.0 expected of the purely ionic character of the bonds, and decreases with the increasing covalent nature of the bonding.

*References*

1. M. Akkurt, S. Ozfuric, S. Ide, *Anal.Sci.* 16 (2000) 667.
2. J.R. Dimmock, R.N. Puthucode, J.M. Smith, M. Hetherington, J.W. Quil, U. Pugazhenthii, *J. Med. Chem.* 39 (1996) 3984.
3. J.R. Dimmock, K.K. Sidhu, S.D. Thumber, S.K. Basran, M. Chen, J.W. Quil, *Eur. J. Chem.* 30 (1995) 287.
4. H. Beraldo, D. Gaminob, *Mini Rev. Med. Chem.* 4 (2004) 31.
5. B.S. Garg, M.R.P. Kurup, S.K. Jain, Y.K. Bhoon, *Trans. Met. Chem.* 13 (1988) 92.
6. B.S. Garg, M.R.P. Kurup, S.K. Jain, Y.K. Bhoon, *Trans. Met. Chem.* 13 (1988) 247.
7. B.S. Garg, M.R.P. Kurup, S.K. Jain, Y.K. Bhoon, *Trans. Met. Chem.* 13 (1988) 309.
8. B.S. Garg, M.R.P. Kurup, S.K. Jain, Y.K. Bhoon, *Trans. Met. Chem.* 16 (1991) 111.
9. B.S. Garg, M.R.P. Kurup, S.K. Jain, Y.K. Bhoon, *Synth. React. Inorg. Met.-Org Chem.* 28 (1998) 321.
10. C.K. Alphonsa, M.R.P. Kurup, *Synth. React. Inorg. Met.-Org Chem.* 29 (1999) 805.
11. U.L. Kala, S. Suma, M.R.P. Kurup, Suja Krishnan, R.P. John, *Polyhedron* 26 (2007) 1427.
12. A. Sreekanth, U.L. Kala, C.R. Nayar, M.R.P. Kurup, *Polyhedron* 23 (2004) 41.

13. T.A. Reena, E.B. Seena, M.R.P. Kurup, *Polyhedron* 27 (2008) 1825.
14. Nonius, MACH3 Software, B.V. Nonius, Delft, The Netherlands, 1997.
15. G.M. Sheldrick, *Acta Cryst.* (2008) A64, 112–122.
16. C.F. Macrae, P.R. Edgington, P. McCabe, E. Pidcock, G.P. Shields, R. Taylor, M. Towler, J. van de Streek, *J. Appl. Crystallogr.* 39 (2006) 453.
17. K. Brandenburg, Diamond Version 3.1f, Crystal Impact GbR, Bonn, Germany, 2008.
18. W.J. Geary, *Coord. Chem. Rev.* 7 (1971) 81.
19. A.W. Addison, J.N. Rao, J. Reedijk, G.C. Vershoor, *J. Chem. Soc., Dalton Trans.* (1984) 1349.
20. E. Manoj, M.R.P. Kurup, *Polyhedron* 27 (2008) 275.
21. T.A. Reena, E.B. Seena, M.R.P. Kurup, *Polyhedron* (2008) (in press).
22. U.L. Kala, *in* Synthesis, spectral and magnetic studies on some transition metal complexes, Ph.D thesis, Kerala University, Kerala, 2007.
23. A. Sreekanth, M.R.P. Kurup, *Polyhedron* 22 (2003) 3321.
24. P. Bindu, M.R.P. Kurup, T.R. Satyakeerty, *Polyhedron* 18 (1998) 321.
25. V. Stefov, V.M. Petrosevski, B. Septrajanov, *J. Mol. Struct.* 293 (1993) 97.
26. M. Joseph, V. Suni, M.R.P. Kurup, M. Nethaji, A. Kishore, S.G. Bhat, *Polyhedron* 23 (2004) 3069.

27. R.P. John, A. Sreekanth, M.R.P. Kurup, S.M. Mobin, *Polyhedron* 21 (2002) 2515.
28. K. Nakamoto, *Infrared and Raman Spectra of Inorganic and Coordination Compounds, Part B*, 5<sup>th</sup> edition, Wiley, New York, 1997.
29. J.R. Wasson, C. Trapp, *J. Phys. Chem.* 73 (1969) 3763.
30. M.J. Bew, B.J. Hathaway, R.R. Faraday, *J. Chem. Soc., Dalton Trans.* (1972) 1229.
31. C.R.K. Rao, P.S. Zacharias, *Polyhedron* 16 (1997) 1201.
32. H. Sacconi, G. Speroni, *J. Am. Chem. Soc.* 87 (1965) 3102.
33. R.P. John, A. Sreekanth, V. Rajakannan, T.A. Ajith, M.R.P. Kurup, *Polyhedron* 23 (2004) 2549.
34. M. Joseph, M. Kuriakose, M.R.P. Kurup, E. Suresh, A. Kishore, G. Bhat, *Polyhedron* 25 (2006) 61.
35. B.N. Bessy Raj, M.R.P. Kurup, E. Suresh, *Spectrochim. Acta A* 71 (2008) 1253.
36. B.J. Hathaway, in: G. Wilkinson, R.D. Gillard, J. A. McCleverty (Eds.), *Comprehensive Coordination Chemistry*, vol. 5, Pergamon, Oxford, 1987, p 533.
37. V. Philip, V. Suni, M.R.P. Kurup, M. Nethaji, *Polyhedron* 24 (2005) 1133.
38. A.H. Maki, B.R. McGarvey, *J. Chem. Phys.* 29 (1958) 31.
39. B.N. Figgis, *Introduction to ligand Fields*, Interscience, New York 1996, p 295.

**SYNTHESES AND SPECTRAL CHARACTERIZATION  
OF MANGANESE(II) COMPLEXES OF *N*(4)-  
PHENYLSEMICARBAZONES**

**5.1. Introduction**

Manganese is the twelfth most abundant element by weight in the earth's crust. Traces of manganese are found in many plants and bacteria, and a healthy human adult has about 10-20 mg of manganese in his body. It is an essential trace element, forming the active sites of a number of metalloproteins. In these metalloproteins, manganese can exist in any of the five oxidation states or in mixed valence states. For inorganic chemists, metalloproteins with two or even more manganese atoms per sub unit are particularly interesting. The largest non-metallurgical use of manganese is in the manufacture of dry-cell batteries in the form of MnO<sub>2</sub>. Metal complexes of manganese play important roles ranging from bioinorganic chemistry to solid state physics.

Manganese(II) complexes are well known for their excellent catalytic activity towards the disproportionation of hydrogen peroxide and a number of them have been shown to catalyze the low temperature peroxide bleaching of fabrics [1]. They are also interesting due to their catalytic antioxidant activity [2]. Potential importance of manganese complexes is evidenced by the realization that the active site in photosystem II (PSII) is a tetranuclear manganese complex [3]. Manganese has a vital role in many enzymatic systems such as superoxide

dismutase, peroxidase, dioxygenase and catalase in which mononuclear Mn active centers are present [4].

Manganese and its compounds are widely used in analytical chemistry, metallurgical processes and paint and pigment industry. Complexes of Mn(II) play an excellent role in catalytic property. Manganese metal has a well established importance in the field of biology and medicine. A lot of articles are available on the physiology and biochemistry of manganese. The most important natural role of manganese is in the oxidation of water in green plant photosynthesis where its presence in photosystem II is essential [5]. Manganese shows oxidation states ranging from (-III) to (+VII). The (+II) state is the most common and  $Mn^{2+}$  ions exist in the solid, in solution and as complexes.

This chapter is focused on the syntheses and spectral studies of six Mn(II) complexes synthesized using the two ligands  $HL^1$  and  $HL^2$ .

## **5.2. Experimental**

### **5.2.1. Materials**

Details regarding the syntheses of  $HL^1$  and  $HL^2$  are described in Chapter 2. Manganese(II) acetate tetrahydrate, manganese sulphate, sodium azide, 1,10-phenanthroline (all Merck) were used as supplied and solvents were purified by standard procedures before use.



5.2.2. Syntheses of complexes

$[\text{MnL}^1\text{phenN}_3] \cdot \text{H}_2\text{O}$  (19)

To a solution of the  $\text{HL}^1$  (0.633 g, 2 mmol) in hot methanol (25 ml), 1,10-phenanthroline (0.360 g, 2 mmol) in methanol was added. To this mixture, manganese acetate tetrahydrate (0.490 g, 2 mmol) was added and heated under reflux for half an hour. Then  $\text{NaN}_3$  (0.130 g, 2 mmol) was added and heated under reflux for three hours. Kept at room temperature for twelve hours. The complex formed was filtered, washed thoroughly with water, methanol and then ether. Finally it was dried over  $\text{P}_4\text{O}_{10}$  *in vacuo*.

$[\text{Mn}(\text{HL}^1)\text{phenSO}_4]$  (20)

To a solution of the  $\text{HL}^1$  (0.633 g, 2 mmol) in hot methanol (25 ml), 1,10-phenanthroline (0.360 g, 2 mmol) in methanol was added. To this mixture, manganese sulphate (0.338 g, 2 mmol) was added and heated under reflux for four hours. Kept at room temperature for two days. The complex formed was filtered, washed thoroughly with water, methanol and then ether. Finally it was dried over  $\text{P}_4\text{O}_{10}$  *in vacuo*.

$[\text{MnL}^1_2] \cdot 3\text{H}_2\text{O}$  (21)

Manganese acetate tetrahydrate (0.245 g, 1 mmol) dissolved in 20 ml of methanol and  $\text{HL}^1$  (0.633 g, 2 mmol) dissolved in 30 ml of hot methanol were mixed and stirred for 5 hrs. The yellow colored solid, which separated on cooling was filtered, washed with hot methanol and ether and dried over  $\text{P}_4\text{O}_{10}$  *in vacuo*.

$[\text{MnL}^2\text{phenN}_3] \cdot 2\text{H}_2\text{O}$  (22)

To a solution of the  $\text{HL}^2$  (0.508 g, 2 mmol) in hot methanol (25 ml), 1,10-phenanthroline (0.360 g, 2 mmol) in methanol was added. To this mixture, manganese acetate tetrahydrate (0.490 g, 2 mmol) was added and heated under reflux for half an hour. Then  $\text{NaN}_3$  (0.130 g, 2 mmol) was added and heated under reflux for three hours. Kept at room temperature for three days. The complex formed was filtered, washed thoroughly with water, methanol and then ether. Finally it was dried over  $\text{P}_4\text{O}_{10}$  *in vacuo*.

 $[\text{Mn}(\text{HL}^2)\text{phenSO}_4]$  (23)

To a solution of the  $\text{HL}^2$  (0.508 g, 2 mmol) in hot methanol (25 ml), 1,10-phenanthroline (0.360 g, 2 mmol) in methanol was added. To this mixture, manganese sulphate (0.338 g, 2 mmol) was added and heated under reflux for four hours. Kept at room temperature for two days. The complex formed was filtered, washed thoroughly with water, methanol and then ether. Finally it was dried over  $\text{P}_4\text{O}_{10}$  *in vacuo*.

 $[\text{MnL}^2_2] \cdot \text{CH}_3\text{OH}$  (24)

Manganese acetate tetrahydrate (0.245 g, 1 mmol) dissolved in 20 ml methanol and  $\text{HL}^2$  (0.508 g, 2 mmol) dissolved in 30 ml hot methanol were mixed and stirred for 5 hrs. The yellow colored solid, which separated on cooling was filtered, washed with hot methanol and ether and dried over  $\text{P}_4\text{O}_{10}$  *in vacuo*.

### **5.2.3. Analytical methods**

Elemental analyses were carried out using a Vario EL III CHNS analyzer at SAIF, Kochi, India. IR spectra were recorded on a Thermo Nicolet AVATAR 370 DTGS model FT-IR Spectrophotometer with KBr pellets and ATR technique at SAIF, Kochi, India. Electronic spectra were recorded on a Cary 5000, version 1.09 UV-Vis-NIR spectrophotometer using solutions in acetonitrile. EPR spectra were recorded on a Varian E-112 X-band EPR spectrometer using TCNE as a standard at SAIF, IIT, Bombay, India. The magnetic susceptibility measurements were carried out at the Indian Institute of Technology, Roorkee, at room temperature in the polycrystalline state on a PAR model 155 Vibrating Sample Magnetometer at 5 kOe field strength. The molar conductivities of the complexes in dimethylformamide solutions ( $10^{-3}$  M) at room temperature were measured using a direct reading conductivity meter.

## **5.3. Results and discussion**

### **5.3.1. Analytical measurements**

All the six Mn(II) complexes are yellow powders, clearly soluble in alcohol, chloroform, dimethylformamide and acetonitrile. In compounds except  $[\text{Mn}(\text{HL}^1)\text{phenSO}_4]$  (**20**) and  $[\text{Mn}(\text{HL}^2)\text{phenSO}_4]$  (**23**), the semicarbazones deprotonate and chelate in monoanionic form  $\text{L}^-$  and in compounds **20** and **23**, the ligand moiety is coordinated in the neutral form as evidenced by the IR spectra. Elemental analyses and conductivity data are in agreement with the general empirical formula  $[\text{MnL}_2]$  for compounds **21** and **24**.

Ligand can exist in keto or enol form or an equilibrium mixture of the two since it has an amide  $\text{-NH-C(=O)}$  function. However, the IR spectrum of  $\text{HL}^1$  and  $\text{HL}^2$  indicates that in the solid state it remains in keto form. The IR spectra of complexes, however, do not show any intense absorption band around  $1698\text{ cm}^{-1}$  and  $1683\text{ cm}^{-1}$  except complexes **20** and **23**, due to the carbonyl stretching of the semicarbazone moiety. This shows that in solution, it tautomerises to the enol form and coordinates to the metal in the enolate form.

The room temperature magnetic moments of powdered samples of complexes are consistent with Mn(II) complexes where there are no significant exchange interactions between adjacent metal centers and are very close to spin-only value (5.91 B.M.).

The complexes  $[\text{MnL}^1\text{phenN}_3] \cdot \text{H}_2\text{O}$  (**19**) and  $[\text{MnL}^2\text{phenN}_3] \cdot 2\text{H}_2\text{O}$  (**22**) were readily formed by the reaction of the ligand, sodium azide and 1,10-phenanthroline with manganese(II) acetate tetrahydrate in the ratio 1:1:1:1. The complexes  $[\text{Mn}(\text{HL}^1)\text{phenSO}_4]$  (**20**) and  $[\text{Mn}(\text{HL}^2)\text{phenSO}_4]$  (**23**) were formed by the reaction of the ligand with 1,10-phenanthroline and manganese sulphate in the ratio 1:1:1. The complexes  $[\text{MnL}^1_2] \cdot 3\text{H}_2\text{O}$  (**21**) and  $[\text{MnL}^2_2] \cdot \text{CH}_3\text{OH}$  (**24**) were obtained when a hot solution of ligand was reacted with a hot filtered methanolic solution of manganese acetate tetrahydrate in the ratio 2:1.

The partial elemental analyses and magnetic susceptibilities of the metal complexes are shown in Table 5.1.

Table 5.1. Partial elemental analyses and magnetic susceptibilities of manganese(II) complexes of HL<sup>1</sup> and HL<sup>2</sup>

Compound	Observed (Calculated) %			$\mu$ (B.M.)
	C	H	N	
[MnL <sup>1</sup> phenN <sub>3</sub> ] · H <sub>2</sub> O (19)	60.65 (60.99)	3.81 (4.13)	21.03 (20.65)	5.64
[Mn(HL <sup>1</sup> )phenSO <sub>4</sub> ] (20)	57.65 (57.41)	4.06 (3.89)	13.35 (12.96)	5.78
[MnL <sup>1</sup> <sub>2</sub> ] · 3H <sub>2</sub> O (21)	62.12 (61.70)	4.49 (4.91)	15.56 (15.15)	5.49
[MnL <sup>2</sup> phenN <sub>3</sub> ] · 2H <sub>2</sub> O(22)	55.62 (55.13)	4.84 (4.45)	22.53 (22.25)	5.81
[Mn(HL <sup>2</sup> )phenSO <sub>4</sub> ] (23)	52.83 (53.24)	3.64 (3.95)	13.96 (14.33)	5.96
[MnL <sup>2</sup> <sub>2</sub> ] · CH <sub>3</sub> OH (24)	58.31 (58.68)	5.22 (5.09)	18.56 (18.88)	5.72

### 5.3.2. IR spectra

The tentative assignments of the IR spectral bands of ligands and its manganese(II) complexes useful for determining the ligand's mode of coordination are listed in Table 5.2. A comparison of the IR spectra of the ligands and the complexes revealed significant variations in the characteristic bands due to coordination with the central metal ion. It is found that the azomethine (C=N) band suffered a negative shift in all the complexes. The shifting of the azomethine band to lower frequency is attributed to the conjugation of the *p* orbitals on the double bond with the *d* orbital on the metal ion with reduction of the force constant.

Table 5.2. Infrared spectroscopic assignments ( $\text{cm}^{-1}$ ) for the ligands and its manganese(II) complexes.

Compound	$\nu(\text{N-H})$	$\nu(\text{C=N})$	$\nu(\text{N-N})$	$\nu(\text{C=O})$	$\nu(\text{Mn-N})$	$\nu(\text{C=N})^a$	$\nu(\text{Mn-O})$
$\text{HL}^1$	3375	1600	1132	1698	-	-	-
$[\text{MnL}^1\text{phenN}_3] \cdot \text{H}_2\text{O}$ ( <b>19</b> )	-	1570	1144	-	420	1542	555
$[\text{Mn}(\text{HL}^1)\text{phenSO}_4]$ ( <b>20</b> )	3337	1533	1138	1687	409	-	554
$[\text{MnL}^1_3] \cdot 3\text{H}_2\text{O}$ ( <b>21</b> )	-	1589	1145	-	407	1525	552
$\text{HL}^2$	3380	1599	1151	1683	-	-	-
$[\text{MnL}^2\text{phenN}_3] \cdot 2\text{H}_2\text{O}$ ( <b>22</b> )	-	1562	1192	-	408	1515	553
$[\text{Mn}(\text{HL}^2)\text{phenSO}_4]$ ( <b>23</b> )	3381	1571	1162	1675	412	-	564
$[\text{MnL}^2_3] \cdot \text{CH}_3\text{OH}$ ( <b>24</b> )	-	1584	1178	-	416	1529	552

<sup>a</sup> indicates newly formed C=N

The IR spectra of the complexes except compounds **20** and **23** show new sharp bands in the 1515-1542  $\text{cm}^{-1}$  range which is assigned to the newly formed C=N. This indicates that the ligand enolizes and coordinates in the enolate form [6]. Strong bands in the region  $\sim 550 \text{ cm}^{-1}$  indicate the presence of Mn–O bond, resulting from the coordination of the enol or keto oxygen [6,7]. Sharp bands at 1600 and 1599  $\text{cm}^{-1}$  in the spectra of the ligands HL<sup>1</sup> and HL<sup>2</sup> are shifted to lower frequencies in the spectra of the complexes (Figs. 5.1–5.6) indicates the coordination via azomethine nitrogen. Additional evidence for coordination of the imine nitrogen is the presence  $\nu(\text{Mn}-\text{N}_{\text{azo}})$  bands in the region 407-420  $\text{cm}^{-1}$  [8-11]. The occurrence of  $\nu(\text{N}-\text{N})$  at higher wavenumbers in the spectra of the complexes compared to that of the ligand confirms the coordination of the azomethine nitrogen.

Medium bands at 3375 and 3380  $\text{cm}^{-1}$  for the ligands HL<sup>1</sup> and HL<sup>2</sup> respectively due to  $\nu(^2\text{N}-\text{H})$  vibration [12,13] and another at 1698 and 1683  $\text{cm}^{-1}$  due to  $\nu(\text{C}=\text{O})$ , disappear in the spectrum of the complexes except **20** and **23** providing a strong evidence for the ligand coordination around manganese(II) ion in the enolate form [14,15]

In the azido complex, strong bands observed at 2037 and 1383  $\text{cm}^{-1}$  corresponding to  $\nu_a$  and  $\nu_s$  of azido group is assigned to the coordinated azido group [16,17]. The prominent bands at 693 and a weak band at 454  $\text{cm}^{-1}$ , assigned to  $\delta(\text{NNN})$  and  $\nu(\text{Mn}-\text{N})$  suggest a non linear Mn–N–N–N band [18].

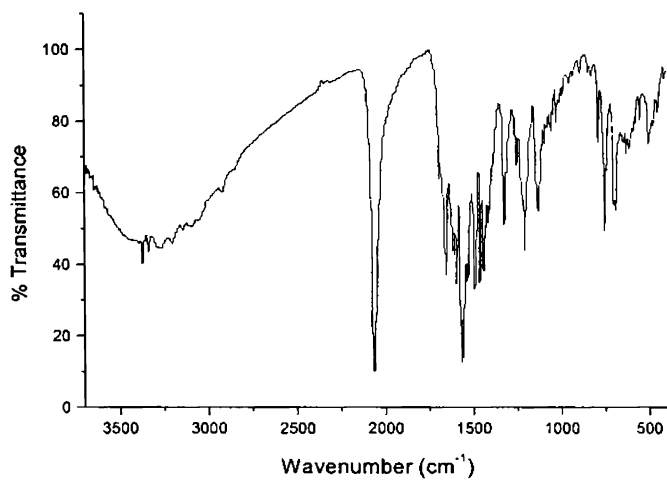


Fig. 5.1. IR spectrum of the complex  $[\text{MnL}^1\text{phenN}_3] \cdot \text{H}_2\text{O}$  (19).

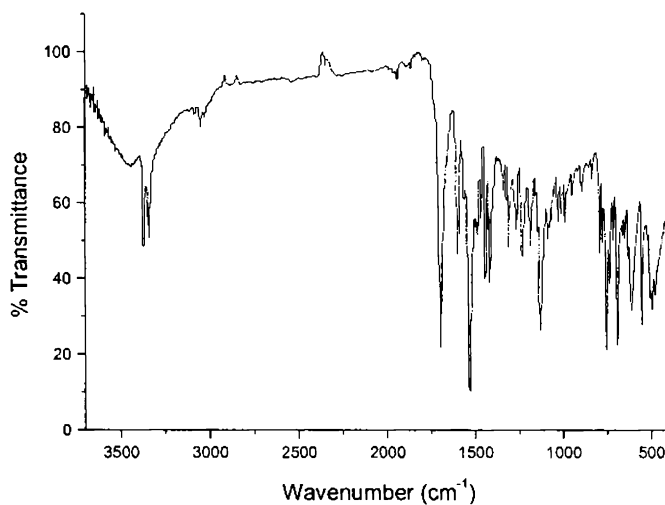


Fig. 5.2. IR spectrum of the complex  $[\text{Mn}(\text{HL}^1)\text{phenSO}_4]$  (20).



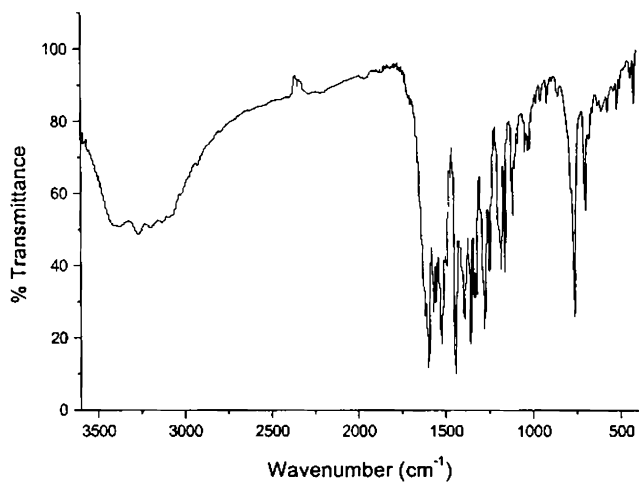


Fig. 5.3. IR spectrum of the complex  $[\text{Mn}(\text{L}^1_2)] \cdot 3\text{H}_2\text{O}$  (**21**).

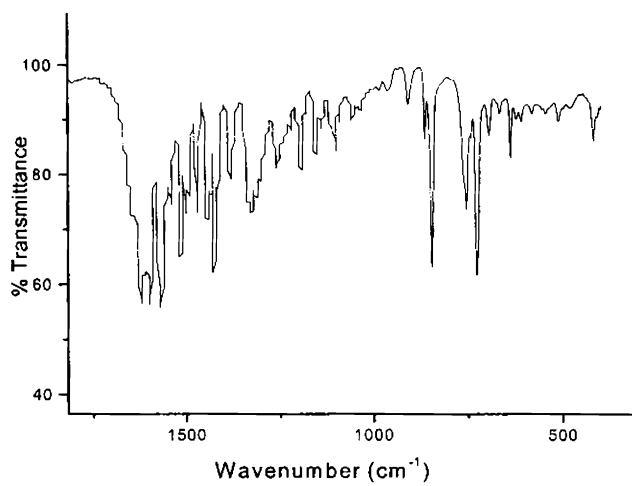


Fig. 5.4. IR spectrum of the complex  $[\text{Mn}(\text{L}^2)\text{phenN}_3] \cdot 2\text{H}_2\text{O}$  (**22**).

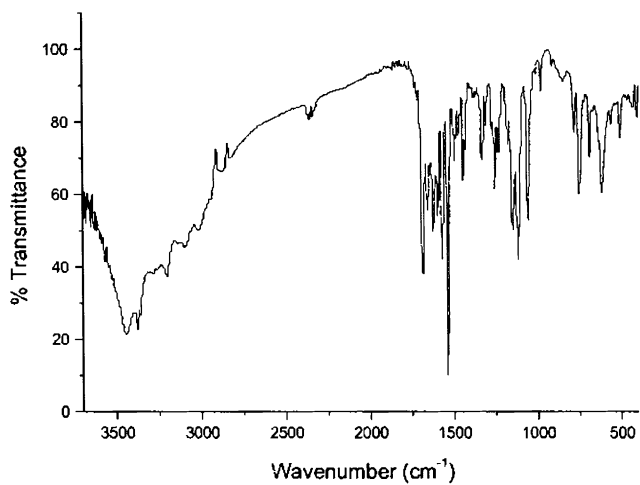


Fig. 5.5. IR spectrum of the complex  $[\text{Mn}(\text{HL}^2)\text{phenSO}_4]$  (23).

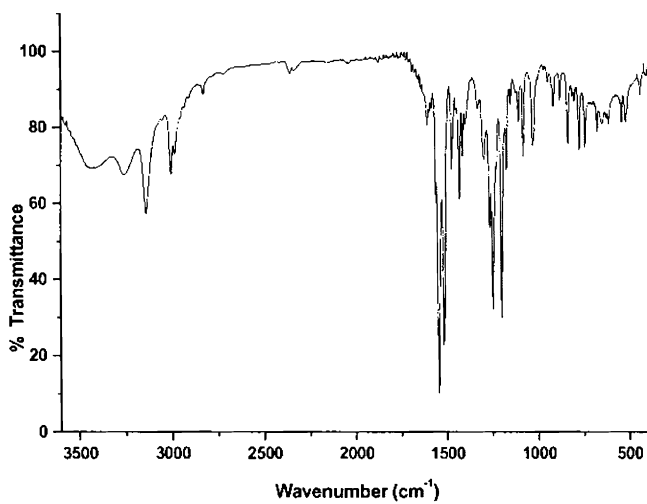


Fig. 5.6. IR spectrum of the complex  $[\text{Mn}(\text{L}^2)_2] \cdot \text{CH}_3\text{OH}$  (24).

The sulfato complex has strong bands at 1120 and 1065  $\text{cm}^{-1}$ , indicating the presence of monocoordinated sulfato group [13,16]. Bands due to heterocyclic base 1,10-phenanthroline are observed at 1500 and 845  $\text{cm}^{-1}$  and the coordination of the base is indicated by the presence of weak bands in the 430-475  $\text{cm}^{-1}$  range.

### **5.3.3. Electronic spectra**

Electronic spectral data are presented in the Table 5.3. Magnetic studies have shown that ground state of  $\text{Mn}^{2+}$  ion is a sextet. There can be no spin allowed transitions. The *d-d* transitions in the manganese(II) systems are doubly forbidden hence they don't register any characteristic bands in the visible region.

The Tanabe-Sugano diagram corresponding to such a system shows that the only high spin state Russell-Sanders term is  ${}^6S$  which in an octahedral geometry changes its notation to  ${}^6A_{1g}$ . Since there are no excited states with spin multiplicity with six, all electronic transitions are not only Laporte forbidden but are spin forbidden also. Consequently all electronic transitions have extremely small molar extinction coefficients and it is very difficult to locate the bands [18,19]. The values are characteristic of a tetragonally distorted octahedral environment. In the visible region the complexes show weak absorptions attributed to the forbidden nature of the spin doublets.

Upon complexation,  $n \rightarrow \pi^*$  and  $\pi \rightarrow \pi^*$  bands are observed at  $\sim 33000$  and  $37000 \text{ cm}^{-1}$  for complexes of both ligands. The absorptions of the organic ligands tailing into the visible region obscure the very weak *d-d*

absorption bands of the manganese(II) complexes. The broad bands in the region 24000-27600  $\text{cm}^{-1}$  is typical of octahedral manganese(II) complexes due to the  ${}^4T_{2g} \leftarrow {}^6A_{1g}$  transitions.

Table 5.3. Electronic spectral assignments ( $\text{cm}^{-1}$ ) of semicarbazones and their Mn(II) complexes.

Compound	${}^4T_{2g} \leftarrow {}^6A_{1g}$	$n \rightarrow \pi^*$	$\pi \rightarrow \pi^*$
HL <sup>1</sup>	-	32890	37410
[MnL <sup>1</sup> phenN <sub>3</sub> ] · H <sub>2</sub> O (19)	27590	33930	37590
[Mn(HL <sup>1</sup> )phenSO <sub>4</sub> ] (20)	24390	32680	37450
[MnL <sup>1</sup> <sub>2</sub> ] · 3H <sub>2</sub> O (21)	27320	33980	37425
HL <sup>2</sup>	-	33900	37010
[MnL <sup>2</sup> phenN <sub>3</sub> ] · 2H <sub>2</sub> O (22)	23960	32390	37560
[Mn(HL <sup>2</sup> )phenSO <sub>4</sub> ] (23)	24480	33900	37260
[MnL <sup>2</sup> <sub>2</sub> ] · CH <sub>3</sub> OH (24)	23820	32460	37330

Electronic spectra of the complexes **19**, **20** and **21** are shown in Figs. 5.7- 5.9.

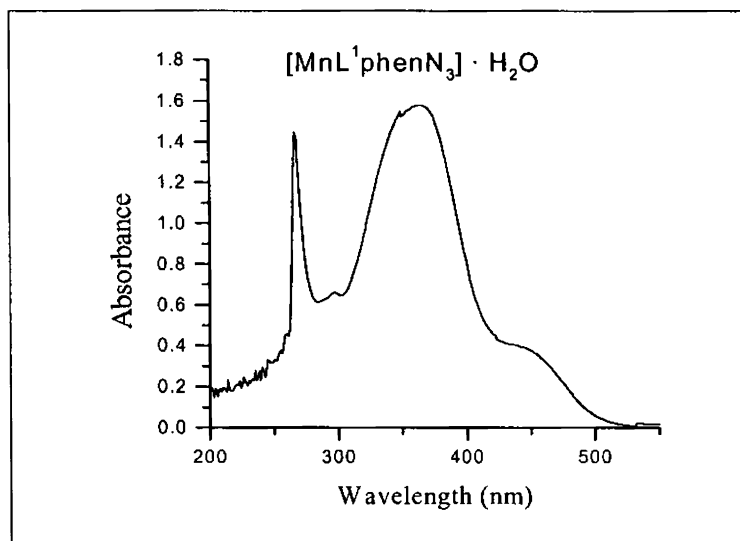


Fig. 5.7. Electronic spectrum of the complex 19.

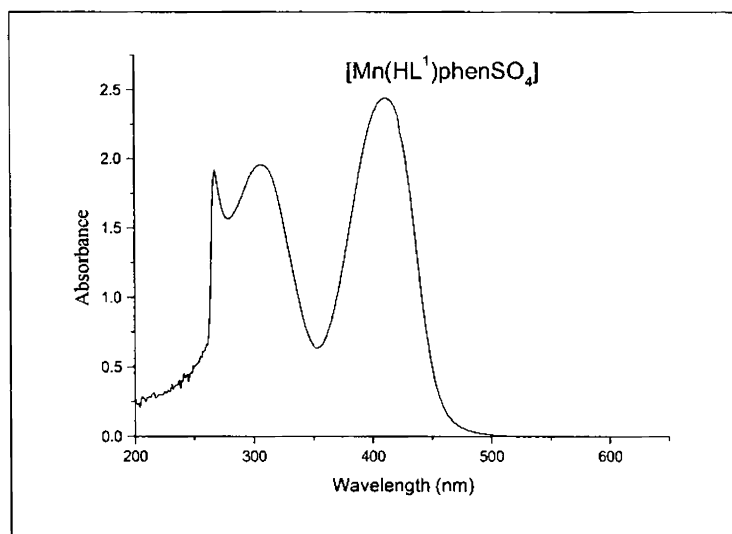


Fig. 5.8. Electronic spectrum of the complex 20.

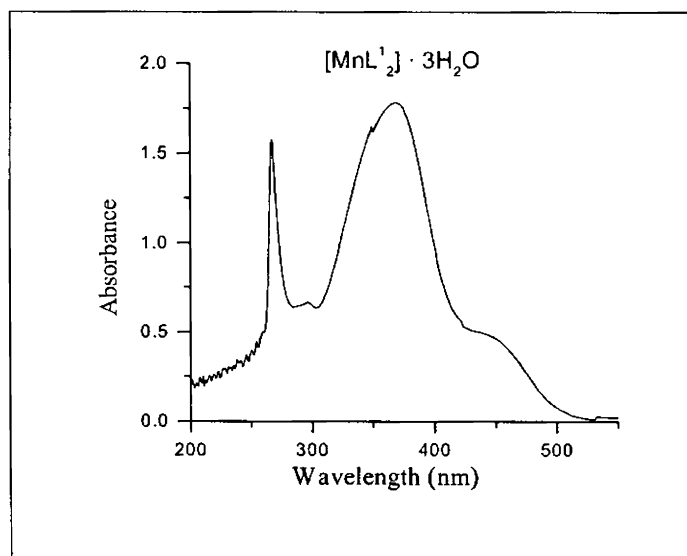


Fig. 5.9. Electronic spectrum of the complex **21**.

#### 5.3.4. EPR spectra

The spin Hamiltonian  $\hat{H}$  used to represent the EPR spectra of Mn(II) is given by

$$\hat{H} = g\beta HS + D[S_z^2 - S(S+1)/3] + E(S_x^2 - S_y^2)$$

where  $H$  is the magnetic field vector,  $g$  is the Lande's splitting factor,  $\beta$  is the Bohr magneton,  $D$  is the axial zero field splitting term,  $E$  is rhombic zero field splitting parameter and  $S$  is the electron spin vector. If  $D$  and  $E$  are very small compared to  $g\beta HS$ , five EPR transitions are expected corresponding to  $\Delta m_s = \pm 1$ .

The EPR data for the compounds are presented in the Table 5.4. The EPR spectra of the compounds at 298 K in polycrystalline state exhibited broad isotropic signals with characteristic  $g$  values with no hyperfine splitting for compounds.

Table 5.4. EPR data of Mn(II) complexes

Compound	Polycrystalline at 298 K $g_0$	DMF at 77 K	
		$g_0$	$A_0^a$
$[\text{MnL}^1\text{phenN}_3] \cdot \text{H}_2\text{O}$ ( <b>19</b> )	2.20	1.99	92
$[\text{Mn}(\text{HL}^1)\text{phenSO}_4]$ ( <b>20</b> )	2.00	1.99	91
$[\text{MnL}^1_2] \cdot 3\text{H}_2\text{O}$ ( <b>21</b> )	2.04	1.99	96
$[\text{MnL}^2\text{phenN}_3] \cdot 2\text{H}_2\text{O}$ ( <b>22</b> )	2.07	2.02	92
$[\text{Mn}(\text{HL}^2)\text{phenSO}_4]$ ( <b>23</b> )	2.01	2.01	92
$[\text{MnL}^2_2] \cdot \text{CH}_3\text{OH}$ ( <b>24</b> )	2.03	2.01	92

<sup>a</sup> A values are expressed in Gauss.

The EPR spectrum of compound **19** at 298 K in polycrystalline state exhibited a broad signal with a  $g$  value at 2.20. (Fig. 5.10)

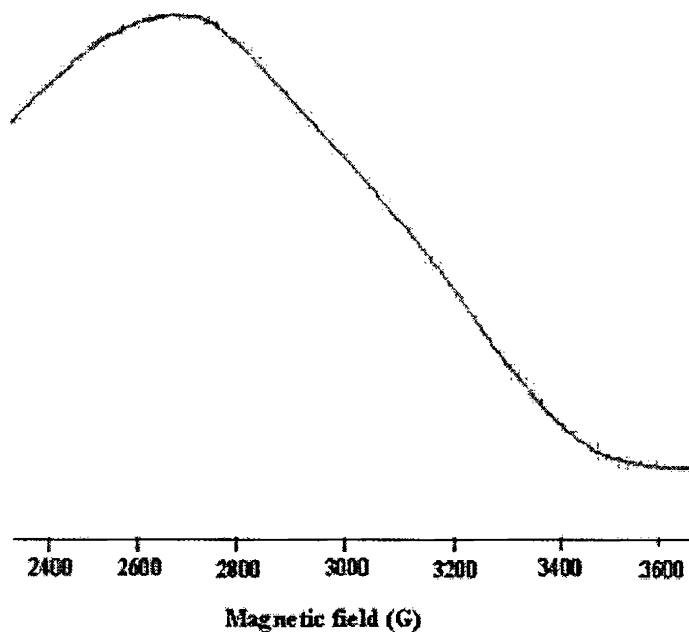


Fig. 5.10. EPR spectrum of compound 19 (polycrystalline form) at 298 K.

The frozen solution spectrum (Fig. 5.11) of the compound in DMF, displayed one  $g$  value 1.992 with a hyperfine sextet. The coupling constant  $A_{iso}$  for the sextet hyperfine lines is found to be 92 G.

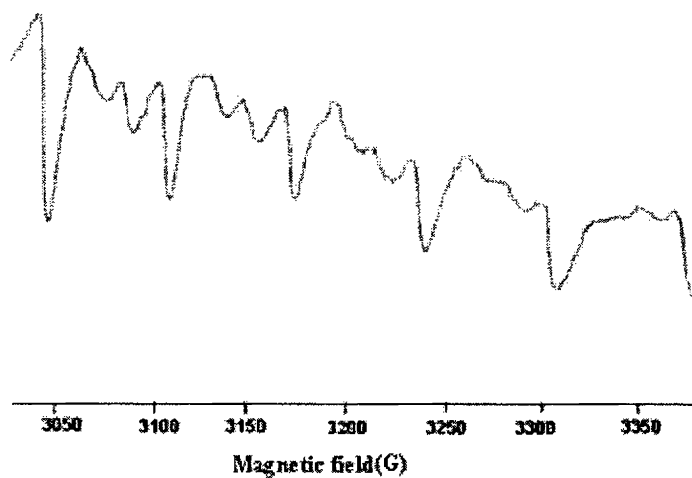


Fig. 5.11. EPR spectrum of compound 19 (DMF at 77 K).



In the case of compound **20**, the EPR spectrum at 298 K in polycrystalline state exhibited a signal with a  $g$  value at 1.999 and in DMF at 77 K reveals one  $g$  value at 1.994 (Figs. 5.12 and 5.13). This signal has split into a hyperfine sextet with a hyperfine coupling constant of 91 G.

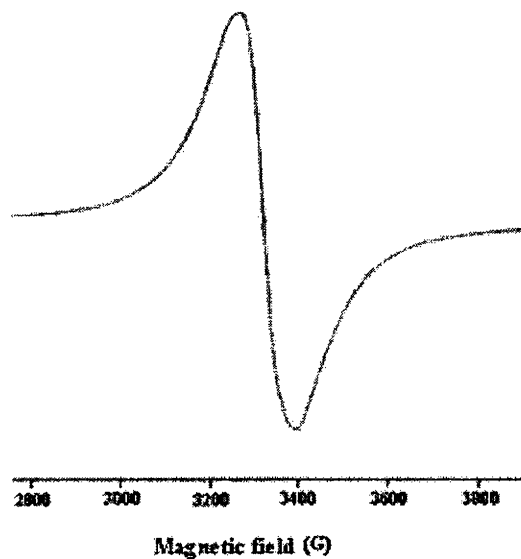


Fig. 5.12. EPR spectrum of compound **20** (polycrystalline form) at 298 K.

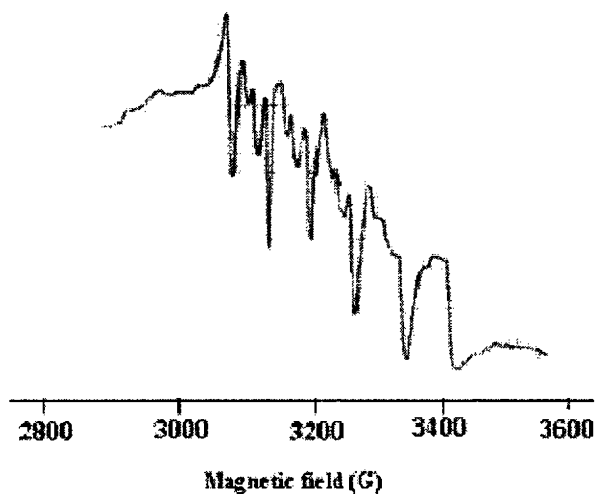


Fig. 5.13. EPR spectrum of compound **20** (DMF at 77 K).

The EPR spectrum of compound **21** at 298 K in polycrystalline state exhibited a broad signal with a  $g$  value at 2.040. The frozen solution spectrum (Fig. 5.14) of the compound in DMF, displayed one  $g$  value 1.992 with a hyperfine sextet. The coupling constant  $A_{iso}$  for the sextet hyperfine lines is found to be 96 G. A pair of low intensity forbidden lines lying between each of the two main hyperfine lines is observed. The forbidden lines in the spectrum arise due to the mixing of the nuclear hyperfine levels by the zero- field splitting factor of the Hamiltonian [20,21].

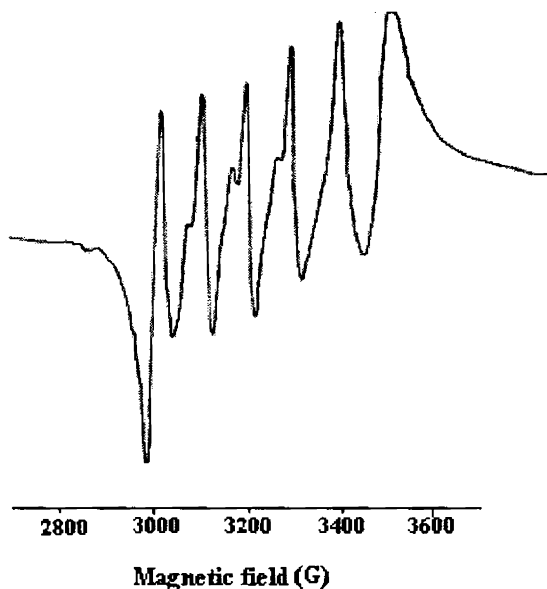


Fig. 5.14. EPR spectrum of compound **21** (DMF at 77 K).

In the case of compound **22**, the EPR spectrum at 298 K in polycrystalline state exhibited a broad signal with a  $g$  value at 2.070 and in DMF at 77 K reveals one  $g$  value at 2.021 (Fig. 5.15). A six line manganese hyperfine sextet with a hyperfine coupling constant 92 G is also observed.

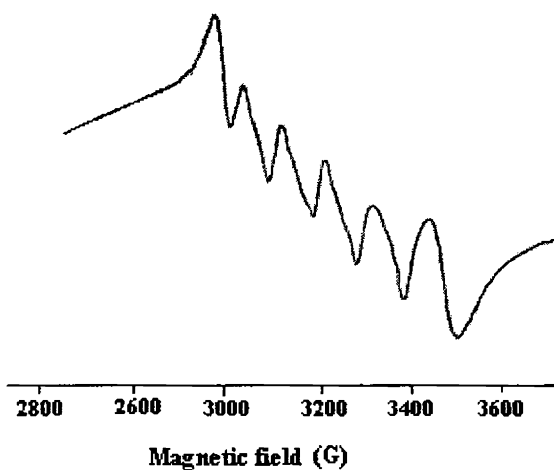


Fig. 5.15. EPR spectrum of compound **22** (DMF at 77 K).

The EPR spectrum of compound **23** at 298 K in polycrystalline state exhibited a broad signal with a  $g$  value at 2.010 with no hyperfine splittings (Fig. 5.16). However, the solution spectrum in DMF at 77 K displayed a hyperfine sextet with  $g_{iso}$  2.012. The  $A_{iso}$  value calculated for the hyperfine sextet is 92 G.

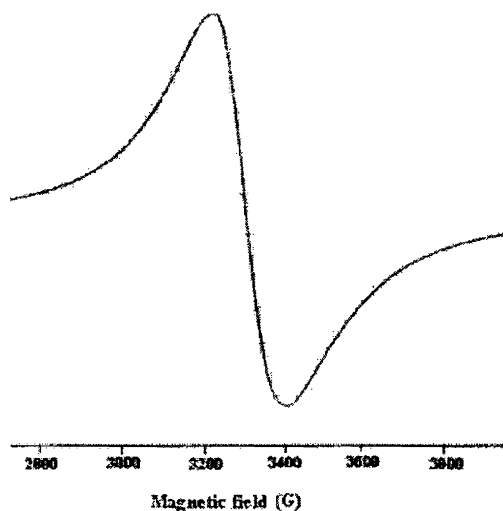


Fig. 5.16. EPR spectrum of compound **23** (polycrystalline at 298 K).

The EPR spectrum of compound **24** at 298 K in polycrystalline state exhibited a broad signal with a  $g$  value at 2.030 with no hyperfine splittings. However, the solution spectrum in DMF at 77 K (Fig. 5.17), displayed a hyperfine sextet with  $g_{\text{iso}}$  2.012. High spin  $\text{Mn}^{2+}$  ions with five unpaired electrons ( $S=5/2$ ) have an orbitally non-degenerate  ${}^6A_{1g}$  ground state. Hence the spin-orbit coupling is expected to be unimportant and the zero field splitting should be rather small. This is usually observed with complexes of weak field ligands, which give only one ' $g$ ' value close to 2.0023, the free electron ' $g$ ' value. The  $A_{\text{iso}}$  value calculated for the hyperfine sextet is 92 G.

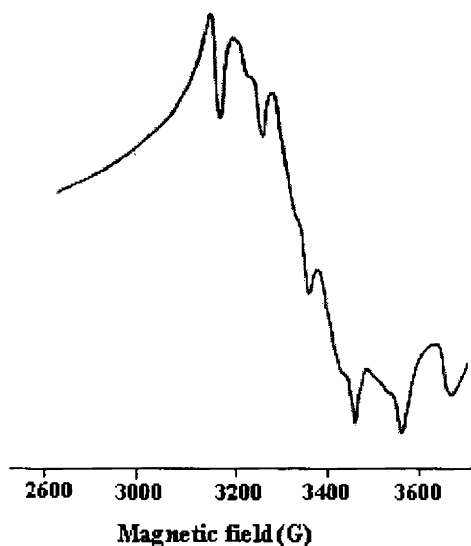


Fig. 5.17. EPR spectrum of compound **24** (DMF at 77 K).

In all the EPR spectra of  $\text{Mn}^{2+}$  complexes under study, it is observed that the separation between adjacent lines in the hyperfine multiplet differ slightly, and this can be attributed to the inequivalent

spacing of the  $2nI+1$  nuclear levels. Mn(II) nuclei with  $S=5/2$  has an appreciable quadrupole moment and the electric field gradient from the surrounding ligand ions compete with the magnetic hyperfine interaction in determining the orientation of the nuclear spin, due to which the degeneracy of the nuclear levels is lost resulting in difference in the separation between adjacent lines in the hyperfine splittings.

**References**

1. M. Devereux, M. McCann, V. Leon, V. McKee, R.J. Ball, *Polyhedron* 21 (2002) 1063.
2. B.J. Day, *Drug Discovery Today* 13 (9) (2004) 557.
3. M. Maneiro, M.R. Bermejo, M. Fondo, A.M. Gonzalez, J. Sanmartyn, J.C. Garcya-Monteagudo, R.G Pritchard, A.M. Tyryshkin, *Polyhedron* 20 (2001) 711.
4. D. Huang, X. Zhang, C. Chen, F. Chen, Q. Liu, D. Liao, L. Li, L. Sun, *Inorg. Chim. Acta* 353 (2003) 284.
5. K. Wieghardt, *Angew.Chem. Int. Ed. Engl.* 28 (1989) 1153.
6. J.R. Dimmock, K.K. Sidhu, S.D. Thumber, S.K.Basran, M. Chen, J.W. Quil, *Eur. J. Chem.* 30 (1995) 287.
7. R.P. John *in* Structural and biological investigations of metal complexes of some thiosemicarbazone ligands, Ph.D. Thesis, Cochin University of Science and Technology, 2002.
8. S.K. Nag, D.S. Joarder, *Can.J.Chem.* 54 (1976) 2827.
9. A.Z. Elsonbati, E.M. Mabroukand, H.E. Megahed, *Trans. Met. Chem.*16 (1991) 280.
10. R. Roy, M. Chaudhury, S.K. Mondal, K. Nag, *J. Chem.Soc., Dalton Trans.* (1984) 1681.
11. P.F. Raphael, E. Manoj, M.R.P. Kurup, *Polyhedron* 26 (2007) 5088.
12. P. Bindu, M.R.P. Kurup, T.R. Satyakeerty, *Polyhedron* 18 (1998) 321.

13. V. Philip, V. Suni, M.R.P. Kurup, M. Nethaji, *Spectrochim. Acta Part A*, 64 (2006) 171.
14. S. Renjusha, M.R.P. Kurup, *Polyhedron* 27 (2008) 3294.
15. K. Nakamoto, *Infrared and Raman Spectra of Inorganic and Coordination Compounds, Part B*, 5<sup>th</sup> edition, Wiley, New York, 1997.
16. R.P. John, A. Sreekanth, M.R.P. Kurup, S.M. Mobin, *Polyhedron* 21 (2002) 2515.
17. D.X. West, J.K. Swearingen, J. Vades-Martinez, S. Hernandez-Ortega, A.K. Ei-Sawaf, van Meurs, A. Castineiras, I. Garcia, E. Bermejo, *Polyhedron* 18 (1999) 2919.
18. Carini, G. Pelizzi, P. Tarasconi, C. Pelizzi, K.C. Molloy, P.C. Waterfield, *J. Chem. Soc., Dalton Trans.* 2 (1989) 289.
19. S. Casas, A. Castiñeiras, A. Sánchez, J. Sordo, A. Vázquez- López, M.C. Rodríguez-Argüelles, U. Russo, *Inorg. Chim. Acta* 221(1994) 61.
20. B. Bleany, R.S. Rubins, *Proc. Phys. Soc. London*, 77 (1961) 103.
21. W. Linert, F. Renz, R. Boca, *J. Coord. Chem.* 40 (1996) 293.

**SYNTHESES AND SPECTRAL CHARACTERIZATION  
OF COBALT(III) COMPLEXES OF  
N(4)-PHENYLSEMICARBAZONES**

**6.1. Introduction**

Cobalt is a ferromagnetic metal of Group VIII of the periodic table, used especially for heat-resistant and magnetic alloys. Cobalt compounds have been used for centuries to impart a rich blue color to glass, glazes, and ceramics. It is a hard, lustrous, silver-gray metal and is ferromagnetic. Cobalt-60, an artificial isotope, is an important  $\gamma$  ray source, and is extensively used as a tracer and a radiotherapeutic agent. Single compact sources of  $^{60}\text{Co}$  are readily available. Cobalt salts in small amounts are essential to many life forms, including humans. It is at the core of a vitamin called vitamin-B<sub>12</sub>. Cobalt was announced to be an element by Georg Brandt about 1739 (or possibly 1735). He had been trying to demonstrate that the blue color of glass was because of a new element, cobalt, rather than bismuth, an element often found in the same locations as cobalt.

Cobalt(III) complexes derived from symmetrical and unsymmetrical Schiff bases have also attracted considerable attention in the past for their relevance as biologically active compounds [1,2]. Many model complexes of cobalt in both +2 and +3 oxidation states have been prepared and investigated, which emphasize on the reactivity of the metal ions in the trans methylation reaction and reversible absorption of molecular oxygen [3,4].



Cobalt compounds should be handled with care due to cobalt's slight toxicity. Powdered cobalt in metal form is a fire hazard.

Cobalt(III) and various tridentate ligands form mainly mixed bis(ligand) complexes. Cobalt(III) complexes of the type  $[\text{CoL}_2]\text{X}$  ( $\text{X} = \text{Cl}, \text{Br}, \text{SCN}, \text{N}_3, \text{NO}_3$  etc.,  $\text{L} =$  anion from the enol form of the semicarbazone ligand of the type, HL) which were proposed to be low-spin, diamagnetic and octahedral [5] have been reported. Extending these works further, this chapter presents the syntheses and characterization of novel cobalt(III) complexes of the ligands  $\text{HL}^1$  and  $\text{HL}^2$ .

## 6.2. Experimental

### 6.2.1. Materials

Details regarding the synthesis of  $\text{HL}^1$  and  $\text{HL}^2$  are described in Chapter 2. Cobalt(II) nitrate hexahydrate, cobalt(II) bromide and cobalt(II) chloride hexahydrate (Merck) were used as supplied and solvents were purified by standard procedures before use.

### 6.2.2. Syntheses of complexes

#### $[\text{CoL}^1_2]\text{NO}_3 \cdot \text{H}_2\text{O}$ (25)

To a hot solution of 1 mmol of  $\text{HL}^1$  in methanol (20 ml) was added a methanolic solution of 0.5 mmol of the cobalt(II) nitrate hexahydrate (0.145 g). The mixture was refluxed for four hours and kept at room temperature. The compound formed was filtered, washed with water, methanol and ether. It was then dried *in vacuo* over  $\text{P}_4\text{O}_{10}$ .

$[\text{CoL}^1_2]\text{Cl}$  (26)

To a hot solution of 1 mmol of  $\text{HL}^1$  in methanol (20 ml) was added a methanolic solution of 0.5 mmol of the cobalt(II) chloride hexahydrate (0.118 g). The mixture was refluxed for three hours and kept at room temperature. The compound formed was filtered, washed with water, methanol and ether. It was then dried *in vacuo* over  $\text{P}_4\text{O}_{10}$ .

$[\text{CoL}^1_2]\text{Br} \cdot \text{H}_2\text{O}$  (27)

To a hot solution of 1 mmol of  $\text{HL}^1$  in methanol (20 ml) was added a methanolic solution of 0.5 mmol of the cobalt(II) bromide (0.109 g). The mixture was refluxed for five hours and kept at room temperature for two days. The compound formed was filtered, washed with water, methanol and ether. It was then dried *in vacuo* over  $\text{P}_4\text{O}_{10}$ .

$[\text{CoL}^2_2]\text{NO}_3 \cdot 2\text{H}_2\text{O}$  (28)

To a hot solution of 1 mmol of  $\text{HL}^2$  in methanol (25 ml) was added a methanolic solution of 0.5 mmol of the cobalt(II) nitrate hexahydrate (0.145 g). The mixture was then heated under reflux for five hours and kept at room temperature for two days. The compound formed was filtered, washed with water, methanol and ether. It was then dried *in vacuo* over  $\text{P}_4\text{O}_{10}$ .

$[\text{CoL}^2_2]\text{Cl}$  (29)

To a hot solution of 1 mmol of  $\text{HL}^2$  in methanol (30 ml) was added a methanolic solution of 0.5 mmol of the cobalt(II) chloride hexahydrate (0.118 g). The mixture was refluxed for three hours and kept at room

temperature. The compound formed was filtered, washed with water, methanol and ether. It was then dried *in vacuo* over  $P_4O_{10}$ .

### 6.2.3. Analytical methods

Elemental analyses were carried out using a Vario EL III CHNS analyzer at SAIF, Kochi, India. IR spectra were recorded on a Thermo Nicolet AVATAR 370 DTGS model FT-IR Spectrophotometer with KBr pellets and ATR technique at SAIF, Kochi, India. Electronic spectra were recorded on a Cary 5000, version 1.09 UV-Vis-NIR spectrophotometer from solutions in acetonitrile. The magnetic susceptibility measurements were carried out at the Indian Institute of Technology, Roorkee, at room temperature in the polycrystalline state on a PAR model 155 Vibrating Sample Magnetometer at 5 kOe field strength. The molar conductivities of the complexes in dimethylformamide solutions ( $10^{-3}$  M) at room temperature were measured using a direct reading conductivity meter.

## 6.3. Results and discussion

### 6.3.1. Analytical measurements

The partial elemental analysis data and molar conductivities of the complexes are listed in Table 6.1. All the complexes are brown in color and soluble in solvents like methanol, ethanol, acetonitrile, chloroform and DMF. They are found to be diamagnetic which confirms oxidation to cobalt(III) during preparation as has been found previously with heterocyclic *N*(4)-substituted semicarbazones and hence corresponds to  $d^6$  ion in strong field [6]. The molar conductivities of  $10^{-3}$  M DMF solutions

of the complexes indicate that they are 1:1 electrolytes [7]. The partial elemental analysis data and conductance measurement data are in consistence with the general formulation of the complexes as  $[\text{CoL}_2]\text{X}$ , where  $\text{X} = \text{NO}_3, \text{Cl}$  and  $\text{Br}$ . For the compounds **25** and **27**, the elemental analysis data matches with stoichiometry containing one molecule of water of crystallization/lattice water, two molecules in the case of **28**, whereas no water molecules are present in **26** and **29**.

Ligand can exist in keto or enol form or an equilibrium mixture of the two since it has an amide  $-\text{NH}-\text{C}=\text{O}$  function. However, the IR spectrum of  $\text{HL}^1$  and  $\text{HL}^2$  indicates that in the solid state it remains in keto form. The IR spectra of complexes, however, do not show any intense absorption bands around  $1698$  and  $1683 \text{ cm}^{-1}$ , due to the carbonyl stretching of the semicarbazone moiety. This shows that in solution, it tautomerises to the enol form and coordinates to the metal in the enolate form.

Table 6.1. Partial elemental analyses and of molar conductivities of cobalt(III) complexes of  $\text{HL}^1$  and  $\text{HL}^2$

Compound	Observed (Calculated) %			$\Lambda_{\text{M}^*}$
	C	H	N	
$[\text{CoL}^1_2]\text{NO}_3 \cdot \text{H}_2\text{O}$ ( <b>25</b> )	59.44(59.22)	3.81(4.32)	15.83(16.36)	86
$[\text{CoL}^1_2]\text{Cl}$ ( <b>26</b> )	62.65(62.86)	4.96(4.30)	14.95(15.43)	78
$[\text{CoL}^1_2]\text{Br} \cdot \text{H}_2\text{O}$ ( <b>27</b> )	57.72(57.88)	3.80(4.22)	13.76(14.21)	80
$[\text{CoL}^2_2]\text{NO}_3 \cdot 2\text{H}_2\text{O}$ ( <b>28</b> )	50.12(50.61)	4.94(4.70)	18.53(18.97)	92
$[\text{CoL}^2_2]\text{Cl}$ ( <b>29</b> )	55.36(55.87)	4.27(4.52)	18.34(18.62)	77

\*Molar conductivity of  $10^{-3}$  M DMF solution, in  $\text{ohm}^{-1}\text{cm}^2 \text{mol}^{-1}$

All complexes were prepared by direct reaction between the ligand and the corresponding cobalt(II) salts in the ratio 2:1. Magnetic susceptibility measurements at 293 K suggest that the compounds are diamagnetic indicating the oxidation of cobalt(II) to cobalt(III) and hence corresponds to  $d^6$  ion in a strong field.

### 6.3.2. IR spectra

Band positions in IR spectra are presented in wavenumbers. IR spectra of the ligands and the complexes have been recorded in KBr pellets. Some of the characteristic vibrational frequencies of the ligands are shifted upon coordination.

The tentative assignments of the IR spectral bands of ligands and its cobalt(III) complexes useful for determining the ligand's mode of coordination are listed in Table 6.2. A medium band in the region  $3380\text{ cm}^{-1}$  in the free ligands due to  $\nu(\text{N-H})$  vibration disappears in the spectra of complexes providing a strong evidence for the ligand coordination around cobalt(III) ion in its deprotonated form. Bands in the region  $1600\text{ cm}^{-1}$  suffer a significant shift in the spectra of complexes, which can be attributed to  $\nu(\text{C=N})$  vibration modes, and their mixing patterns are different from that in the spectra of ligands. The positive shift of bands corresponding to  $\nu(\text{C=N})$  in complexes is consistent with coordination of azomethine nitrogen to the central Co(III) ion. Medium bands around  $430\text{--}450\text{ cm}^{-1}$  corresponding to  $\nu(\text{Co-N})$  further support azomethine nitrogen coordination [8,9]. The enolization of the ligands and coordination of azomethine nitrogen is also evidenced from the increase in the  $\nu(\text{N-N})$

Table 6.2. Infrared spectroscopic assignments ( $\text{cm}^{-1}$ ) for the ligands and its cobalt(III) complexes

Compound	$\nu(\text{N-H})$	$\nu(\text{C=N})$	$\nu(\text{N-N})$	$\nu(\text{Co-N}_{\text{py}})$	$\nu(\text{C=O})$	$\nu(\text{Co-N}_{\text{azo}})$
$\text{HL}^1$	3375	1600	1132	-	1698	-
$[\text{CoL}_2]\text{NO}_3 \cdot \text{H}_2\text{O}$ (25)	3428	1608	1137	624	-	438
$[\text{CoL}_2]\text{Cl}$ (26)	3402	1605	1139	617	-	441
$[\text{CoL}_2]\text{Br} \cdot \text{H}_2\text{O}$ (27)	3386	1607	1138	628	-	439
$\text{HL}^2$	3380	1599	1151	-	1683	-
$[\text{CoL}_2]\text{NO}_3 \cdot 2\text{H}_2\text{O}$ (28)	3405	1609	1176	635	-	446
$[\text{CoL}_2]\text{Cl}$ (29)	3426	1631	1157	622	-	434

frequencies. This is further supported by the appearance of a new peak in the range  $720\text{-}780\text{ cm}^{-1}$  indicating  $\nu(\text{Co-O})$ .

A positive shift corresponding to out-of-plane bending vibrations of pyridine ring in the free ligands ( $613\text{-}622\text{ cm}^{-1}$ ) to higher frequencies ( $617\text{-}635\text{ cm}^{-1}$ ) in complexes is confirmative of pyridine nitrogen coordination to cobalt(III) ion [10,11].

In the spectra of the complexes **25** and **28**, the absence of the combination bands ( $\nu_1 + \nu_4$ ) in the region  $1700\text{-}1800\text{ cm}^{-1}$  rule out the possibility for coordinated nitrato group. The bands at  $840\text{ cm}^{-1}$  ( $\nu_2$ ),  $1384\text{ cm}^{-1}$  ( $\nu_3$ ) and  $706\text{ cm}^{-1}$  ( $\nu_4$ ) for **25** and bands at  $725$ ,  $1384$  and  $842\text{ cm}^{-1}$  for **28** clearly points out the uncoordinated nature of the nitrato group [12].

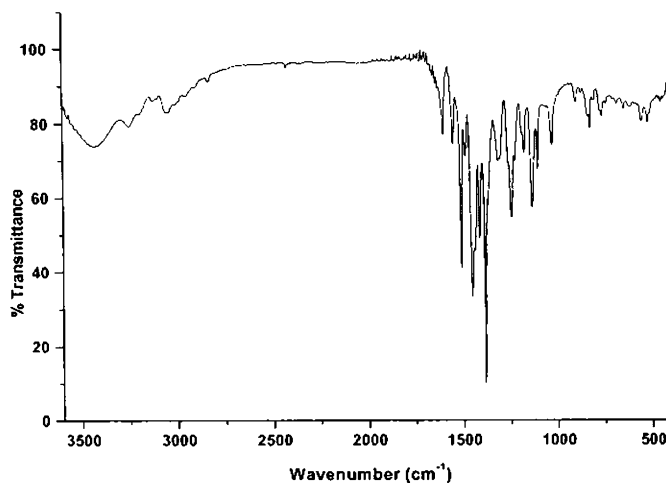


Fig. 6.1. IR spectrum of the complex  $[\text{CoL}^1_2]\text{NO}_3 \cdot \text{H}_2\text{O}$  (**25**).

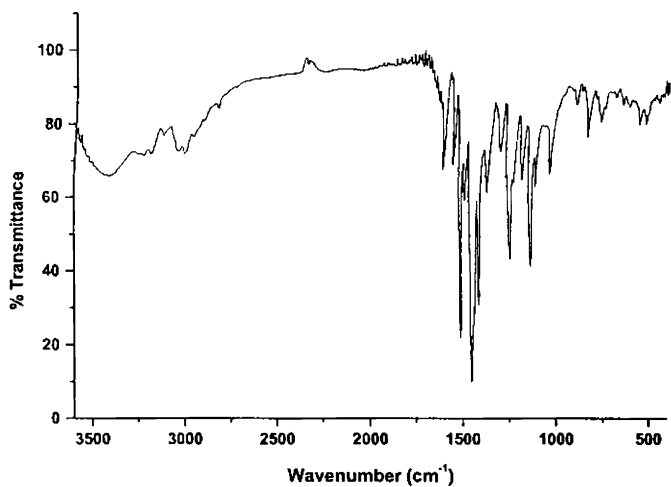


Fig. 6.2. IR spectrum of the complex  $[\text{CoL}^1_2]\text{Cl}$  (26).

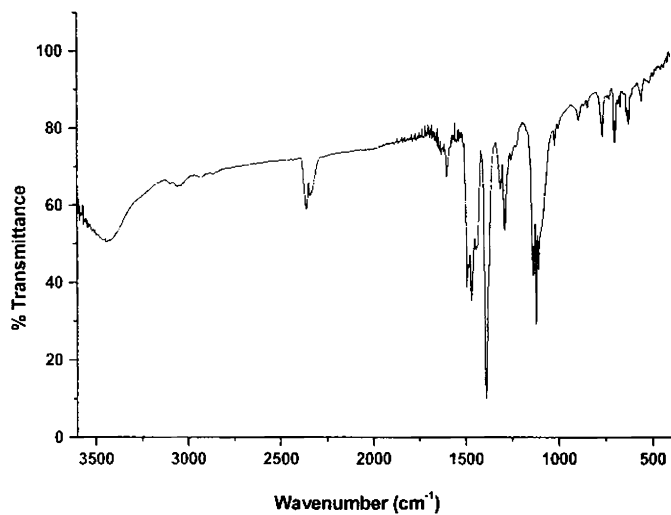


Fig. 6.3. IR spectrum of the complex  $[\text{CoL}^1_2]\text{Br} \cdot \text{H}_2\text{O}$  (27).



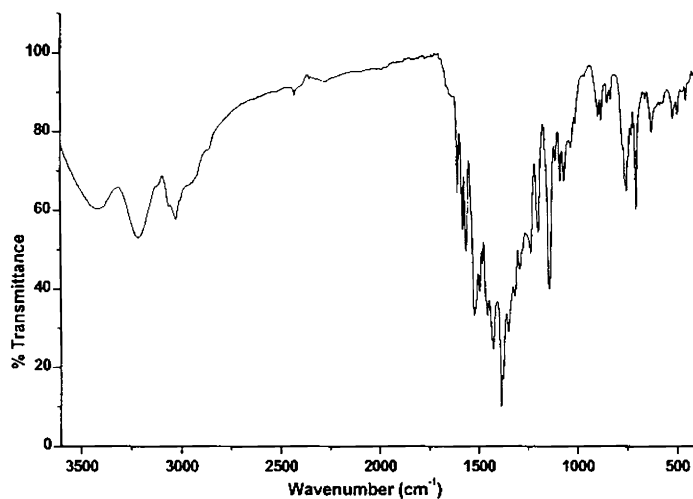


Fig. 6.4. IR spectrum of the complex  $[\text{CoL}_2]\text{NO}_3 \cdot 2\text{H}_2\text{O}$  (28).

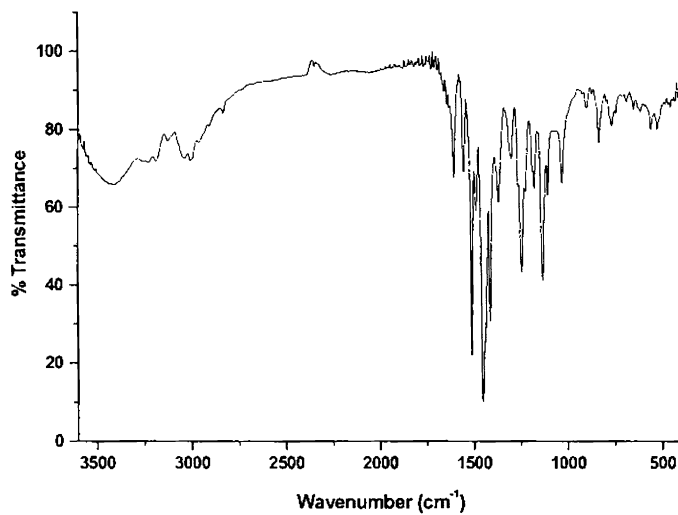


Fig. 6.5. IR spectrum of the complex  $[\text{CoL}_2]\text{Cl}$  (29).

The spectral band  $\nu(\text{N-H})$  of semicarbazones disappear in the complexes indicating deprotonation of NH proton and coordination *via* the

enolate oxygen [13]. The absence of spectral bands in the region of coordinated water according to Stefov *et al.* in the spectra of complexes indicates that the water molecules are not coordinated but are present as lattice water [14,15].

### 6.3.3. Electronic spectra

The electronic spectral assignments for the free ligands (HL<sup>1</sup> and HL<sup>2</sup>) and their Co(III) complexes are presented in Table 6.3.

Table 6.3. Electronic spectral assignments (cm<sup>-1</sup>) of the ligands and its Co(III) complexes

Compound	$\pi - \pi^*$	$n - \pi^*$	LMCT	$d - d$
HL <sup>1</sup>	37410	32890	-	-
[CoL <sup>1</sup> <sub>2</sub> ]NO <sub>3</sub> · H <sub>2</sub> O (25)	38050	32490	24630	17250
[CoL <sup>1</sup> <sub>2</sub> ]Cl (26)	38760	33710	25230	16520
[CoL <sup>1</sup> <sub>2</sub> ]Br · H <sub>2</sub> O (27)	37620	32640	25880	16930
HL <sup>2</sup>	37010	33900	-	-
[CoL <sup>2</sup> <sub>2</sub> ]NO <sub>3</sub> · 2H <sub>2</sub> O (28)	37290	33440	25200	17510
[CoL <sup>2</sup> <sub>2</sub> ]Cl (29)	37740	32940	24410	16180

Both the semicarbazones and their cobalt(III) complexes show a ring  $\pi \rightarrow \pi^*$  band in the range 37000–39000 cm<sup>-1</sup> and an  $n \rightarrow \pi^*$  band in the range 32000–34000 cm<sup>-1</sup> involving transitions within the semicarbazone moiety.

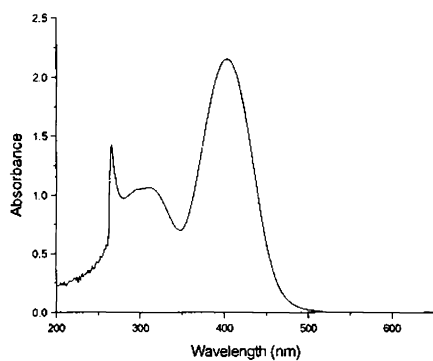
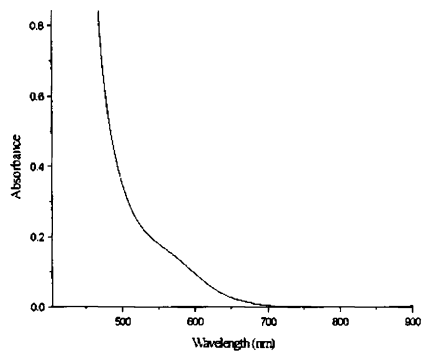
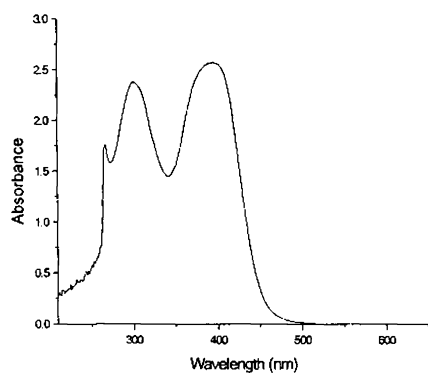
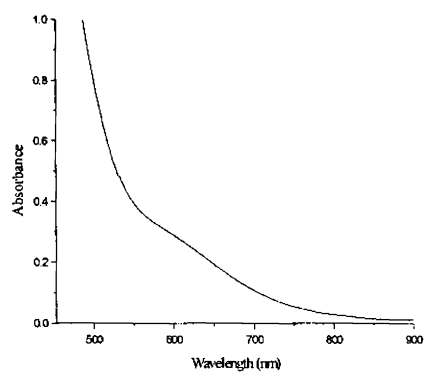
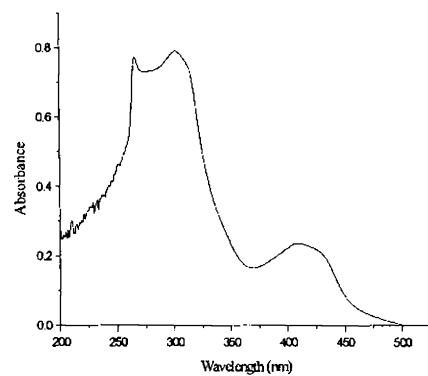
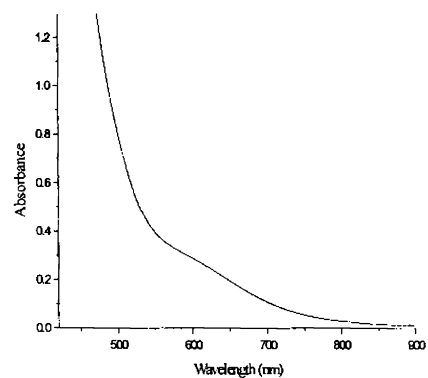
 $[\text{CoL}^1_2]\text{NO}_3 \cdot \text{H}_2\text{O}$  (25) $[\text{CoL}^1_2]\text{NO}_3 \cdot \text{H}_2\text{O}$  (25) $[\text{CoL}^2_2]\text{NO}_3 \cdot 2\text{H}_2\text{O}$  (28) $[\text{CoL}^2_2]\text{NO}_3 \cdot 2\text{H}_2\text{O}$  (28) $[\text{CoL}^2_2]\text{Cl}$  (29) $[\text{CoL}^2_2]\text{Cl}$  (29)

Fig. 6.6. Electronic spectra of cobalt complexes 25, 28 and 29.

The spectra of the complexes have bands with reduction in intensity than those of the ligands [16]. In the case of complexes having NNO donor ligands, the ligand to metal charge transfer bands are found in the 24400–25900  $\text{cm}^{-1}$  range.

The electronic spectra of spin paired trivalent cobalt complexes of approximate  $O_h$  symmetry have the following assignments of  $d-d$  bands: two spin allowed transitions at relatively low energy,  ${}^1T_{1g} \leftarrow {}^1A_{1g}$ ,  ${}^1T_{2g} \leftarrow {}^1A_{1g}$ . There are additional spin-forbidden transitions  ${}^3T_{1g} \leftarrow {}^1A_{1g}$  and  ${}^3T_{2g} \leftarrow {}^1A_{1g}$  at higher energies and these are usually complicated by the overlap of intraligand and charge transfer transitions [17].

In all the complexes, only one broad band is observed for the  $d-d$  band. The bands assigned are all spin allowed transitions. The band corresponding to  ${}^3T_{1g} \leftarrow {}^1A_{1g}$  is weak and difficult to assign because it is spin forbidden.

**References**

1. R.K. Parashar, R.C. Sharma, A. Kumar, G. Mohan, *Inorg. Chim. Acta* 151 (1988) 201.
2. H. Chen, D. Han, H. Yan, W. Tang, Y. Yang, H. Wang, *Polyhedron* 12 (1993) 1097.
3. J.P. Costes, G. Cros, M.H. Darbieu, J.P. Laurent, *Inorg. Chim. Acta* 60 (1982) 111.
4. A. Bottcher, T. Takeuchi, K.I. Hardcastle, T.J. Meade, H.B. Gray, D.C. Wickel, M. Kapon, Z. Dori, *Inorg. Chem.* 36 (1997) 2498.
5. S.K. Chattopadhyay, M. Hossain, S. Ghosh, A.K. Guha, *Transition Met. Chem.* 15 (1990) 473.
6. D.X. West, C.S. Carlson, *Trans. Met. Chem.* 15 (1990) 383.
7. N.M. Samus, V.I. Tsapkov, A.P. Gulya, *Russian Journal of General Chemistry* 74 (2004) 1428.
8. A. Sreekanth, U.L. Kala, C.R. Nayar, M.R.P. Kurup, *Polyhedron* 23 (2004) 41.
9. V. Suni, M.R.P. Kurup, M. Nethaji, *Polyhedron* 26 (2007) 5203.
10. D.F. Little, C.J. Long, *Inorg. Chem.* 7 (1968) 3401.
11. P.F. Raphael, E. Manoj, M.R.P. Kurup, E. Suresh, 26 (2007) 607.
12. D.N. Sathyanarayana, *Vibrational Spectroscopy*, New Age International, New Delhi (2004) 400.
13. P. Bindu, M.R.P. Kurup, T.R. Satyakeerty, *Polyhedron* 18 (1998) 321.
14. V. Stefov, V.M. Petrosevski, B. Septrajanov, *J. Mol. Struct.* 293 (1993) 97.

15. M. Joseph, V. Suni, M.R.P. Kurup, M. Nethaji, A. Kishore, S.G. Bhat, *Polyhedron* 23 (2004) 3069.
16. D.X. West, M.M. Salberg, G.A. Bain, A.E. Liberta, *Trans. Met. Chem.* 22 (1997) 180.
17. R.P. John, A. Sreekanth, M.R.P. Kurup, S.M. Mobin, *Polyhedron* 21 (2002) 2515.

**SYNTHESES AND SPECTRAL CHARACTERIZATION  
OF ZINC(II) COMPLEXES OF  
*N*(4)-PHENYLSEMICARBAZONES**

**7.1. Introduction**

Zinc with atomic number 30, atomic weight 65.39 and oxidation state +2 is an essential element in all living systems and play a structural role in many proteins and enzymes. It has an important role in several enzymes, both as metallo-enzyme and enzyme-activator, as well as filling a structural role [1]. Zinc(II)- sulfur interactions are of great interest in biochemical systems, due to the presence of sulfur at the active sites of several enzymes, vitamins and proteins [2]. Biologically it is the second most important transition metal. Its most vital function may be concerned with the synthesis of DNA and RNA. Zinc deficiency leads to impaired DNA synthesis, delayed wound healing and decrease in collagen synthesis [2,3]. Surprisingly, zinc was found to have important physiological and pharmaceutical functions involving insulin-mimetic activity. Although Zn(II) ion has been revealed to have an insulin-mimetic activity, zinc complexes have never been examined. Glucose normalizing effects of zinc complexes are also reported [4,5].

Zinc is an essential element, necessary for sustaining all life. In the human body, generally, 2-3 g of zinc is present and about 15 mg per day is necessary for the maintenance of healthy condition. It is estimated that about 3000 proteins in the human body contain zinc. It stimulates the

activity of approximately 100 enzymes, which are substances that promote biochemical reactions in the body [6].

Today more than 200 different zinc proteins are known which include numerous essential enzymes [7]. Zn is present as enzyme in most body cells of human beings, but its concentration is very low. The wound healing effect of zinc containing ointment was already known in the ancient world and during the last decades, zinc has increasingly been used as a remedy for growth disorders due to malnutrition [8].

Advantageous features of zinc in the above-mentioned functions and its applications for medical use are well explained by the following basic physicochemical aspects of zinc ion and its complexes. 1) Zinc ion has a small radius and acts as a Lewis acid and hence it can play an advantageous role as a catalyst in hydrolysis reactions. 2) The stability of zinc complexes with some ligands present in living system is satisfactorily high but not too high, so that zinc is reactive in complexation. This means high probability of ligand-exchange reactions in zinc complexes in living systems. Irving-Williams stability order applicable to various divalent metal complexes with common ligands shows that the stability of zinc complexes is generally lower than that of copper and is comparable to that of nickel and much higher than that of calcium or magnesium. 3) The bivalent state is stable because of the fully occupied  $3d$  orbital, and it is maintained even in highly oxidizing and reducing environments. 4) Fairly high affinity is shown towards the main coordinating atoms such as sulfur, nitrogen and oxygen. This means high flexibility in the structure, coordination mode, and coordination number of the complexes produced [9].



The electron configuration [Ar]  $3d^{10} 4s^2$  provides a filled (n-1)*d* state for zinc. In view of the stability of the filled *d* sublevel, the element shows few of the characteristics of transition metals despite its position in the *d*-block of the periodic table. It resembles other transition metals in the formation of stable complexes with O, N and S-donor ligands and with ions like cyanide, halide etc. The  $d^{10}$  configuration affords no crystal field stabilization, which implies that the stereochemistry of a  $Zn^{2+}$  complex depends on the size and polarizing power of this ion. Because of this versatility towards different kinds of ligands and its flexibility towards coordination number ranging from two to six, the zinc(II) ion provides various types of chelate complexes. Among these complexes, some have attracted special attention as model compounds for the active sites of zinc-containing enzymes [10,11] and their functions strongly depend upon the coordination environment around the zinc ion. Therefore, for understanding or creating functional zinc complexes, it is important to consider the relationship of the coordination characteristics peculiar to the zinc ion. Heterocyclic carbaldehyde thiosemicarbazones have been extensively investigated for activity against various bacterial and viral infections [12,13]. Biological activity of semicarbazones and thiosemicarbazones are found to increase on complexation with transition metals [14], higher activity being incorporated with substitution at *N*(4) position [15]. These observations were the impetus for us to build an *N*(4)-substituted semicarbazone moiety on 2-benzoylpyridine and 2-acetylpyridine and synthesize zinc(II) complexes to study the coordinating behavior. In this chapter we describe the structural and spectral studies of six new Zn(II) complexes of the ligands, 2-benzoylpyridine-*N*(4)-phenyl semicarbazone (HL<sup>1</sup>) and 2-acetylpyridine-*N*(4)-phenylsemicarbazone (HL<sup>2</sup>).

## 7.2. Experimental

### 7.2.1. Materials

Details regarding the syntheses of HL<sup>1</sup> and HL<sup>2</sup> are described in Chapter 2. Zinc(II) nitrate hexahydrate, zinc(II) chloride, zinc(II) bromide and zinc(II) sulphate heptahydrate (Merck) were used as supplied. The solvents were purified by standard procedures before use.

### 7.2.2. Syntheses of complexes

#### [Zn(HL<sup>1</sup>)Cl<sub>2</sub>] · H<sub>2</sub>O (30)

To a solution of 1 mmol of HL<sup>1</sup> (0.316 g) in 15 ml hot methanol was added 10 ml of a methanolic solution of 1 mmol of ZnCl<sub>2</sub> (0.136 g). The mixture was heated under reflux for two hours and cooled. The yellow colored complex formed was filtered, washed thoroughly with water, methanol and then ether and dried *in vacuo* over P<sub>4</sub>O<sub>10</sub>.

#### [Zn(HL<sup>1</sup>)<sub>2</sub>](NO<sub>3</sub>)<sub>2</sub> (31)

To a solution of 1 mmol of HL<sup>1</sup> (0.316 g) in 20 ml hot methanol was added 10 ml of a methanolic solution of 1 mmol of Zn(NO<sub>3</sub>)<sub>2</sub> · 6H<sub>2</sub>O (0.297 g). The mixture was stirred for four hours. The yellow colored complex formed was filtered, washed thoroughly with water, methanol and then ether and dried *in vacuo* over P<sub>4</sub>O<sub>10</sub>.

$[\text{Zn}_2(\text{L}^1)_2\text{SO}_4] \cdot 2\text{CH}_3\text{OH}$  (32)

To a solution of 1 mmol of HL<sup>1</sup> (0.316 g) in 20 ml hot methanol was added a suspension of 1 mmol of ZnSO<sub>4</sub> · 7H<sub>2</sub>O (0.287 g) in a mixture of 10 ml of methanol and 10 ml of ethanol. The mixture was stirred for 30 minutes. The yellow colored complex formed was filtered, washed thoroughly with water, methanol and then ether and dried *in vacuo* over P<sub>4</sub>O<sub>10</sub>.

 $[\text{Zn}(\text{HL}^2)\text{Cl}_2]$  (33)

To a solution of 1 mmol of HL<sup>2</sup> (0.254 g) in 20 ml hot methanol was added 10 ml of a methanolic solution of 1 mmol of ZnCl<sub>2</sub> (0.136 g). The mixture was refluxed for two hours. The yellow colored complex formed was filtered, washed thoroughly with water, methanol and then ether and dried *in vacuo* over P<sub>4</sub>O<sub>10</sub>.

 $[\text{ZnL}^2\text{Br}] \cdot \text{CH}_3\text{OH}$  (34)

To a solution of 1 mmol of HL<sup>2</sup> (0.254 g) in 20 ml hot methanol was added 10 ml of a methanolic solution of 1 mmol of ZnBr<sub>2</sub> (0.225 g). The mixture was heated under reflux for three hours and cooled. The yellow colored complex formed was filtered, washed thoroughly with water, methanol and then ether and dried *in vacuo* over P<sub>4</sub>O<sub>10</sub>.

 $[\text{Zn}_2(\text{L}^2)_2\text{SO}_4] \cdot 2\text{H}_2\text{O}$  (35)

To a solution of 1 mmol of HL<sup>2</sup> (0.254 g) in 20 ml hot methanol was added a suspension of 1 mmol of ZnSO<sub>4</sub> · 7H<sub>2</sub>O (0.287 g) in a mixture of 10 ml of methanol and 10 ml of ethanol. The mixture was stirred for one hour. The complex formed was filtered, washed thoroughly with water, methanol and then ether and dried *in vacuo* over P<sub>4</sub>O<sub>10</sub>.

### 7.2.3. Analytical methods

Elemental analyses were carried out using a Vario EL III CHNS analyzer at SAIF, Kochi, India. Infrared spectra were recorded on a Thermo Nicolet AVATAR 370 DTGS model FT-IR spectrophotometer with KBr pellets at SAIF, Kochi, India. Electronic spectra were recorded on a Cary 5000, version 1.09 UV-Vis-NIR spectrophotometer from solutions in acetonitrile. Molar conductance measurements of the solutions of complexes in DMF ( $10^{-3}$  M) at room temperature were done using a digital conductivity meter.

## 7.3. Results and discussion

### 7.3.1. Analytical measurements

The colors, molar conductivity measurements and partial elemental analysis data of the complexes are listed in Table 7.1. Zn complexes were found to form readily in methanol medium under reflux or upon stirring. Molar conductivity measurements show that except **31** all of them are non-electrolytes, **31** being an electrolyte. From the elemental analysis, the compounds **30** and **33** were assigned the empirical formulae  $[\text{Zn}(\text{HL}^1)\text{Cl}_2]$  and  $[\text{Zn}(\text{HL}^2)\text{Cl}_2]$  respectively, while **31**, **32**, **34** and **35** were assigned the formulae  $[\text{Zn}(\text{HL}^1)_2](\text{NO}_3)_2$ ,  $[\text{Zn}_2(\text{L}^1)_2\text{SO}_4] \cdot 2\text{CH}_3\text{OH}$ ,  $[\text{ZnL}^2\text{Br}] \cdot \text{CH}_3\text{OH}$  and  $[\text{Zn}_2(\text{L}^2)_2\text{SO}_4] \cdot 2\text{H}_2\text{O}$  respectively. The complexes **30**, **31** and **33** have ligands in the keto form, whereas **32**, **34** and **35** have ligands coordinated in the enolate form as evidenced by the IR spectra. The complexes are found to be diamagnetic as expected for a  $d^{10}$  Zn(II) system.

Table 7.1. Stoichiometries, partial elemental analyses, colors and molar conductivities of the complexes.

Compound	Color	$\lambda_M^*$	Observed (Calculated)%		
			C	H	N
$[\text{Zn}(\text{HL}^1)\text{Cl}_2] \cdot \text{H}_2\text{O}$ (30)	Yellow	64	48.15 (48.49)	3.46 (3.85)	15.24 (15.06)
$[\text{Zn}(\text{HL}^1)_2](\text{NO}_3)_2$ (31)	Yellow	166	60.66 (60.20)	3.88 (4.25)	18.14 (18.48)
$[\text{Zn}_2\text{L}^1_2\text{SO}_4] \cdot 2\text{CH}_3\text{OH}$ (32)	Yellow	58	52.49 (52.01)	4.78 (4.37)	12.56 (12.13)
$[\text{Zn}(\text{HL}^2)\text{Cl}_2]$ (33)	Yellow	52	43.38 (43.05)	3.42 (3.61)	14.78 (14.34)
$[\text{ZnL}^2\text{Br}] \cdot \text{CH}_3\text{OH}$ (34)	Yellow	56	41.68 (41.84)	3.56 (3.98)	12.85 (13.01)
$[\text{Zn}_2(\text{L}^2)_2\text{SO}_4] \cdot 2\text{H}_2\text{O}$ (35)	Yellow	62	43.24 (43.59)	4.41 (4.18)	14.25 (14.53)

\*Molar conductivity of  $10^{-3}$  M DMF solution, in  $\text{ohm}^{-1}\text{cm}^2 \text{mol}^{-1}$

Ligand can exist in keto or enol form or an equilibrium mixture of the two since it has an amide  $-\text{NH}-\text{C}=\text{O}$  function. However, the IR spectra of  $\text{HL}^1$  and  $\text{HL}^2$  indicate that in the solid state they remain in keto form.

The IR spectra of complexes except 30, 31 and 33, however, do not show any intense absorption bands around  $1698$  and  $1683 \text{ cm}^{-1}$ , due to the carbonyl stretching of the semicarbazone moiety. This shows that in solution, the complexes tautomerise to the enol form and coordinates to the metal in the enolate form.

### 7.3.2. IR spectra

The IR spectra of the free ligands when compared with those of complexes confirm the coordination of the semicarbazone to the metal. The significant bands observed in the IR spectra of ligands and its complexes with the tentative assignments are presented in the Table 7.2.

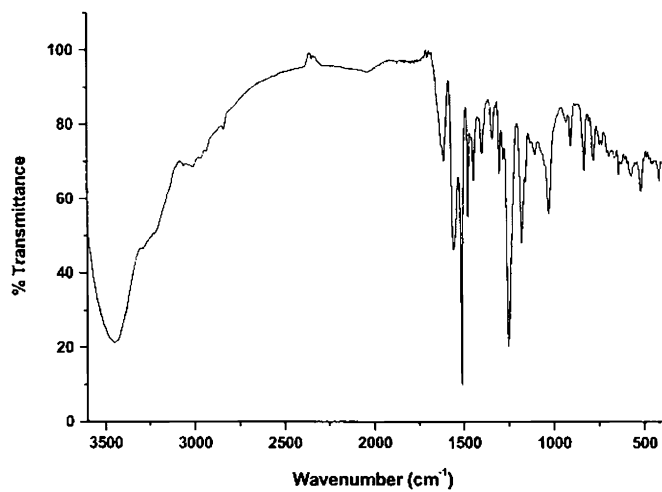
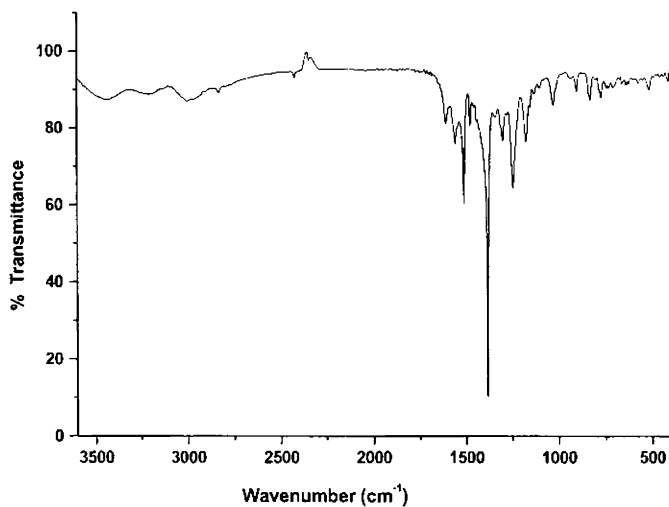
In the IR spectra of the ligands HL<sup>1</sup> and HL<sup>2</sup>, the bands at 3052 and 3094 cm<sup>-1</sup> respectively corresponding to the  $\nu(\text{N-H})$  indicate that the ligands remain as keto tautomers in the solid state [16]. These bands are absent in all the complexes except in **30**, **31** and **33**. Bands at 1698 and 1683 cm<sup>-1</sup> attributable to  $\nu(\text{C=O})$  stretching in the ligand spectrum is absent in the complexes except compounds **30**, **31** and **33** indicate the coordination in the enolate form. In compounds **30**, **31** and **33**, the ligand is coordinated in the keto form. In the spectra of complexes **32**, **34** and **35**, the bands corresponding to the newly formed C=N bond due to the enolization of the ligands are observed around 1570 cm<sup>-1</sup>. In compounds **30**, **31** and **33**, the ligand is in the keto form which is confirmed by the appearance of bands at 1696, 1668 and 1687 cm<sup>-1</sup>, due to  $>\text{C=O}$  in these complexes.

The  $\nu(\text{C=N})$  bands of semicarbazones are found to be shifted to lower frequencies by 30-40 cm<sup>-1</sup> in all complexes representing the coordination *via* the azomethine nitrogen. The coordination of this nitrogen is also supported by a shift in  $\nu(\text{N-N})$  frequencies [17,18]. A shift to lower frequency is due to the conjugation of *p*-orbital on the double bond with the *d*-orbital on the metal atom with the reduction of the force constant. In the IR spectra of the complexes, the bands at 420-435 cm<sup>-1</sup> assignable to  $\nu(\text{Zn-N}_{\text{azo}})$  further confirms the coordination of the metal through azomethine nitrogen [19,20].

Table 7.2. Infrared spectral assignments ( $\text{cm}^{-1}$ ) of semicarbazones and their Zn(II) complexes.

Compound	$\nu(\text{N-H})$	$\nu(\text{C=N})$	$\nu(\text{N-N})$	$\nu(\text{C=O})$	$\nu(\text{C=N})^a$	$\nu(\text{Zn-N}_{\text{av.}}$ )
HL <sup>1</sup>	3375	1600	1132	1698	-	-
[Zn(HL <sup>1</sup> )Cl <sub>2</sub> ] · H <sub>2</sub> O (30)	3448	1561	1025	1692	-	424
[Zn(HL <sup>1</sup> ) <sub>2</sub> ](NO <sub>3</sub> ) <sub>2</sub> (31)	3439	1560	1029	1668	-	429
[Zn <sub>2</sub> L <sup>1</sup> <sub>2</sub> SO <sub>4</sub> ] · 2CH <sub>3</sub> OH (32)	3419	1564	1129	-	1572	428
HL <sup>2</sup>	3380	1599	1151	1683	-	430
[Zn(HL <sup>2</sup> )Cl <sub>2</sub> ] (33)	3425	1568	1056	1668	-	435
[ZnL <sup>2</sup> Br] · CH <sub>3</sub> OH (34)	3422	1566	1058	-	1574	428
[Zn <sub>2</sub> L <sup>2</sup> <sub>2</sub> SO <sub>4</sub> ] · 2H <sub>2</sub> O (35)	3445	1567	1113	-	1570	425

<sup>a</sup> indicates newly formed C=N

Fig. 7.1. IR spectrum of  $[\text{Zn}(\text{HL}^1)\text{Cl}_2] \cdot \text{H}_2\text{O}$  (30).Fig. 7.2. IR spectrum of  $[\text{Zn}(\text{HL}^1)_2](\text{NO}_3)_2$  (31).



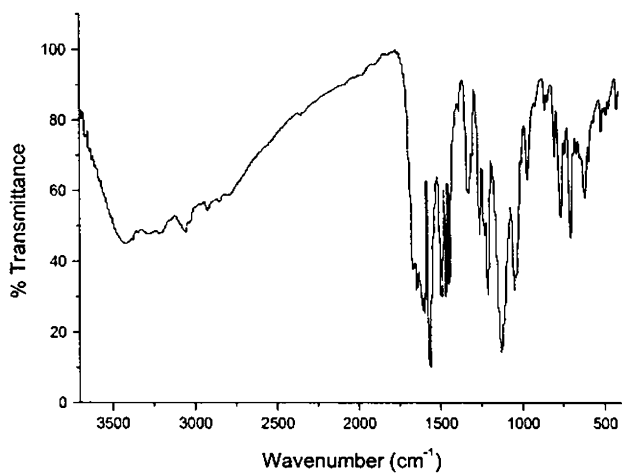


Fig. 7.3. IR spectrum of  $[\text{Zn}_2\text{L}^1_2\text{SO}_4] \cdot 2\text{CH}_3\text{OH}$  (32).

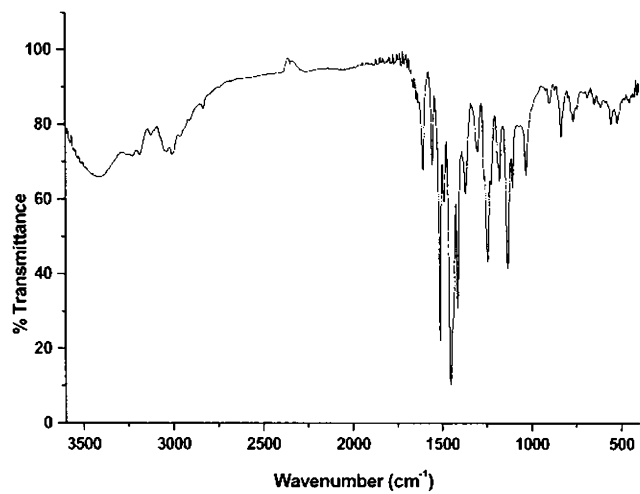
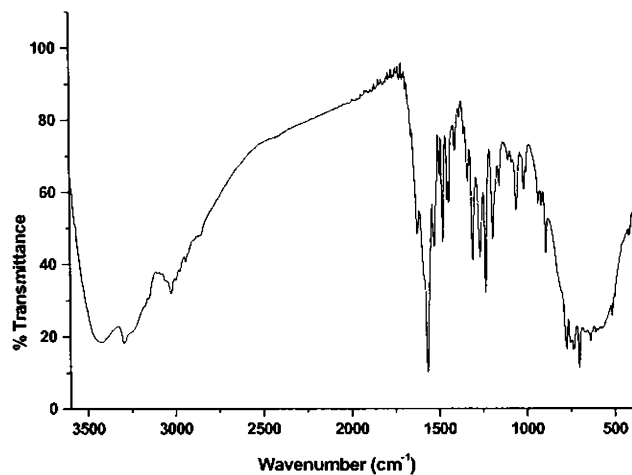
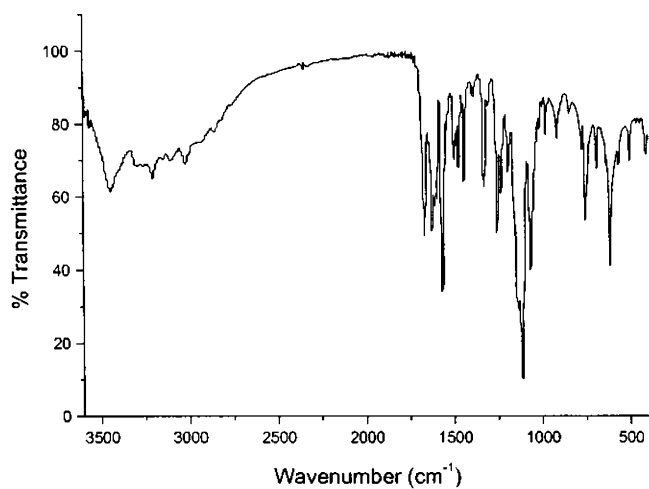


Fig. 7.4. IR spectrum of  $[\text{Zn}(\text{HL}^2)\text{Cl}_2]$  (33).

Fig. 7.5. IR spectrum of  $[\text{ZnL}^2\text{Br}] \cdot \text{CH}_3\text{OH}$  (34).Fig. 7.6. IR spectrum of  $[\text{Zn}_2\text{L}^2\text{SO}_4] \cdot 2\text{H}_2\text{O}$  (35).

In the spectrum of the complex **31**, the absence of the combination bands ( $\nu_1+\nu_4$ ) in the region  $1700-1800\text{ cm}^{-1}$  rules out the possibility for coordinated nitrate group. The bands at  $837\text{ cm}^{-1}(\nu_2)$ ,  $1385\text{ cm}^{-1}(\nu_3)$  and  $712\text{ cm}^{-1}(\nu_4)$  clearly point out the uncoordinated nature of the nitrate group [21].

The IR spectrum of the complex **32** shows bands at 1213, 1129 and  $1052\text{ cm}^{-1}$  and that of complex **35** shows bands at 1197, 1113 and  $1067\text{ cm}^{-1}$  can be attributed to the  $\nu_3$  vibrations of the bridging bidentate sulfato group with  $C_{2v}$  symmetry. The appearance of medium bands at 662 and  $413\text{ cm}^{-1}$  and a weak band at  $964\text{ cm}^{-1}$  for complex **32** and medium bands at 618 and  $411\text{ cm}^{-1}$  and a weak band at  $982\text{ cm}^{-1}$  for complex **35** can be assigned to  $\nu_4$ ,  $\nu_2$  and  $\nu_1$  vibrations which also supports the presence of bridging bidentate sulfato group [21,22].

According to Stefov *et al.*, coordinated water should exhibit bands at 825, 575 and  $500\text{ cm}^{-1}$ . The absence of bands in these regions in the spectra of **30** and **35** show that the water molecules are not coordinated but are present as lattice water [23].

### 7.3.3. Electronic spectra

The electronic spectral assignments for the free ligands ( $HL^1$  and  $HL^2$ ) and their Zn(II) complexes are presented in Table 7.3. The electronic spectra of the Zn(II) complexes were recorded in acetonitrile.

The ligand  $HL^1$  showed bands at 37410 and  $32890\text{ cm}^{-1}$  and the ligand  $HL^2$  showed bands at 37010 and  $33900\text{ cm}^{-1}$  attributable to the  $\pi\rightarrow\pi^*$  and  $n\rightarrow\pi^*$  transitions of the azomethine group [24,25]. The energy of these bands is slightly shifted on complexation (Figs. 7.7 and 7.8). The

shift shows donation of a lone pair of electrons to the metal by the coordination of azomethine nitrogen [26,27].

Table 7.3. Electronic spectral assignments ( $\text{cm}^{-1}$ ) of the ligands and its Zn(II) complexes.

Compound	$\pi - \pi^*$	$n - \pi^*$	MLCT
$\text{HL}^1$	37410	32890	-
$[\text{Zn}(\text{HL}^1)\text{Cl}_2] \cdot \text{H}_2\text{O}$ (30)	36100	31060	24360
$[\text{Zn}(\text{HL}^1)_2](\text{NO}_3)_2$ (31)	36870	31250	24040
$[\text{Zn}_2\text{L}^1_2\text{SO}_4] \cdot 2\text{CH}_3\text{OH}$ (32)	37590	31750	23920
$\text{HL}^2$	37010	33900	-
$[\text{Zn}(\text{HL}^2)\text{Cl}_2]$ (33)	37680	33590	24200
$[\text{ZnL}^2\text{Br}] \cdot \text{CH}_3\text{OH}$ (34)	37480	32370	24810
$[\text{Zn}_2(\text{L}^2)_2\text{SO}_4] \cdot 2\text{H}_2\text{O}$ (35)	38020	32680	25250

In addition to these intra-ligand bands, a new band around 23900–25300  $\text{cm}^{-1}$  range is observed in the spectra of the complexes. This band can safely be assigned to metal $\rightarrow$ O charge-transfer band. The appearance of metal $\rightarrow$ O charge-transfer band in the electronic spectra of Zn(II) complex is a strong evidence that the keto oxygen atoms of the ligands are coordinated to the Zn(II) ion. The MLCT maxima of the complexes show line broadening into the visible part of the spectra. No appreciable absorptions occurred below 20000  $\text{cm}^{-1}$  indicating the absence of  $d-d$  bands, which is in accordance with the  $d^{10}$  configuration of the Zn(II) ion.

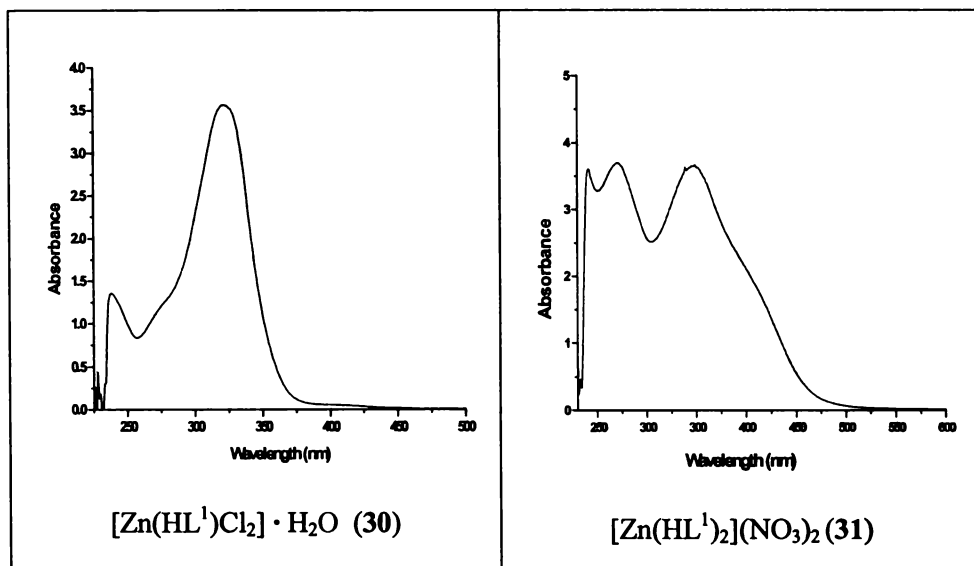


Fig. 7.7. Electronic spectra of zinc(II) complexes (30 and 31).

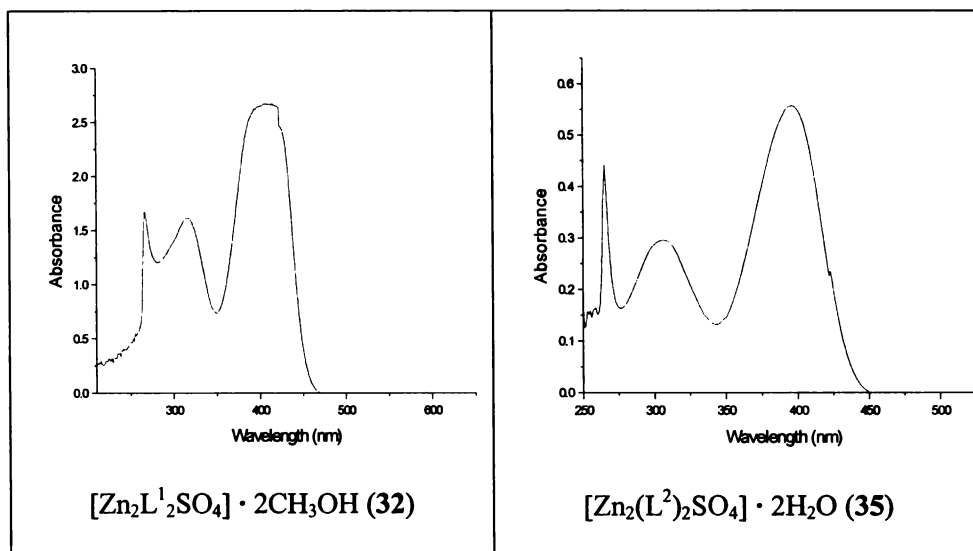


Fig. 7.8. Electronic spectra of zinc(II) complexes (32 and 35).

The semicarbazones and their zinc(II) complexes show a  $\pi \rightarrow \pi^*$  band in the range 37000–38100  $\text{cm}^{-1}$  and an  $n \rightarrow \pi^*$  band in the range 31000–34000  $\text{cm}^{-1}$  involving transitions within the semicarbazone moiety. The spectra of the complexes have bands with reduction in intensity than those of the ligands [28].

**References**

1. R.H. Prince, *Adv. Inorg. Radiochem.* 22 (1979) 349.
2. L.S. Sarma, J.R. Kumar, K.J. Reddy, T. Thriveni, A.V. Reddy, J. *Braz. Chem. Soc.* 17 (2006) 463.
3. T. Walsh, H. Sandstead, A.S. Prasad, P.M. Newberne, J. Pamela . *Zinc: Health Effects*, Carol Boston University School of Medicine, Boston, 1990.
4. H. Sakurai, Y. Kojima, K. Kawabe. *Coord. Chem. Rev.* 226 (2002) 187.
5. M.B. Ferrari, G.G. Fava, C. Pelizzi, P. Tarasconi, *J. Chem. Soc., Dalton Trans.* 2153 (1992).
6. H.H. Sandstead, *J. Lab. Clin. Med.* 124 (1994) 322.
7. W. Kaim, B. Schwderski, *Bioinorganic Chemistry, Inorganic Elements in the Chemistry of Life*, Wiley, New York, 1991.
8. B.C. Cunningham, M.G. Mulkerrin, J.A. Wells, *Dimerization of human growth hormone by zinc*, *Science*, 253 (1991) 545.
9. T. Matsukura, H. Tanaka, *Biochemistry* 65 (2000) 817.
10. G. Parkin, *Chem. Commun.* 1971 (2000).
11. M. Doring, M. Ciesielski, O. Walterand, H. Gorls, *Eur. J. Inorg. Chem.* (2002) 1615.
12. P. Malatesta, G.P. Accinelli, G.P. Quaglia, *Ann. Chim. Rome* 49 (1959) 397.
13. J.C. Logan, M.P. Fox, J.H. Morgan, A.M. Makohon, C.J. Pfau, J. *Gen. Virol.* 28(1975) 271.
14. D.X. West, A.E. Liberta, S.B. Padhye, R.C. Chikate, P.B. Sonawane,

- A.S. Kumbhar, R.G. Yerande, *Coord. Chem. Rev.* 123 (1993) 49.
15. D.L. Klayman, J.F. Bartosevich, T.S. Griffin, C.J. Manson, J.P. Scovill, *J. Med. Chem.* 22 (1979) 885.
16. Y.-P. Tian, W.-T. Yu, C.-Y. Zhao, M.-H. Jiang, Z.-G. Cai, H.-K. Fun, *Polyhedron* 21 (2002) 1217.
17. A. Sreekanth, M. Joseph, H.-K. Fun, M.R.P. Kurup, *Polyhedron* 25 (2006) 1408.
18. E.B. Seena, M.R.P. Kurup, *Spectrochim. Acta A* 69 (2008) 726.
19. E. Bermejo, A. Castineiras, I.G. Santos, D.X. West, *Z. Anorg. Allg. Chem.* 630 (2004) 1097.
20. Leji Latheef, E. Manoj, M.R.P. Kurup, *Polyhedron* 26 (2007) 4107.
21. D.N. Sathyanarayana, *Vibrational Spectroscopy*, New Age International, New Delhi (2004) 400.
22. M. Joseph, V. Suni, M.R.P. Kurup, M. Nethaji, A. Kishore, S.G. Bhat, *Polyhedron* 23 (2004) 3069.
23. V. Stefov, V.M. Petrusevski, B. Soptrajanov, *J. Mol. Struct.* 293 (1993) 97.
24. A. Sreekanth, U.L. Kala, C.R. Nayar, M.R.P. Kurup, *Polyhedron* 23 (2004) 41.
25. E. Bermejo, D.X. West, L.J. Ackerman, J.V. Martinez, S.H. Ortega, *Polyhedron* 18 (1999) 1469.
26. N.C. Bhardwaj, R.V. Singh, *Proc. Indian Acad. Sci. (Chem.Sci.)* 106 (1994).
27. E.W. Ainscough, A.M. Brodie, J. Ranford, J.M. Waters, *J. Chem. Soc., Dalton Trans.* (1997) 279.
28. D.X. West, M.M. Salberg, G.A. Bain, A.E. Liberta, *Trans. Met. Chem.* 22 (1997) 180.



## SUMMARY AND CONCLUSION

The work presented in this thesis aims on the syntheses of some novel semicarbazone ligands and their transition metal complexes together with their physico-chemical characterization. The coordination geometries have been confirmed by X-Ray diffraction studies. The thesis is divided into seven chapters.

Chapter 1 deals with an extensive literature survey relating the history, applications and recent developments in the field of semicarbazones and their transition metal complexes. A brief introduction to the various analytical methods is also furnished.

Chapter 2 deals with the syntheses of two semicarbazone ligands.

The ligands synthesized are:

- 2-Benzoylpyridine-*N*(4)-phenylsemicarbazone [HL<sup>1</sup>]
- 2-Acetylpyridine-*N*(4)-phenylsemicarbazone [HL<sup>2</sup>]

The ligands are characterized by elemental analyses, IR, UV and <sup>1</sup>H NMR techniques. The IR spectra of ligands indicate that in solid state they remain in keto form.

Chapter 3 describes the syntheses and physico-chemical characterizations by partial elemental analyses, conductivity and room temperature magnetic susceptibility measurements and IR, electronic and EPR spectral studies of nine copper(II) complexes (**1-9**) of the ligand HL<sup>1</sup>. The principal ligand HL<sup>1</sup> undergoes deprotonation to L<sup>-</sup> and chelates in enolate form as evidenced by the IR spectra. However, for complexes **4** and **5**, the semicarbazone remains in the neutral form. The conductivity measurements were made in DMF solutions and the values are found to be

less than  $20 \Omega^{-1}\text{mol}^{-1}\text{cm}^{-1}$  and all complexes are found to be non-electrolytes which indicates that the anion and the ligand are coordinated to the central copper(II). The room temperature magnetic susceptibilities of the complexes in the polycrystalline state except complexes **1** and **5** fall in the range of 1.70-2.00 B.M., which are very close to the spin-only value of 1.73 B.M. for a typical  $S=1/2$   $d^9$  copper(II) system. The low value of complexes **1** and **5** is an evidence for their behavior as dimers. From the EPR spectra of the complexes, the EPR parameters, the bonding parameters and the orbital reduction factors are calculated. The EPR spectra of all the Cu(II) complexes were recorded both in polycrystalline state at 298 K and in DMF at 77 K. The solution EPR spectra of compounds **1** and **5** at 77 K, exhibit a half field signal which indicate that indeed a weak interaction between two Cu(II) ions within this compound is present. The  $g$  values calculated indicate that in all the complexes the unpaired electron is present in the  $d_{x^2-y^2}$  orbital. In the electronic spectral studies, the  $d-d$  transitions are found to be broad. IR spectral data indicates that the ligand  $\text{HL}^1$  is tridentate, coordinating *via* the azomethine nitrogen, the pyridyl nitrogen and keto or enolate oxygen. The single crystal X-ray diffraction study of the compound  $[\text{Cu}_2\text{L}^1_2(\text{OAc})_2]$  (**1a**) shows that the compound exists as oxygen bridged dimer with a distorted square pyramidal geometry.

Syntheses and spectral characterization of nine copper(II) complexes (**10-18**) of the ligand  $\text{HL}^2$  are discussed in Chapter 4. It presents the physico-chemical characterization by partial elemental analyses, conductivity and room temperature magnetic susceptibility measurements and also by IR, electronic and EPR spectral studies. The principal ligand  $\text{HL}^2$  undergoes deprotonation to  $\text{L}^-$  and chelates in enolate form as

evidenced by the IR spectra. The room temperature magnetic susceptibilities of the complexes in the polycrystalline state formulated with one metal centre except complexes **10**, **11**, **14** and **18** fall in the range of 1.60-2.00 B.M., which are very close to the spin-only value of 1.73 B.M. The magnetic susceptibilities of the polynuclear complexes **10**, **11**, **14** and **18** suggest considerable interaction between metal centers and the magnetic moments fall in the range 1.03-1.16 B.M. which makes an evidence for their behavior as dimers. The EPR spectra of all the Cu(II) complexes were recorded both in polycrystalline state at 298 K and in DMF at 77 K. The solution EPR spectrum of compound **10** at 77 K and the spectra of compounds **11**, **14** and **18** in polycrystalline form at 298 K exhibit a half field signal. The single crystal X-ray diffraction study of the compound  $[\text{Cu}_2\text{L}_2(\mu\text{-N}_3)_2]$  (**10a**) shows that the compound exists as an end-on azido bridged dimer.

Chapter 5 represents the syntheses and spectral characterization of six Mn(II) complexes (**19-24**). In compounds except **20** and **23**, the semicarbazones deprotonate and chelate in monoanionic form  $\text{L}^-$  and in compounds **20** and **23**, the ligand moiety is coordinated in the neutral form as evidenced by the IR spectra. The room temperature magnetic moments of powdered samples of complexes are consistent with Mn(II) complexes where there are no significant exchange interactions between adjacent metal centers and are very close to spin-only value (5.91 B.M.). From the magnetic susceptibility measurements, they are found to be high spin complexes. The coordination behaviour was assessed by IR and electronic spectroscopy. EPR spectra of the complexes showed six hyperfine splitting with forbidden transitions.

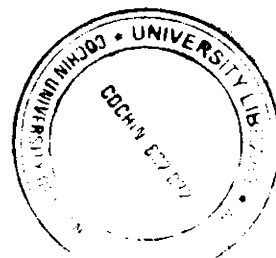
Syntheses and spectral characterization of five cobalt(III) complexes (**25-29**) of the ligands HL<sup>1</sup> and HL<sup>2</sup> are discussed in Chapter 6. Magnetic susceptibility measurements at 293 K suggest that the compounds are diamagnetic indicating the oxidation of cobalt(II) to cobalt(III) and hence corresponds to  $d^6$  ion in a strong field. The molar conductivities of  $10^{-3}$  M DMF solutions of the complexes indicate that they are 1:1 electrolytes.

Chapter 7 presents the syntheses and spectral characterization of six zinc(II) complexes (**30-35**) of HL<sup>1</sup> and HL<sup>2</sup>. These complexes are characterized by partial elemental analyses, molar conductivity and magnetic susceptibility measurements, IR and electronic spectral studies. Molar conductivity measurements show that except **31** all of them are non-electrolytes, **31** being an electrolyte. The complexes **30**, **31** and **33** have ligands in the keto form, whereas **32**, **34** and **35** have ligands coordinated in the enolate form as evidenced by the IR spectra. The complexes are found to be diamagnetic as expected for a  $d^{10}$  Zn(II) system.

# Curriculum Vitae

## PERSONAL PROFILE

Date of Birth 16<sup>th</sup> May 1979  
Permanent address Parayil House,  
Near 'Kala' Auditorium  
Kothamangalam P.O  
Ernakulam, Kerala 686 691  
Ph. No. 0485 - 2824440



## EDUCATION

1994 SSLC  
Rajarshi memorial HS, Vadavucode  
(87%)

1994-1996 Pre-Degree  
Mar Thoma College for Women,  
Perumbavoor  
(82%)

1996-1999 B. Sc. Chemistry  
St. Teresa's College, Ernakulam  
(89%)

1999-2001 M. Sc. Applied Chemistry  
Sree Sankara College, Kalady  
(71.4%)  
1<sup>st</sup> rank in M.G. University, Kottayam

2001 CSIR-UGC (NET)

2001-2002 B. Ed. Physical Science  
St. Joseph's Training College, Ernakulam  
(75%)